EUMETSAT Satellite Application Facility on
Support to Operational Hydrology and Water Management

Product Validation Report (PVR) for products H60B (P-IN-SEVIRI-PMW) and H63 (P-IN-SEVIRI_E)

Precipitation rate at ground by GEO/IR supported by LEO/MW

Reference Number:	SAF/HSAF/PVR-60-63
Issue/Revision Index:	2.0
Last Change:	27 February 2022
About this document	This Document has been prepared by the Product Validation Cluster Leader, with the support of the Project Management Team and of the Validation and Development Teams of the Precipitation Cluster

DOCUMENT CHANGE RECORD

Issue / Revision	Date	Description
1.0	30/09/2021	Final document
2.0	27/02/2022	Updated document

Index

List of tables

List of figures

1 Introduction to the Product Validation Report

The Product Validation Report (PVR) contains all the useful information for users to acquire more about the limits and potentials of the precipitation product. The document collects all the information and all the results obtained from the Quality and Monitoring Assessment cluster.
The precipitation product under review, during the analyzes carried out by the cluster, is on "in-development" phase. The objective of this report is to determine and quantify both the limits and the potential of the product in order to assess the overall quality and make it available to end users.

The report is structured as follows:

In **Chapter 2** there is a brief description of the product and the precipitation algorithm retrieval. More details about this can be found on the PUM (Product User Manual) and on the ATBD (Algorithm Theoretical Baseline Document) of the products themselves.

The main part of this document is contained in **Chapters 3, 4 and 5**, dedicated to the description of the validation results obtained for case studies, analyses over a long period, and intercomparison between two SEVIRI products, respectively.

For more information about the analysis, validation, and quality assessment methodology, compare **Appendix 1**.

All detailed information on the data used to compare the products is contained in **Appendix 2**.

Please note that Appendix 1 and 2 are common to all PVRs.

Any further results obtained and not included in chapters 3-5, are included from **Appendix 3** onwards.

Finally, the last **Appendix 6** is dedicated to the list of numerous acronyms used in this document.

For any errors, oversights, or requests for updates or changes, please contact us via H SAF project website: **http://h-saf.eumetsat.int**

2 P-IN-SEVIRI-PMW (H60B) and P-IN-SEVIRI_E (H63) products

P-IN-SEVIRI-PMW and P-IN-SEVIRI_E products are two instantaneous precipitation products based on 15 minutes time frequency SEVIRI rainfall acquisitions blended with LEO MW-derived precipitation rate estimates (i.e. PUM document).
The spatial coverage of P-IN-SEVIRI-PMW product includes the H SAF area (Europe and Mediterranean basin), Africa and Southern Atlantic Ocean, while the spatial coverage of the P-IN-SEVIRI_E product corresponds to the MSG IODC Full Disk and it includes the Mediterranean basin, Africa, Middle East, and Indian Ocean. Both products are provided on the MSG SEVIRI grid. Figure 1 shows the geographical regions covered by the two products.

Figure 1: P-IN-SEVIRI-PMW coverage and P-IN-SEVIRI_E coverage (from left to right, respectively).

2.1 Sensing principle

The products P-IN-SEVIRI-PMW and P-IN-SEVIRI_E are based on the IR images from the SEVIRI instrument on-board Meteosat Second Generation (MSG) satellites blended with all the available precipitation MW estimates (PMW). There is no difference in the algorithm used for these products (even if the availability of PMW could be different), they differ only in the geographical coverage. The spatial coverage of P-IN-SEVIRI-PMW product includes the H SAF area (Europe and Mediterranean basin), Africa and Southern Atlantic Ocean, while the spatial coverage of the P-IN-SEVIRI_E product corresponds to the MSG IODC Full Disk and it includes the Mediterranean basin, Africa, Middle East, and Indian Ocean. Both products are provided on the MSG SEVIRI grid, at the 15-min imaging rate of SEVIRI, and the spatial resolution is consistent with the SEVIRI pixel (3 km at nadir).
The processing method adopted for both products is called “Rapid Update” (RU). Following this technique, the precipitation estimates are obtained by combining IR GEO equivalent blackbody temperatures (TB) at 10.8 μm with rain rates (RR) from Precipitation Micro-Wave (PMW) measurements. Algorithm, described below, is based on a collection of time and space overlapping of both GEO IR imagers and Low Earth Orbit (LEO) PMW sensors (SSMIS, AMSU/MHS, AMSR-2, ATMS, and GMI) overpasses. Such a collection consists of a look up table of geolocated

relationships of rain rate vs TB, updated as soon as new overlapping GEO IR and LEO PMW overpasses (i.e., products P-IN-SSMIS, P-IN-MHS, P-IN-ATMS, H-AUX-17, etc.) are available (Mugnai et al., 2013b, Casella et al., 2013, Sanò et al., 2013, Sanò et al., 2015, Sanò et al., 2016, Casella et al.,2017). Precipitation estimation of both products (H60B and H63) is based on the heritage of P-IN-SEVIRI (H03B) rain retrieval and P-IN-SEVIRI-CO (H15A) products, being the latter specific for convective clouds only. Indeed, H60B production chain identifies convective areas and computes a different RR-TB relationships by distinguish between convective and stratiform clouds. The convective areas are identified with the automatic tool for nowcasting applications NEFODINA (Melfi et al., 2012).

2.2 Algorithm principle

The following sections describe the principal characteristics of the various software modules that compose both P-IN-SEVIRI-PMW and P-IN-SEVIRI_E generation chains. The methodology implemented for the ingestion of mandatory input data from both PMW and IR radiometers is the same adopted for P-IN-SEVIRI, apart from the inputs and their format. However, P-IN-SEVIRI-PMW and P-IN-SEVIRI_E consider not only P-IN-SSMIS and P-IN-MHS as PMW radiometer data, but also P-IN-ATMS, H-AUX-17, and H-AUX-20. Furthermore, P-IN-SEVIRI-PMW and P-IN-SEVIRI_E implement different way to calculate stratiform and convective precipitations.
Rainy pixel of PMW radiometer orbital grid is processed differently depending on whether rainfall is convective or stratiform. The choice of one or the other case depends on the convection file obtained by combining the information deriving from both the NEFODINA SW (an automatic tool for detection and classification of convective cloud systems and the monitoring of their lifecycles) output and the SEVIRI-MSG file containing the Channel 9 (10.8 μm) TB (K). When a PMW radiometer's file is selected, a cycle is performed on the number of pixels, searching the coincidence between TB from IR radiometer and rainfall estimates from PMW radiometer based on both the geographical coordinates and time.
When the coincidence has been found, firstly, the number of pixels of SEVIRI-MSG belonging to the selected PMW radiometer's one is identified. So, if more than one pixel of the SEVIRI grid has been found, those referring to convective rain are counted (according to the NEFODINA software).
In that case, a factor f is calculated depending on both the overall area of the convective pixels and their number in the following way:

$$f = \frac{N^2}{A}$$

where N is the number of SEVIRI-MSG pixels (IFOVs) and A represents the number of convective pixels detected by the SEVIRI sensor (dimensionless). Then, f is utilized to correct the PMW radiometer's rainfall estimates, being the latter multiplied by the factor. However, PMW radiometer's estimates are corrected for convective case only if f is greater or equal than 1.
If none of the SEVIRI pixels related to the same PMW IFOV is labelled as convective, the rain is considered as produced by stratiform clouds and the rainfall estimation is not corrected with the proposed method.

2.3 Main operational characteristics

The horizontal resolution (Δx). The SEVIRI instantaneous field of view (IFOV) is 4.8 km at nadir, and it degrades moving away from nadir, becoming about 8 km over Europe. The sampling distance at the sub-satellite point is ~ 3 km. Conclusion:
• resolution Δx ~ from 4.8 to 8 km - sampling distance: ~ 3 km at the sub-satellite point.

The observing cycle (Δt). It is defined as the average time interval between two measurements over the same area. In the case of P-IN-SEVIRI-PMW the product is generated soon after each SEVIRI new acquisition. Thus:
• observing cycle Δt = 15 min - sampling time: 15 min.

The timeliness (δ).
timeliness δ ~ 15 min.

The accuracy is evaluated a-posteriori by means of the validation activity.

3 Validation results: case study analysis

3.1 Introduction

As reported in the Appendix 1 the common validation methodology is composed of large statistic (multi-categorical and continuous), and case study analysis. Both components (large statistics and case study analysis) are considered complementary in assessing the accuracy of the implemented algorithms. Large statistics helps in identifying existence of pathological behavior, selected case studies are useful in identifying the roots of such behavior, when present.

This Chapter collects the case study analysis performed by PPVG. The Chapter is structured by Country / Team, one section each. The analysis has been conducted to provide information to the User of the product on the variability of the performances with climatological and morphological conditions, as well as with seasonal effects.

Each section presents the case studies analysed giving the following information:

- description of the meteorological event;
- comparison of ground data and satellite products;
- visualization of ancillary data deduced by nowcasting products or lightning network;
- discussion of the satellite product performances;
- indication on the ground data (if requested) availability into the H SAF project.

3.2 Product information

Some main product information are summarized in table.

PRODUCT NAME: **P-IN-SEVIRI-PMW (H60B)**		
PRODUCT DEVELOPER INSTITUTE: GEO-K	Developers: Giorgi C. (Leader), Melfi D.	Contact point: claudio.giorgi@geo-k.co davide.melfi@aeronautica.difesa.it
OPERATIONAL CHAIN INSTITUTE: CNMCA	Responsables: Zauli F., Melfi D.	Contact points: francesco.zauli@aeronautica.difesa.it davide.melfi@aeronautica.difesa.it

3.3 Case study analysis in Belgium (RMI)

3.3.1 Case study: 27 September 2020

PRODUCT NAME	H60B
CASE STUDY PERIOD	27 September 2020
CASE STUDY AREA	Belgium
METEOROLOGICAL EVENT	Autumn showers
VALIDATION INSTITUTE	RMI
PRODUCT DEVELOPER INSTITUTE	GEO-K
OPERATIONAL CHAIN INSTITUTE	CNMCA

METEOROLOGICAL EVENT DESCRIPTION

A vast system of low pressure over Europe accompanied by many fronts is influencing the weather in Belgium and the surrounding countries. During the night of 26 to 27 September, an active perturbation associated with this system traversed the country from northeast and produced locally abundant rain with moderate to strong winds.
The barometric state of the atmosphere, including fronts, is summarized in the following maps:

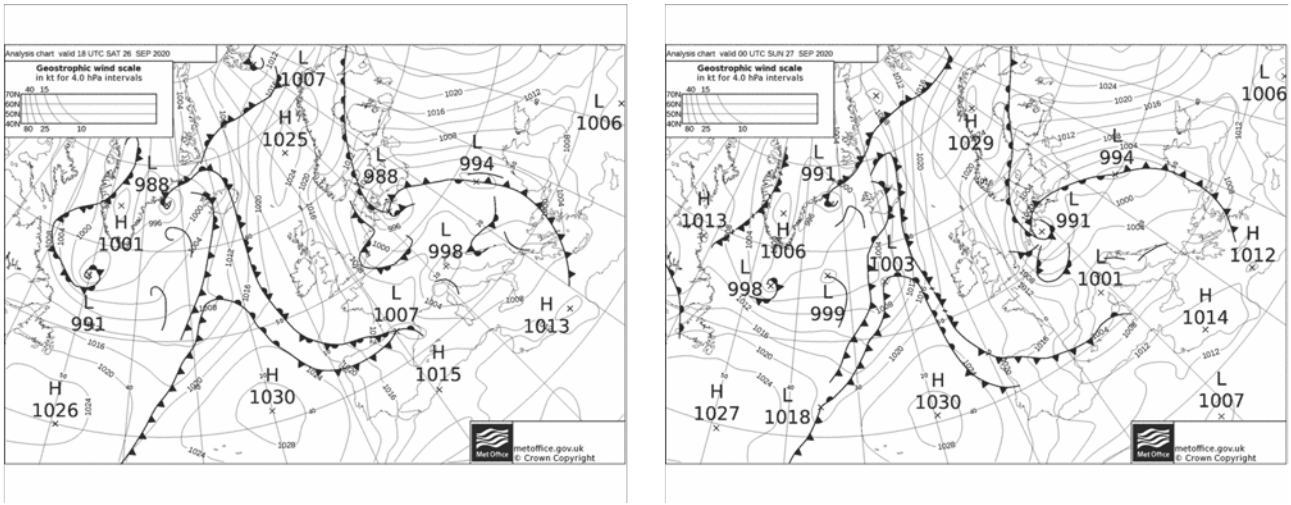

Figure 2: Analysis charts valid for 26 (left) and 27 (right) September 2020 at 18:00 and 00:00 UTC respectively (Contains public sector information licensed under the Open Government Licence v3.0).

DATA/PRODUCTS USED

Reference data: Belgian Radar located at Wideumont, Wallonia (RMI)
Precipitation product H60B (H-SAF/EUMETSAT)
Weather charts (MetOffice analyses from Wetterzentrale archive)

RESULTS OF COMPARISON

In Figure 3 and Figure 4 we can see the result of upscaling of radar data to the H60B grid at 03:00 and 03:30, together with the corresponding H60B data. The upscaled radar data serve as basis for comparison between radar and H60B.

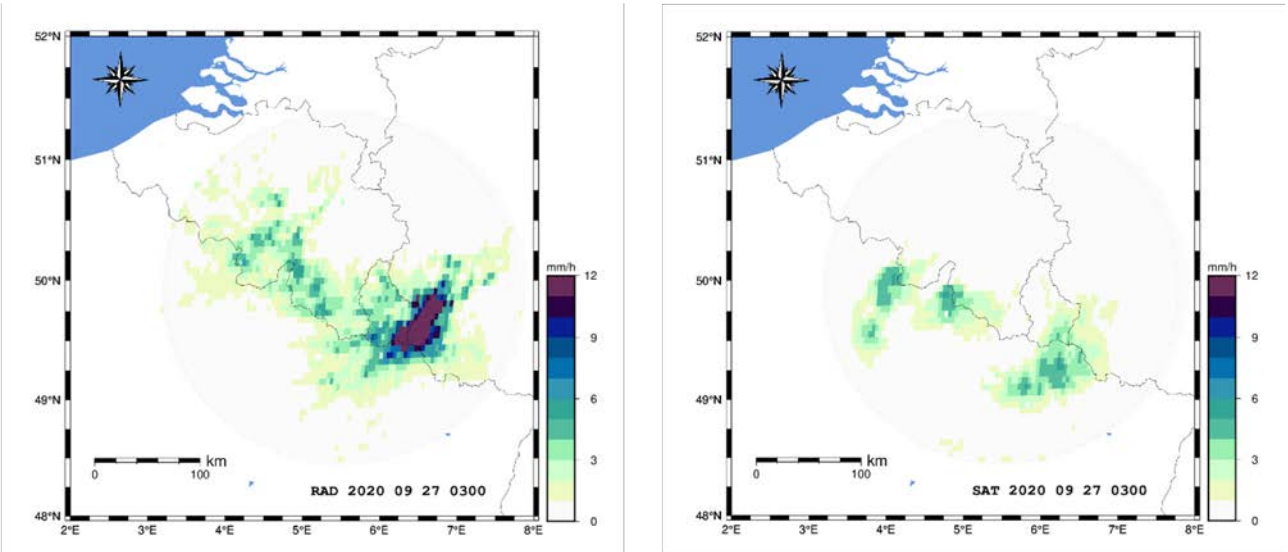

Figure 3: Upscaled radar (left) and H60B (right) valid for 27 September 2020 at 03:00.

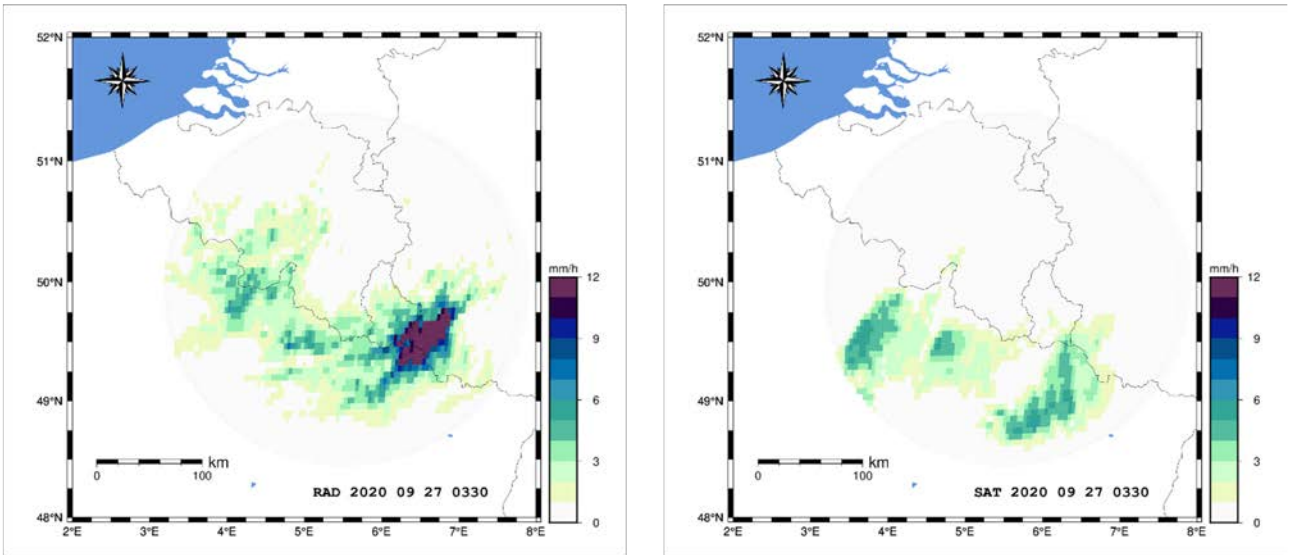

Figure 4: Upscaled radar (left) and H60B (right) valid for 27 September 2020 at 03:30.

In both cases the precipitation detection with the product H60B manages to capture the spatial distribution of the rain, although there are noticeable deviations from the radar images and a significant underestimation of the intensities in one area. In particular, in Figure 27 the percentage of grid cells in which the rainfall exceeds 1 mm/h is 35.1% for the upscaled radar image and 16.8% for the H60B image. Considering a higher threshold of 5 mm/h, these percentages become 4% and 0.17% while the highest rain rates are 30.2 mm/h and 5.6 mm/h respectively.

For the two previous cases we have computed statistical scores shown in the following tables.

H60B vs. RADAR	0.25 mm/h < rr < 1 mm/h	1 mm/h < rr < 10 mm/h	rr > 0.25 mm/h
ME [mm/h]	-0.28	-1.63	-1.18
STD [mm/h]	0.59	1.83	2.42
MB [-]	0.50	0.37	0.35
RMSE [mm/h]	0.65	2.45	2.69
FSE [%]	1.17	0.94	1.48

H60B vs. RADAR	rr > 0.25 mm/h	rr > 1 mm/h
POD [-]	0.38	0.33
FAR [-]	0.18	0.30
CSI [-]	0.35	0.29

Table 1: Statistical scores obtained from the comparison between H60B and radar acquisition, valid for 27 September 2020 at 03:00.

H60B vs. RADAR	0.25 mm/h < rr < 1 mm/h	1 mm/h < rr < 10 mm/h	rr > 0.25 mm/h
ME [mm/h]	0.02	-1.48	-1.12
STD [mm/h]	1.06	1.99	2.84
MB [-]	1.04	0.45	0.46
RMSE [mm/h]	1.06	2.48	3.05
FSE [%]	1.95	0.92	1.47

H02B vs. RADAR	rr > 0.25 mm/h	rr > 1 mm/h
POD [-]	0.46	0.41
FAR [-]	0.08	0.31
CSI [-]	0.45	0.34

Table 2: Statistical scores obtained from the comparison between H60B and radar acquisition, valid for 27 September 2020 at 03:30.

FINAL COMMENTS

In the present case of intense showers, the product H60B shows a tendency to underestimate the precipitation intensities and extent. The general conclusion from the two pairs of images examined here is qualitatively the same, with the negative bias as prominent feature.

3.4 Case study analysis in Hungary (OMSZ))

3.4.1 Case study: 22 April 2021

PRODUCT NAME	H60B
CASE STUDY PERIOD	22 April 2021
CASE STUDY AREA	Hungary
METEOROLOGICAL EVENT	Convective precipitation evolved on a cold front
VALIDATION INSTITUTE	OMSZ – Hungarian Meteorological Service
PRODUCT DEVELOPER INSTITUTE	GEO-K
OPERATIONAL CHAIN INSTITUTE	COMET

METEOROLOGICAL EVENT DESCRIPTION

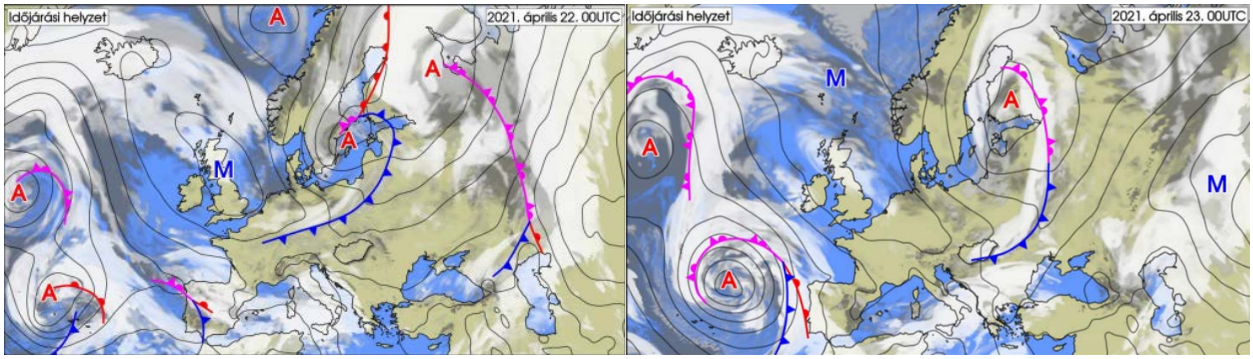

Figure 5: The location of the cold front at 00 UTC on 22nd (left) and 23rd (right) of April 2021.

In the dawn of the 22nd of April 2021, a cold front spread from Finland over Poland to Luxembourg. During the day this quick-moving cold front passed over Hungary from northwest to southeast (Figure 5). The frontal cloud and the evolved convective clouds caused showers and thunderstorms in numerous places of the country, in some places even hail occurred. In the night precipitation ended in most parts of Hungary, but in the northeastern counties showers, in mountain Bükk snow shower occurred. The daily sum of precipitation was between trace and 15 mm (Figure 6).

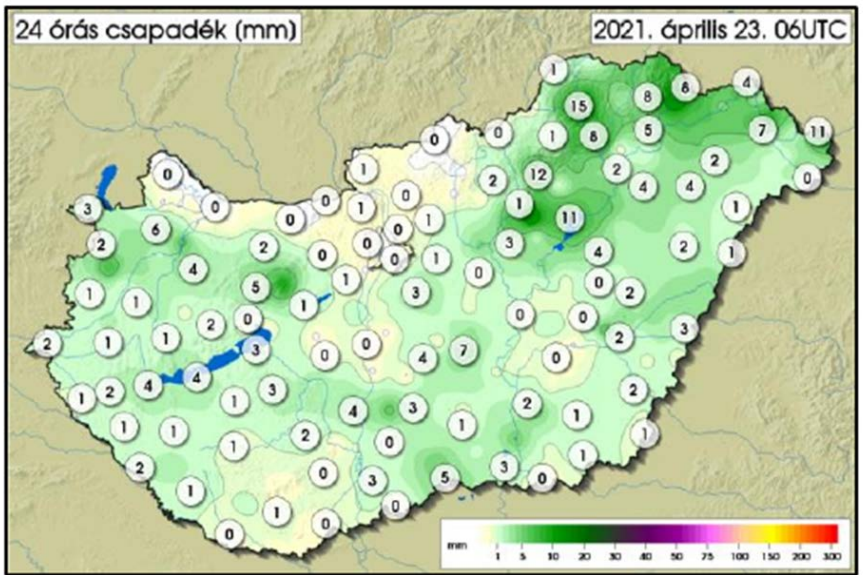

Figure 6: 24 h precipitation measured until 06:00 UTC on 23rd April 2021.

DATA/PRODUCTS USED

Product to validate:

Instantaneus precipitation values from the H60B products (EUMETSAT HSAF)

Reference data:

Precipitation values from the Hungarian radar network (OMSZ), precipitation from synop data, MSG IR and RGB images, lightning data of the Hungarian LINET network, operational H03B instantaneous precipitation product, H15A instantaenous convective precipitation product

SAF products, radar images, lightning and synop maps were visualised with the **HAWK-3** (Hungarian Advanced Weather WorKStation) software, which is the operational visualisation tool developed by the Hungarian Meteorological Service.

RESULTS OF COMPARISON

The case was selected because on 22 April a lot of convective cloud was formed on the cold front and we wanted to compare the new product to both the general H03B and the convective H15A products as well. The H15A products unfortunately contained very little data as the convection was not strong enough (Figure 7).

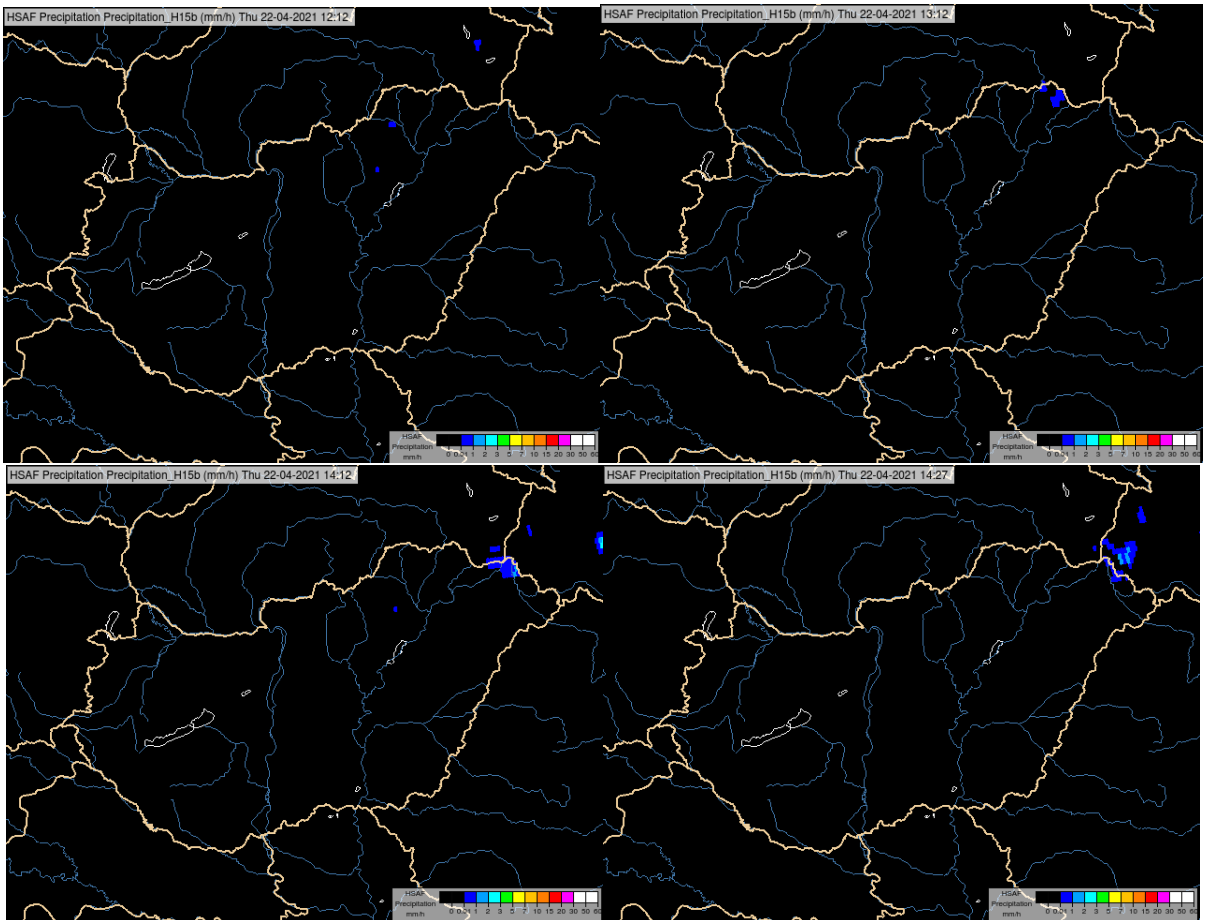

Figure 7: H15A convective precipitation product in 4 time slots from the first nonzero values until the system left Hungary (12:12 UTC top left, 13:12 UTC top right, 14:12 UTC bottom left, 14: 27 UTC bottom right)

During the detailed comparison we used the following fields, as they will appear in the images below:

1	2	3
4	5	6

1. Instantaneous precipitation values from the H60B product
2. Precipitation values from the Hungarian radar network (OMSZ),
3. Calibrated MSG IR 10.8 µm image
4. Operational H03B instantaneous precipitation product
5. Precipitation from synop data of OMSZ (10 min measurements were multiplied by 6 to have comparable mm/h values),
6. SEVIRI HRV Cloud RGB image with lightning data of the Hungarian LINET network (OMSZ). Lightning of the last 1 hour is visualised, red colour represents the latest and light pink colour the oldest strokes.

In the images the IR, RGB and ground data have +10min timestamps as it is used in OMSZ, because the timestamp of the original MSG satellite images and thus most of the HSAF MSG products (excluding H15A e.g.) refer to the start of the scanning, but Hungary is scanned about 10 minutes after.

At 9 UTC the first lightning strokes appeared on the lightning map (Figure 8). At the same time the first precipitation patch appeared in H60B image. In the IR image we can see a very cold point there as top of the convective cloud. The radar composite gave precipitation earlier and in an extended area, also higher amount. But compared to H03B which still gave no precipitation, the H60B is better.

We can see similar result in images at 10:30 (Figure 9) but at 11:00 (Figure 10) the precipitating area is bigger in H60B than in radar image, but the intensity values are still lower in H60B than in radar. This is acceptable here as the resolution of the satellite image is less than of the radar image.

The selected convective cell leaves Hungary at about 14:30 (Figure 11) reaching its highest precipitation intensity. The values in the radar can reach 60 mm/h. In H60B the values are between 10-15mm/h, but in a more extended area. At this timeslot the H03B has similar extension for precipitating area, but the values are much lower (less than 3mm/h). Synop stations were avoided by the highest intensity peaks, 8.4 mm/h were the maximum intensity values caught.

For all the selected timeslots we can say that H60B gives better estimate of the precipitation than H03B or H15A compared to radar data.

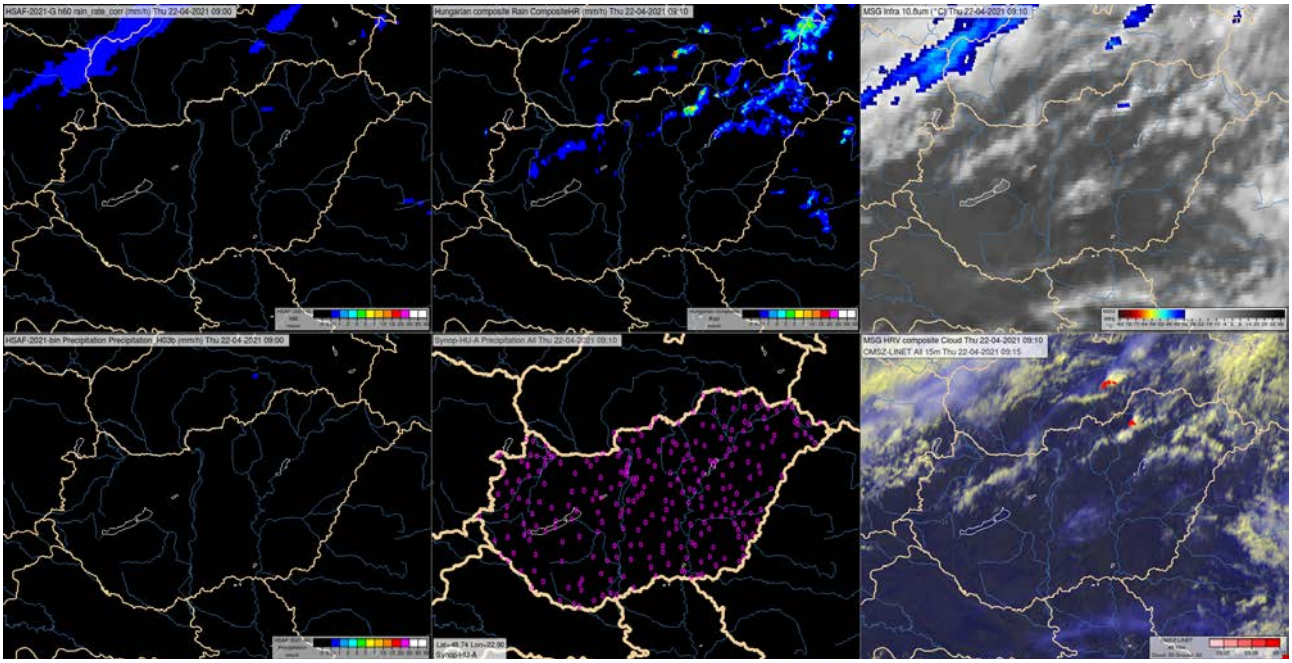

Figure 8: Precipitation fields (1-6 as above descripted) for 22 April 2021. 09:00 UTC

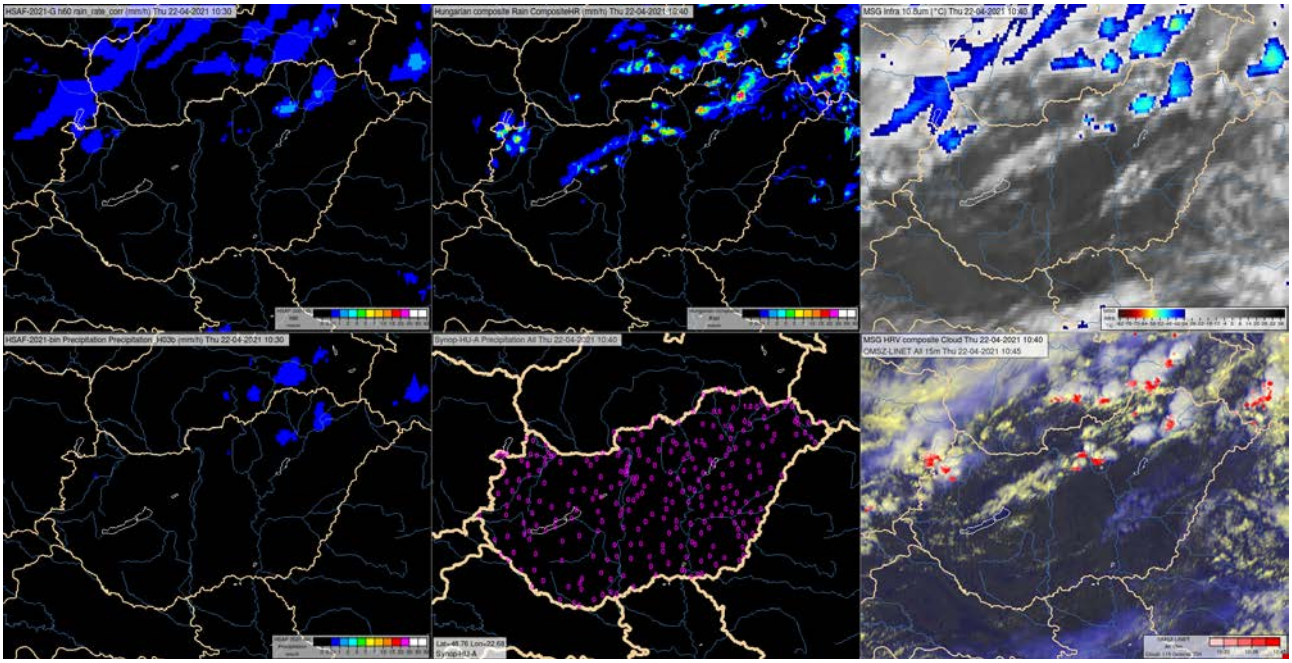

Figure 9: Precipitation fields (1-6 as above descripted) for 22 April 2021. 10:30 UTC.

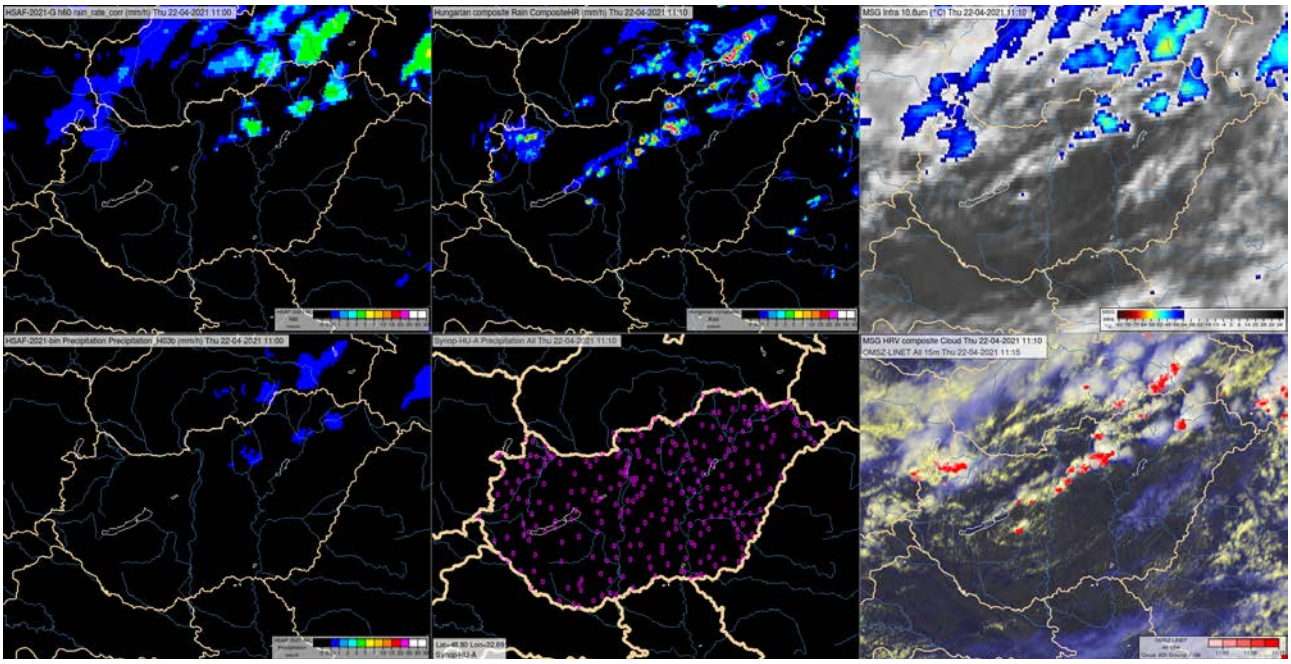

Figure 10: Precipitation fields (1-6 as above descripted) for 22 April 2021. 11:00 UTC.

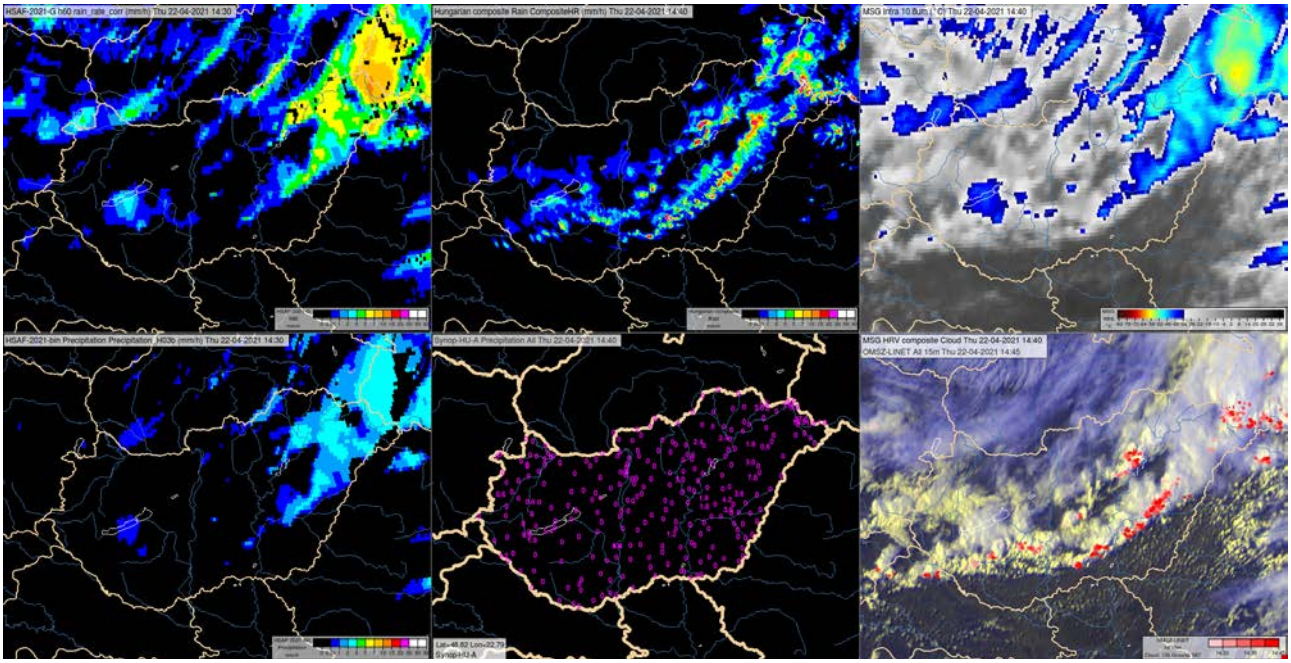

Figure 11: Precipitation fields (1-6 as above descripted) for 22 April 2021. 14:30 UTC.

FINAL COMMENTS

At this case the convective precipitation is better represented in H60B than in H03B and much better then in H15A. It is appreciated that we can have the advantages of H03B and H15A in one product now!

It would be useful to indicate in the quality flag (or some other layer) if the convective or non-convective algorithm is used for the given pixel.

3.5 Case study analysis in Slovakia (SHMI))

3.5.1 Case study: 12 July 2020

PRODUCT NAME	H60B
CASE STUDY PERIOD	12 July 2020
CASE STUDY AREA	Slovakia
METEOROLOGICAL EVENT	Thunderstorms on a convergence line moving over Slovakia
VALIDATION INSTITUTE	Slovak Hydrometeorological Institute (SHMI)
PRODUCT DEVELOPER INSTITUTE	GEO-K
OPERATIONAL CHAIN INSTITUTE	CNMCA

METEOROLOGICAL EVENT DESCRIPTION

Ahead of cold front approaching from Western Europe, a convergence line formed in the warm, originally tropical air mass in the Central Europe. Associated thunderstorms were moving over Slovakia in the SW-NE direction during the day 2 July 2021 00:00UTC. The movement of cold front is evident from synoptical analyses at the end of the day, dated 3 July 2021 00:00UTC.

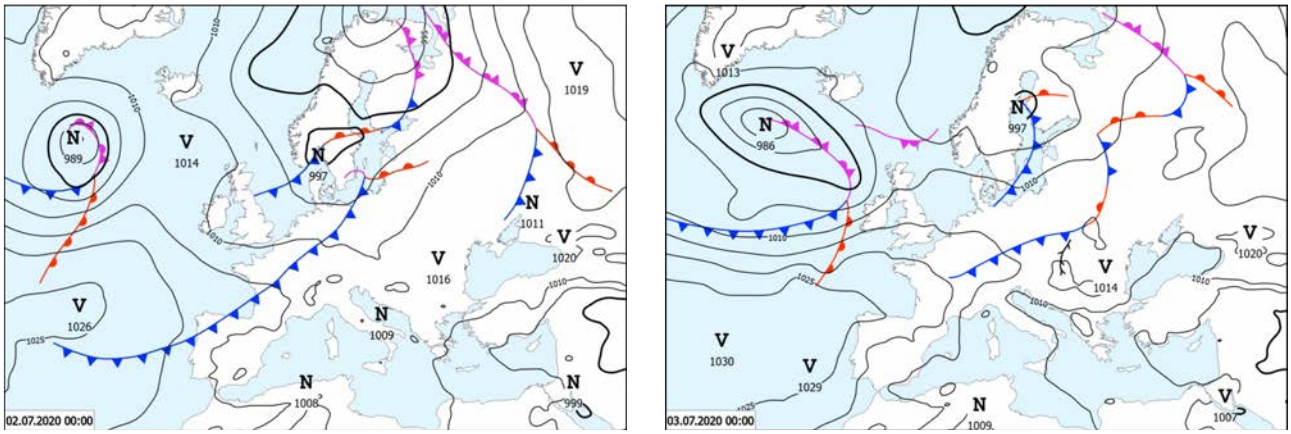

Figure 12: Synoptical analyses at the end of the day, dated 3 July 2021 00:00UTC

DATA/PRODUCTS USED

P-IN-SEVIRI-PMW (H60B, Full disk product) precipitation intensity fields from following satellite timeslots (mean scan times of SHMI radar domain are stated): 2 July 2020 00-23:15 UTC.

Meteosat imagery to document synoptic situation: 2 July 2020 03:15, 5:00, 17:00 and 19:00 UTC.

Precipitation intensity fields from SHMI radars derived from CAPPI 2km product using quality indices, thresholded to overall radar QI > 0.3, and the same but for comparison with threshold QI>0.6.

Statistical results (RMSE, bias, correlation, Fractional Standard Error, Nash-Sutcliffe Coefficient) of radar and satellite data comparison and evaluation.

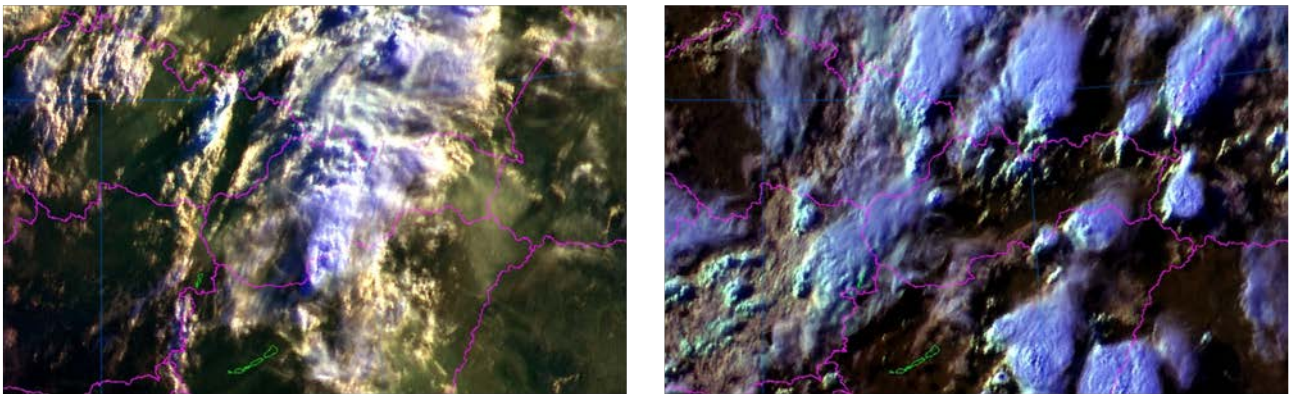

Figure 13: MSG HRV imagery showing development of thunderstorm over Slovakia during studying period. Left - 2 July 2020 03:15 UTC early morning storms. Right - 2 July 2020 17:00 UTC, afternoon storms.

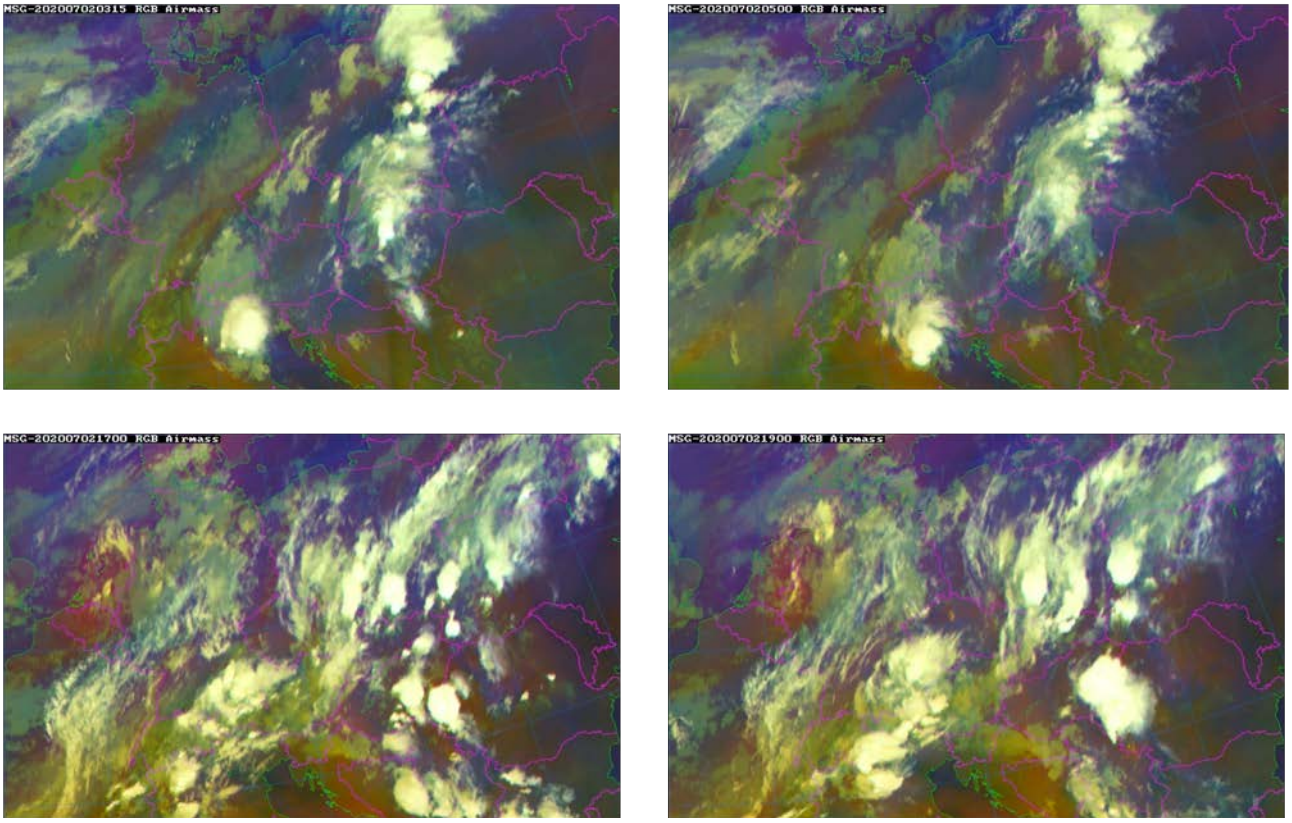

Figure 14: MSG Airmass RGB imagery is showing scattered thunderstorms over southern and central Europe: 3:15, 5:00, 17:00 and 19:00 UTC 2 July 2020.

RESULTS OF COMPARISON

By visual comparison with radars, the satellite product overestimated area of the precipitation and mostly underestimated maxima of precipitation intensities (see Figure 15). The structure of precipitation matched well; only small dislocations we found as typical feature of convective systems over central Europe observed from geostationary orbit.

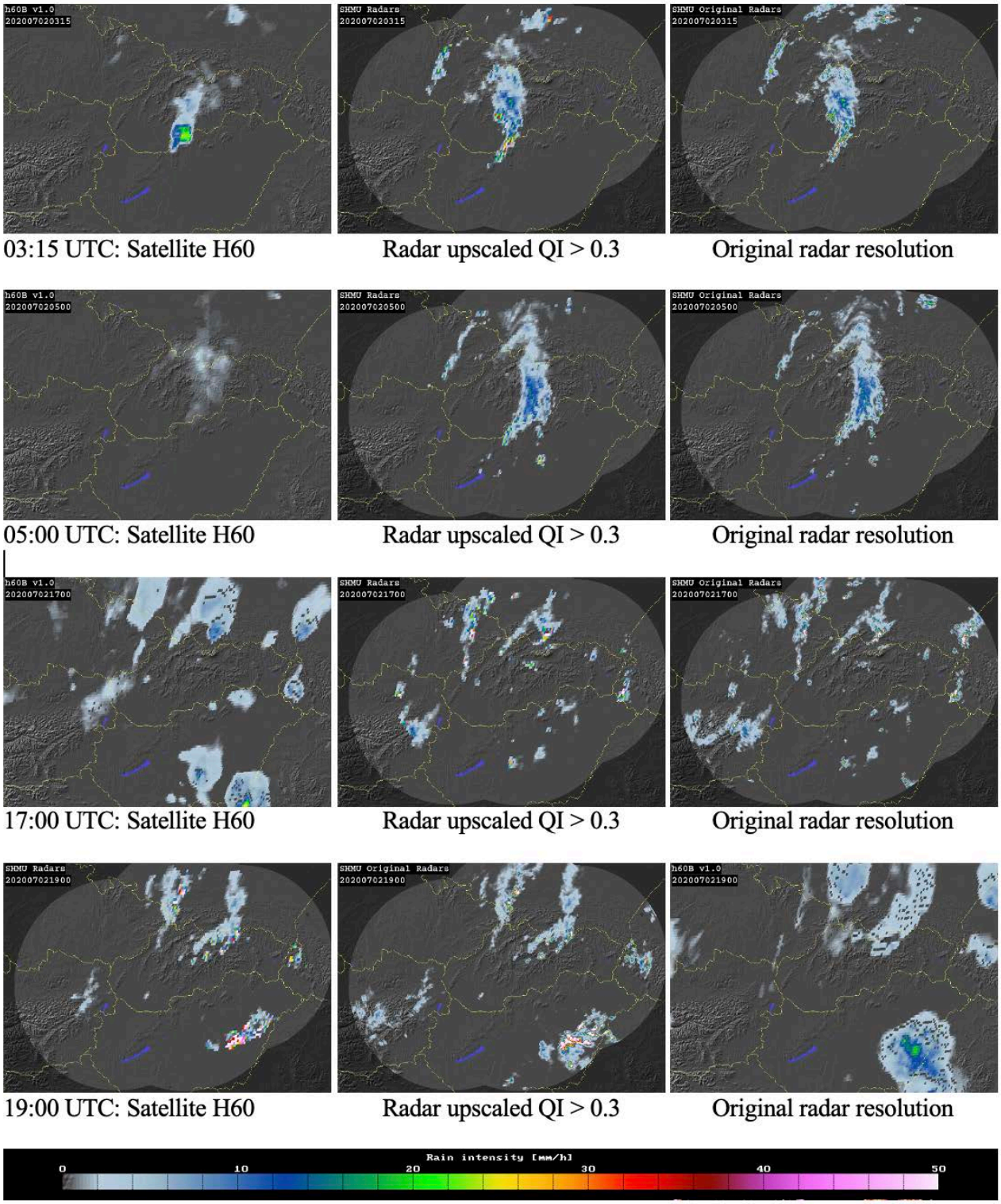

Figure 15: Instantaneous precipitation fields from 2 July 2020 observed by H60B product (left column), SHMU radars upscaled to satellite grid (middle) and SHMU radars in original 1km resolution (right column). Data in rows: MSG timeslots 2 July 2020 03:15, 05:00, 17:00 and 19:00 UTC. The radar precipitation values are corresponding to satellite IFOVs projected over the radar domain. Comparison is limited to area where overall radar quality index QI > 0.3. Because of lower quality, also radar data in more distant ranges are taken into account in validation statistics.

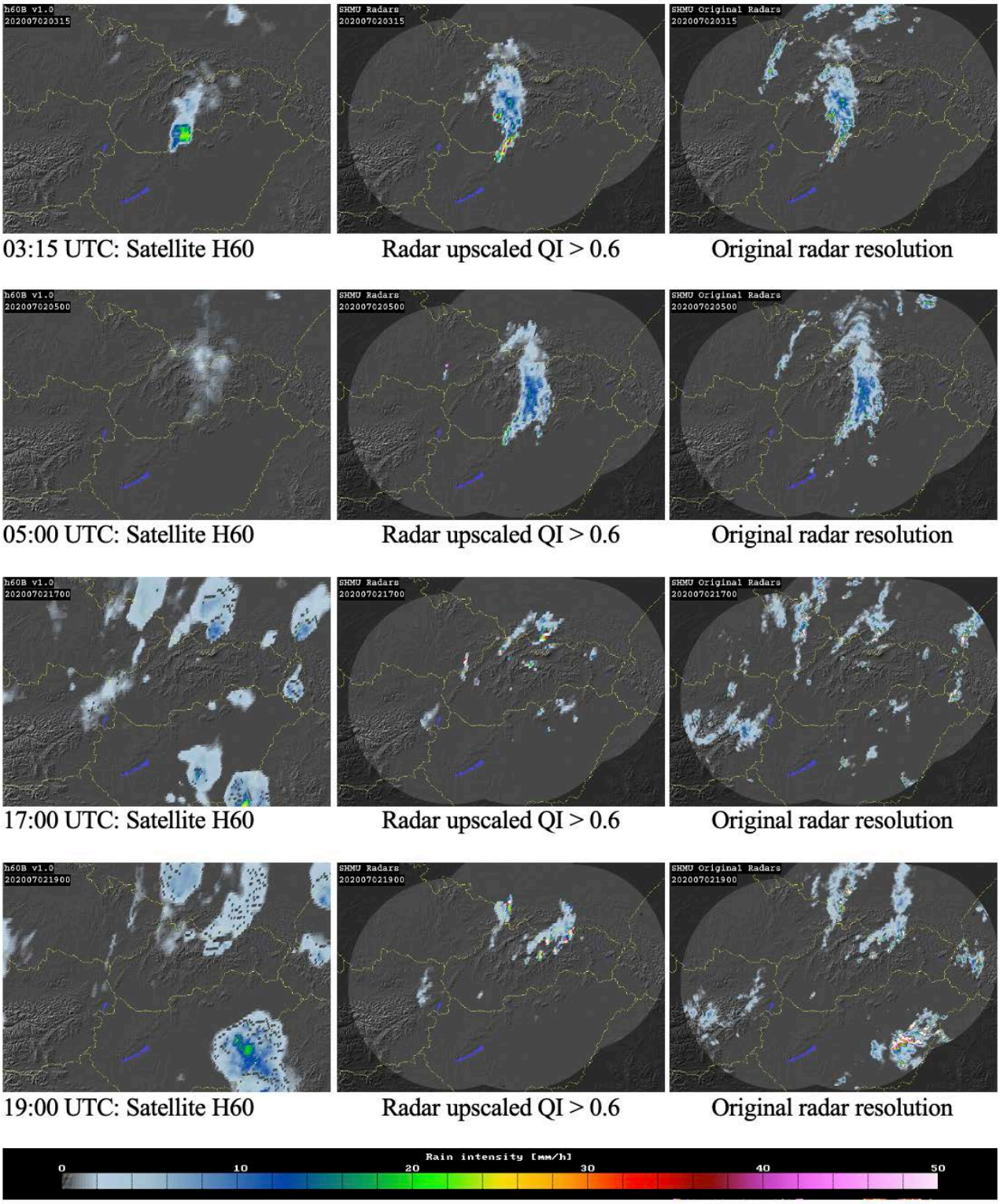

Figure 16: Instantaneous precipitation fields from 2 July 2020 observed by H60B product (left column), SHMU radars upscaled to satellite grid (middle) and SHMU radars in original 1km resolution (right column). Data in rows: MSG timeslots 2 July 2020 03:15, 05:00, 17:00 and 19:00 UTC. The radar precipitation values are corresponding to satellite IFOVs projected over the radar domain. Comparison is limited to area where overall radar quality index QI > 0.6. Because of higher quality, only radar data in closer ranges are taken into account in validation statistics.

Results of statistical comparison of the satellite product with radars for the whole case study period are shown in the following tables.

Precipitation class (mm/h)	**0.25 - 1**	**1 - 10**	**≥ 10**	**≥ 0.25**
1 Number of satellite obs.	40404	51102	1986	93492
2 Number of radar obs.	29006	51645	8544	89195
3 Mean error (mm/h)	0.167	-2.273	-22.755	-3.441
6 Multiplicative bias	1.298	0.352	0.124	0.268
7 Correlation coefficient	0.014	0.117	0.208	0.279
9 URD-RMSE (%)	3.936	1.159	0.878	2.427
10 Fractional Standard Error (x100%)	3.109	1.082	1.190	2.136
11 Nash-Sutcliffe Coefficient	-64.568	-1.910	-1.086	-0.045

Table 3: Selected scores of continuous statistics for radar QI > 0.3.

Precipitation threshold (mm/h	**≥ 0.25**	**≥ 1**
POD	0.457	0.324
FAR	0.564	0.633
CSI	0.288	0.208

Table 4: Selected scores of dichotomous statistics for radar QI > 0.3.

Precipitation class (mm/h)	**0.25 - 1**	**1 - 10**	**≥ 10**	**≥ 0.25**
1 Number of satellite obs.	22561	24936	990	48487
2 Number of radar obs.	14322	26301	3843	44466
3 Mean error (mm/h)	0.152	-2.470	-22.399	-3.348
6 Multiplicative bias	1.272	0.301	0.121	0.252
7 Correlation coefficient	0.007	0.110	0.218	0.274
9 URD-RMSE (%)	4.089	1.119	0.888	2.489
10 Fractional Standard Error (x100%)	3.204	1.088	1.207	2.139
11 Nash-Sutcliffe Coefficient	-67.788	-1.982	-1.029	-0.054

Table 5: Selected scores of continuous statistics for radar QI > 0.6.

Precipitation threshold (mm/h)	**≥ 0.25**	**≥ 1**
POD	0.440	0.277
FAR	0.596	0.678
CSI	0.266	0.175

Table 6:Selected scores of dichotomous statistics for radar QI > 0.6.

High negative Mean error and low Multiplicative bias of heavy precipitation class (see Table 3, PR ≥ 10 mm/h) confirm the observed underestimation of precipitation maxima by H60B. On the other hand, both scores corresponding to medium precipitation class (1 – 10 mm/h) and overall precipitation (PR ≥ 0.25 mm/h) are much better. The same applies to Nash-Sutcliffe Coefficient.

POD values 0.45 (are lower than we observed in older case studies 0.80 for H03B product) for lower threshold (see Table 4) and indicates medium detection capability of the satellite product. FAR values are quite high (above 0.5 or 0.6 for higher precipitation intensities) which agrees with the observed overestimation of spatial precipitation extent by H60B and are comparable to the

previous H03B product. However, it is varying from case to case according to meteorological situation.

Correlation Coefficient reached positive values for all precipitation classes though the values are relatively low, not exceeding 0.3. It is evident that higher precipitation rates had better correlate with reference data than low rates.

COMMENTS

In this case, study, the radar data come from 4 Doppler radars, which were replaced in frame of building of new SHMI radar network.

This case study is comparing the performance of validation procedure using two different radar quality thresholds: QI>0.3 and QI>0.6. Results show that lower quality of radar data is increasing the area extent where satellite data are validated, but we do not observe significant impact on overall statistical results. Both results are comparable, and this is positive finding.

4 Validation results: long-term analysis

4.1 Overview

Product ID (Acronym)	H60B (P-IN-SEVIRI-PMW)		
Product name	Precipitation rate at ground by GEO/IR supported by LEO/MW		
Algorithm version number	Latest version:		1.0
	Version considered for Q.A.:		1.0
Covered period	07/2020 – 04/2021		
Q.A. methods applied	Continuous statistics	ME, SD, MAE, MB, RMSE, FSE	
	Multi-categorical statistics	POD, FAR, CSI	
	Contributing countries	BE, BU, DE, HU, IT, PL, SK, TU	

The validation has been performed over the period between July 2020 and April 2021 by European countries belonging to PPVG and supervised by DPC. The product release currently in force at the time of writing has been evaluated. The results are showed both for European area in comparison with radar and rain gauge data (section 4.2), and over the MSG full disk area in comparison with DPR-NS product (section 4.3). The surface type classification is taken in account (land, sea and coast areas) as well as different precipitation rate classes (<1mm/h; 1-10mm/h; ≥10mm/h). The validation procedure evaluates only high-quality precipitation data. Satellite Field Of Views not fully covered by reference data (or with percentage of coverage less than 50%) are discarded by the Q.A. procedure in order to increase the significance of the statistical sample.

4.2 Validation results over European area

Validation has been performed using rain gauge and radar data as reference in Belgium, Bulgaria, Germany, Italy, Hungary, Poland, Slovakia and Turkey, for the period as above descripted. Each institute has used the Unique Common Code (UCC Version 2.0) developed by PPVG to evaluate every H SAF precipitation product in terms of different statistical scores. More than 20 millions of ground and satellite pairs of data were analyzed. For H60B product, the accuracy requirements depend by FSE score as indicated in Table 7: Accuracy requirements for product P-IN-SEVIRI-PMW in term of FSE(%).

Precipitation Rate	Threshold	Target	Optimal
≥ 1 mm/h	200	150	100

Table 7: Accuracy requirements for product P-IN-SEVIRI-PMW in term of FSE(%).

The FSE score (mathematical formula shown in Table 23) defines the accuracy of the H SAF product under analysis.

4.2.1 Monthly accuracy

The monthly accuracy computed for H60B in comparison with radar, rain gauge and overall ground observations is shown in Figure 17 in panel a, b and c respectively. In every panel, the background color indicates the region inside each requirement accuracy threshold as defined in Table 7: Accuracy requirements for product P-IN-SEVIRI-PMW in term of FSE(%). and also used in Table 11. The black dotted line represents the mean FSE value over the full period (12 months). Panel d shows the percentage contribution for different instruments and observation's surfaces respect to the full dataset.

The product has different trend and performances respect to radar and gauge. The overall accuracy is representative of all results computed: the mean value is equal to the target requirement. As for the gauge, the requirement score is always below the target (<150%) for all months with a mean annual value equals to 120%; whereas for the radar it is quite over the target for a couple of months and always below the target (<150%) for the other months, this results in a mean annual value around 170%.

The percentage contribution highlights how radar over land (45%) and gauge (39%) represent most of the full dataset. While coast and sea areas cover only 9% and 8%, respectively.

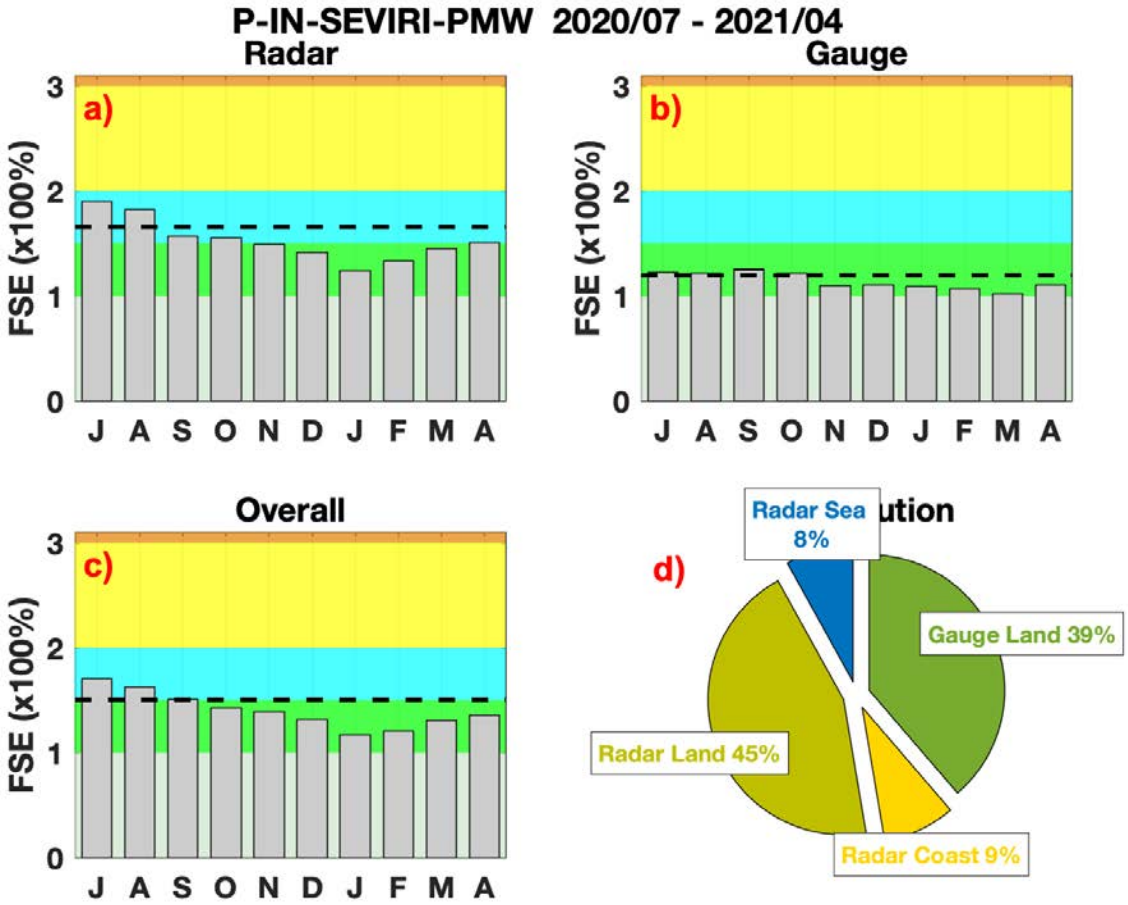

Figure 17: H60B monthly accuracy using Radar (a) and Gauge (b) as ground reference. The Overall Q.A. is shown in the panel c). Background colours highlight the requirement accuracy thresholds in terms of FSE as reported in Table 7. The horizontal black dotted line indicates the mean annual value. The single ground percentage contribution is shown in the panel d).

4.2.2 Monthly continuous statistical scores

In Figure 18 the H60B monthly trend respect to radar over land (green line), sea (blue line), coast (red line) and rain gauge (black dotted line) for all precipitation rates above 1 mm/h is shown for six continuous statistical scores: ME, SD, MAE, MB, RMSE and FSE. Results over land areas are quite coherent in the various months with there over sea and coast.
The decrease of error over time is highlighted in trends of SD, MAE, RMSE and FSE score. ME and MB show a strong tendency to underestimate the precipitation intensity. A better agreement can be found with gauge rather than radar. More continuous statistical scores are shown in Appendix.

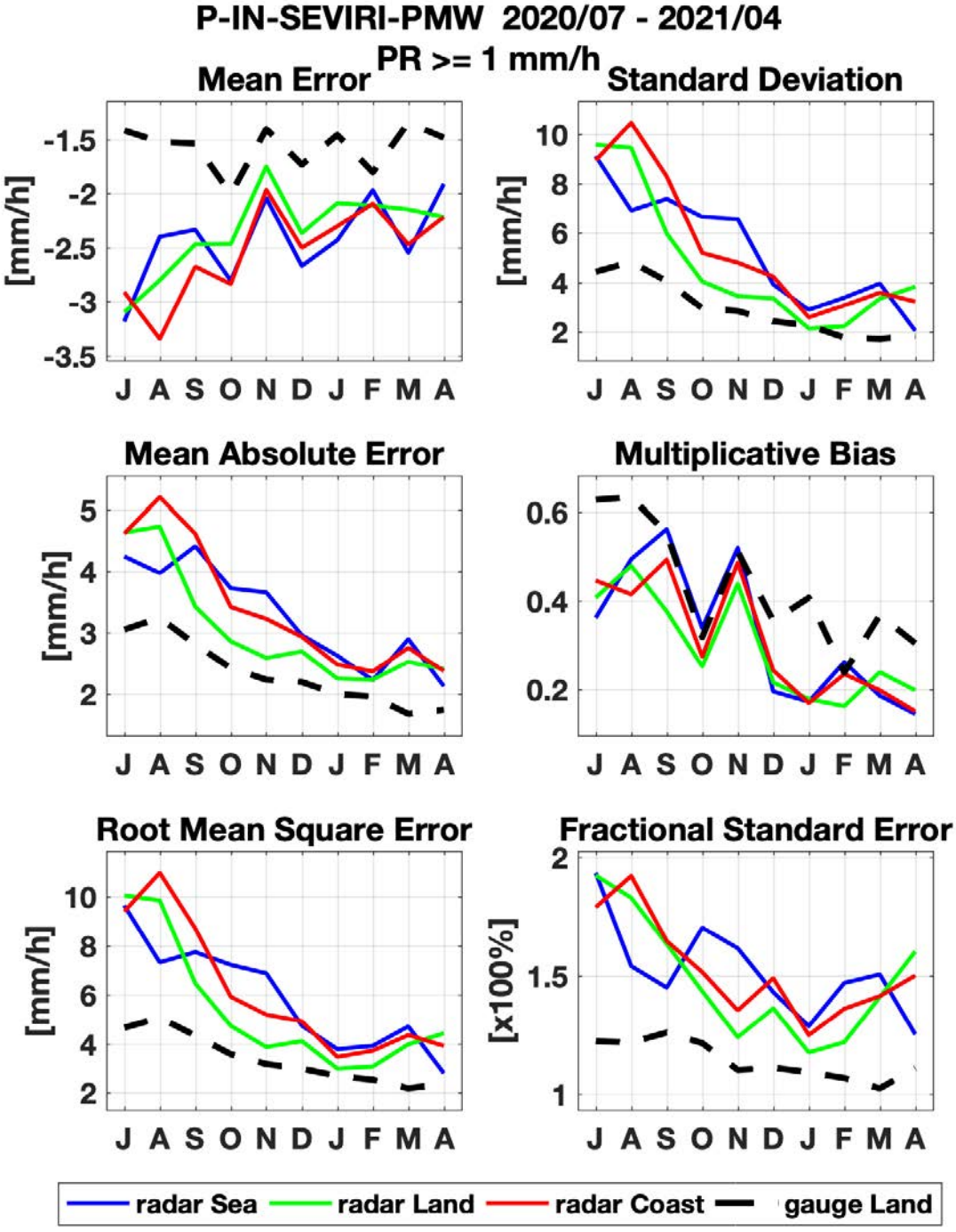

Figure 18: Monthly continuous statistical scores resulting for H60B relatively to the precipitation regime above 1 mm/h.

4.2.3 Multi-categorical statistics

The multi-categorical statistics are below shown. In each table, the first column indicates the precipitation classes of the satellite product, while along the columns are reported the ground precipitation classes. The first class detects the no-rain class (0≤PR<0.25 mm/h), the second class detects the light rain (0.25≤PR<1 mm/h), the third class identifies the stratiform rain rates (1≤PR<10 mm/h), while the last one classifies the convective rates (PR≥10 mm/h).
The H60B product well detects the no-rain area in 90% of cases. Light rain rates are not well detected, mainly over land (17% vs gauge and 12% vs radar) and coast (13%). An evident tendency to underestimate this intensity is observable. Stratiform rain rates are detected in only 28% of total cases. Finally, convective precipitation areas are correctly identified in only 10% of cases. More multi-categorical statistics are shown in Appendix.

Radar Land | Sea | Coast												
Multi-Categorical Statistics												
	[0 - 0.25[mm/h			[0.25 - 1[mm/h			[1 - 10[mm/h			≥10 mm/h		
[0 - 0.25[mm/h	93%	93%	93%	72%	73%	72%	58%	60%	60%	40%	36%	38%
[0.25 - 1[mm/h	4%	4%	4%	12%	13%	13%	14%	14%	15%	11%	12%	13%
[1 - 10[mm/h	3%	3%	3%	15%	13%	15%	26%	24%	24%	42%	41%	40%
≥10 mm/h	0%	0%	0%	0%	0%	1%	1%	1%	1%	8%	10%	9%

Table 8: Multi-categorical table for product H60B – radar validation over land, sea and coast areas. The precipitation classes along the columns (rows) are relative to ground (satellite) precipitation.

Gauge Land				
Multi-Categorical Statistics				
	[0 - 0.25[mm/h	[0.25 - 1[mm/h	[1 - 10[mm/h	≥10 mm/h
[0 - 0.25[mm/h	85%	68%	48%	20%
[0.25 - 1[mm/h	9%	17%	20%	14%
[1 - 10[mm/h	5%	15%	30%	55%
≥10 mm/h	0%	0%	1%	11%

Table 9: Multi-categorical table for product H60B– rain gauge validation over land. The precipitation classes along the columns (rows) are relative to ground (satellite) precipitation.

Overall				
Multi-Categorical Statistics				
	[0 - 0.25[mm/h	[0.25 - 1[mm/h	[1 - 10[mm/h	≥10 mm/h
[0 - 0.25[mm/h	90%	70%	54%	32%
[0.25 - 1[mm/h	6%	15%	18%	12%
[1 - 10[mm/h	4%	15%	28%	46%
≥10 mm/h	0%	0%	1%	10%

Table 10: Multi-categorical table for product H60B– Overall validation. The precipitation classes along the columns (rows) are relative to ground (satellite) precipitation.

4.2.4 Product requirement compliance

The accuracy of H60B, for the validation period July 2020 - April 2021, respect to ground measurements and overall results are reported in Table 11.
All FSE score values are always between the threshold and target. Only that referred to the gauge is below the target requirement (150%) and close to the optimal requirement (100%). The overall accuracy for H60B is equal to 150%.

Between target and optimal	Between threshold and target	Threshold exceeded by < 50 %	Threshold exceeded by ≥ 50 %

H60B	Annual average of FSE (%)							
Precipitation Class	**Requirement (FSE %)**			**Radar (Land)**	**Radar (Sea)**	**Radar (Coast)**	**Gauge (Land)**	**OVERALL**
	thresh	**target**	**optimal**					
≥ 1 mm/h	200	150	100	171	158	162	120	**150**

Table 11: Product requirement and compliance analysis for product H60B

4.3 Validation results over Full Disk (FD) area

The validation procedure over full disk area has been developed by the PPVG and coordinated by DPC. DPR-NS product represents the reference for precipitation over the full area considered. As the validation on the European area, this one is performed over the same period and the FSE score defines the accuracy of H60B (as indicated in Table 7, mathematical formula shown in Table 23). More than 20 millions of gridded data over boxes of 0.5° x 0.5° are compared. Next sections deal about the statistical scores obtained between the two intersected products. In addition, a more detailed analysis for different geographical areas is reported in section 4.3.5. More maps over the MSG full disk area are shown in Appendix.

4.3.1 Monthly accuracy

The monthly accuracy computed for H60B in comparison with DPR-NS product is shown in Figure 19 over land, sea, and overall areas in panel a), b) and c) respectively. In every panel, the background color indicates the region inside each requirement accuracy threshold. The black dotted line represents the mean FSE value over the full period (12 months). Panel d shows the percentage contribution for different areas respect to the full dataset. Sea areas represent the most part of dataset (61%) respect to land (29%) and coast areas (10%).
The mean annual value is always close to the target value (150%).
As for the land, for most months, the accuracy is below the target value and three times between the threshold and the target. As regards the sea, the accuracy is always below the target except for July. Overall results show a mean accuracy value very close to the target requirement.

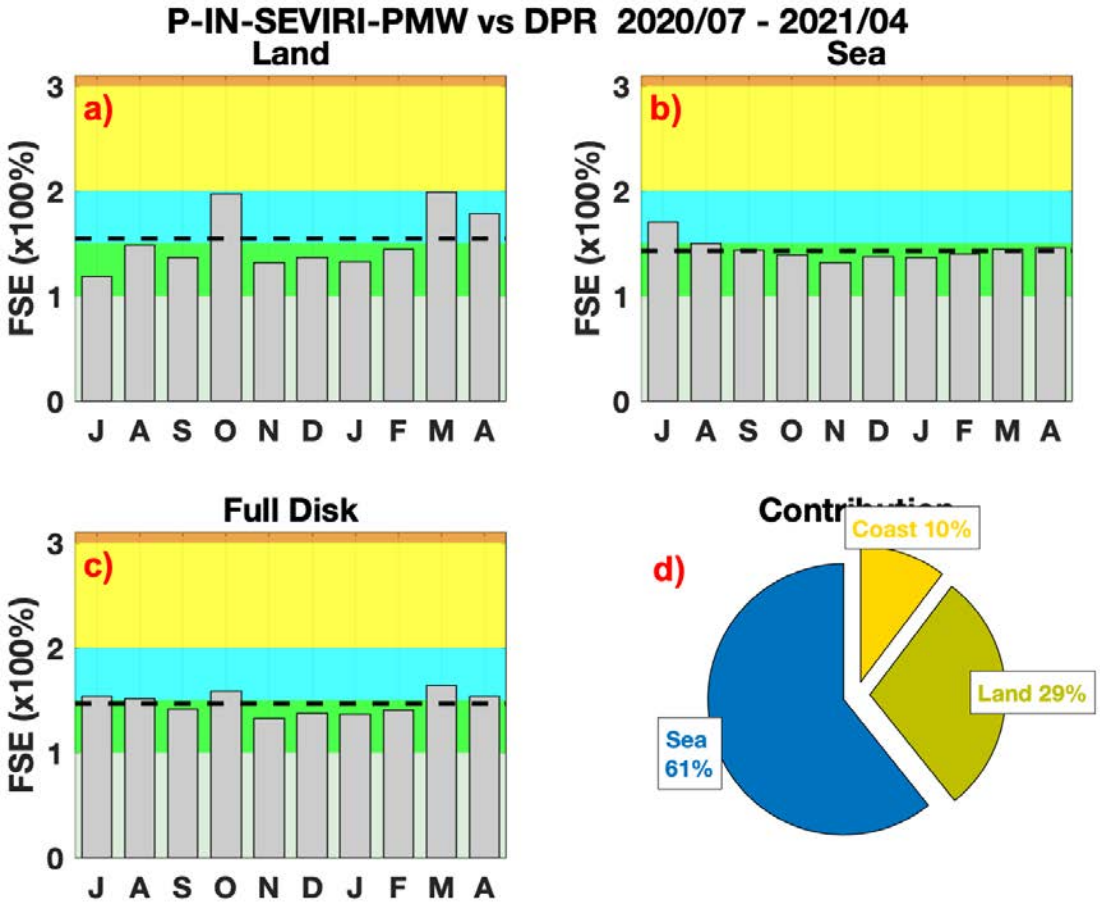

Figure 19: H60B monthly accuracy using DPR-NS as reference over Land (a) and Sea (b) MSG full disk areas. The Overall Q.A. is shown in the panel c). Background colours highlight the requirement accuracy thresholds in terms of FSE as reported in Table 7: Accuracy requirements for product P-IN-SEVIRI-PMW in term of FSE(%). and Table 11.
The horizontal black dotted line indicates the mean annual value.
The single ground percentage contribution is shown in the panel d).
Note: Coast is not shown.

4.3.2 Monthly continuous statistical scores

H60B monthly tendency over land (green line), coast (red line) and sea (blue line) areas for all rain rates above 1 mm/h is shown in Figure 20 for six continuous statistical scores: ME, SD, MAE, MB, RMSE and FSE. Results show a seasonal trend: indeed, over the sea (61% of whole dataset), in cold months the errors are generally lower.
More continuous statistical scores are shown in Appendix.

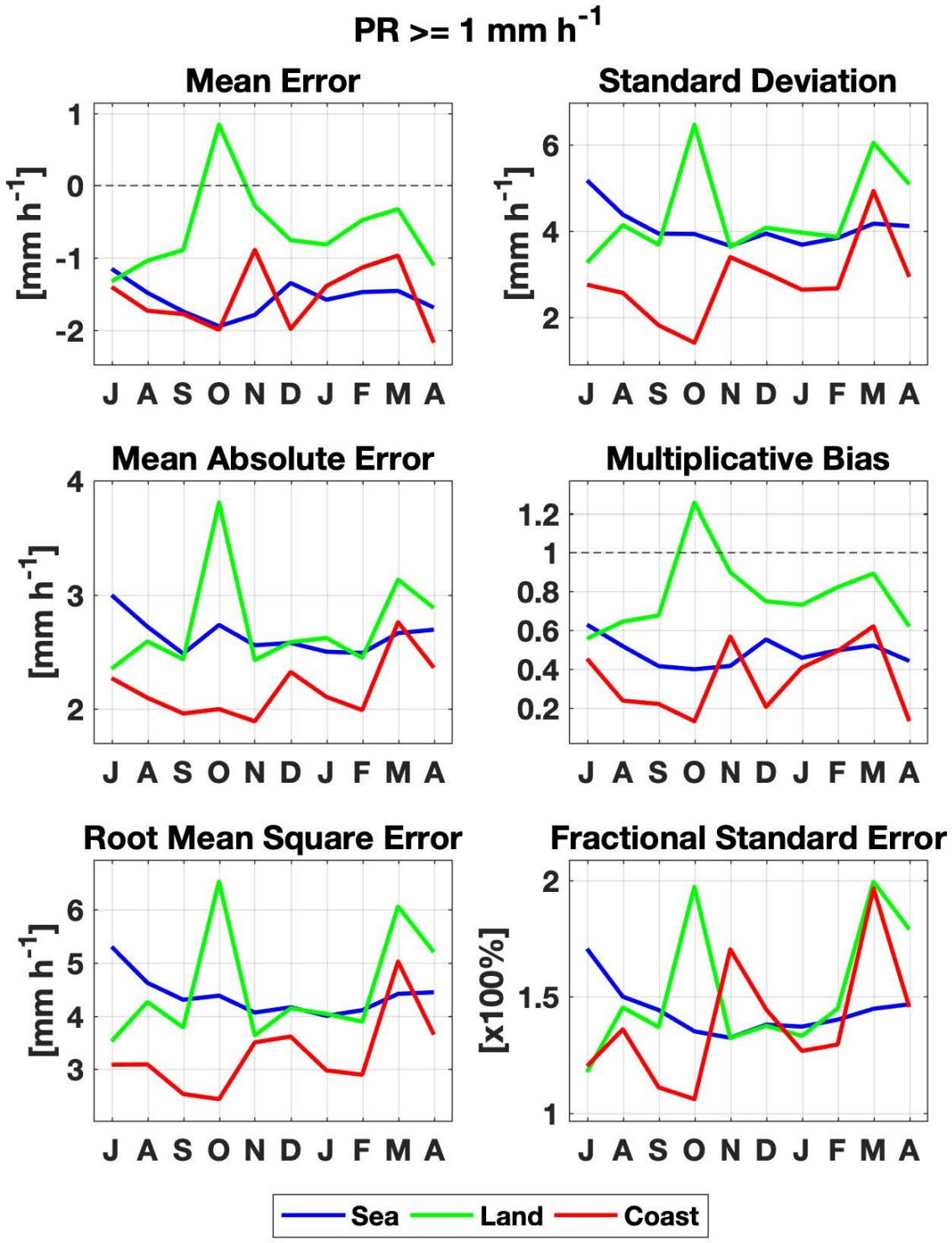

Figure 20: Monthly continuous statistical scores resulting for H60B vs DPR-NS over MSG full disk area relatively to the precipitation regime above 1 mm/h.

4.3.3 Multi-categorical statistics

The multi-categorical statistics are below shown. In each table, the first column indicates the precipitation classes of the H SAF (H60B) product, while along the columns are reported the reference (DPR-NS product) precipitation classes. The first class detects the no-rain class

(0≤PR<0.25 mm/h), the second class detects the light rain (0.25≤PR<1 mm/h), the third class identifies the stratiform rain rates (1≤PR<10 mm/h), while the last one classifies the convective rates (PR≥10 mm/h).
The detection of no-rain areas for H60B in comparison with DPR-NS product reaches in mean the 98% of cases. Light PR are often underestimated (82%). Stratiform rain rates are detected in only 28% of total cases, whereas a high underestimation can be detected (69%). Convective precipitation is not well detected: the mean POD is equal to 20%; it reaches 27% over land, 19% over the sea and only 11% over the coast. More multi-categorical statistics are shown in Appendix.

Land | Sea | Coast - Full Disk												
Multi-Categorical Statistics												
	[0 - 0.25[mm/h			[0.25 - 1[mm/h			[1 - 10[mm/h			≥10 mm/h		
[0 - 0.25[mm/h	97%	98%	98%	72%	83%	88%	43%	55%	70%	15%	19%	51%
[0.25 - 1[mm/h	2%	1%	1%	14%	9%	7%	18%	16%	12%	9%	12%	9%
[1 - 10[mm/h	1%	1%	1%	14%	8%	5%	36%	27%	17%	49%	50%	29%
≥10 mm/h	0%	0%	0%	1%	0%	0%	4%	2%	1%	27%	19%	11%

Table 12: Multi-categorical table for product H60B over land, sea and coast MSG full disk areas. The precipitation classes along the columns (rows) are relative to DPR-NS (H60B) precipitation.

Overall - Full Disk				
Multi-Categorical Statistics				
	[0 - 0.25[mm/h	[0.25 - 1[mm/h	[1 - 10[mm/h	≥10 mm/h
[0 - 0.25[mm/h	98%	82%	53%	20%
[0.25 - 1[mm/h	1%	9%	16%	11%
[1 - 10[mm/h	1%	9%	28%	48%
≥10 mm/h	0%	0%	2%	20%

Table 13: Multi-categorical table for product H60B over the MSG full disk area. The precipitation classes along the columns (rows) are relative to DPR-NS (H60B) precipitation.

4.3.4 Product requirement compliance

The accuracy of H60B over MSG full disk area for the period between July 2020 and April 2021 is reported in Table 14. All FSE score values are very close to the target requirement (150%). The mean annual overall accuracy for H60B over the MSG full disk area reaches the value of 147%.

Between target and optimal	Between threshold and target	Threshold exceeded by < 50 %	Threshold exceeded by ≥ 50 %

H60B vs DPR	Annual average of FSE (%)						
Precipitation Class	**Requirement (FSE %)**			**Land**	**Sea**	**Coast**	**OVERALL**
	thresh	**target**	**optimal**				
≥ 1 mm/h	200	150	100	154	143	154	147

Table 14: Product requirement and compliance analysis for H60B in comparison with DPR-NS product.

4.3.5 Results for different geographical areas

The analysis over different geographical areas is here shown. The full disk area is divided over three regions: European area (36°N-66°N; 30°W-60°E), African area (36°S-36°N;30°W-60°E) and the rest part of the coverage namely "Ocean" (mainly oceans and Brazil). The spatial distribution of the 0.5°x0.5° DPR-H60B coincident grid boxes is shown in Figure 21.

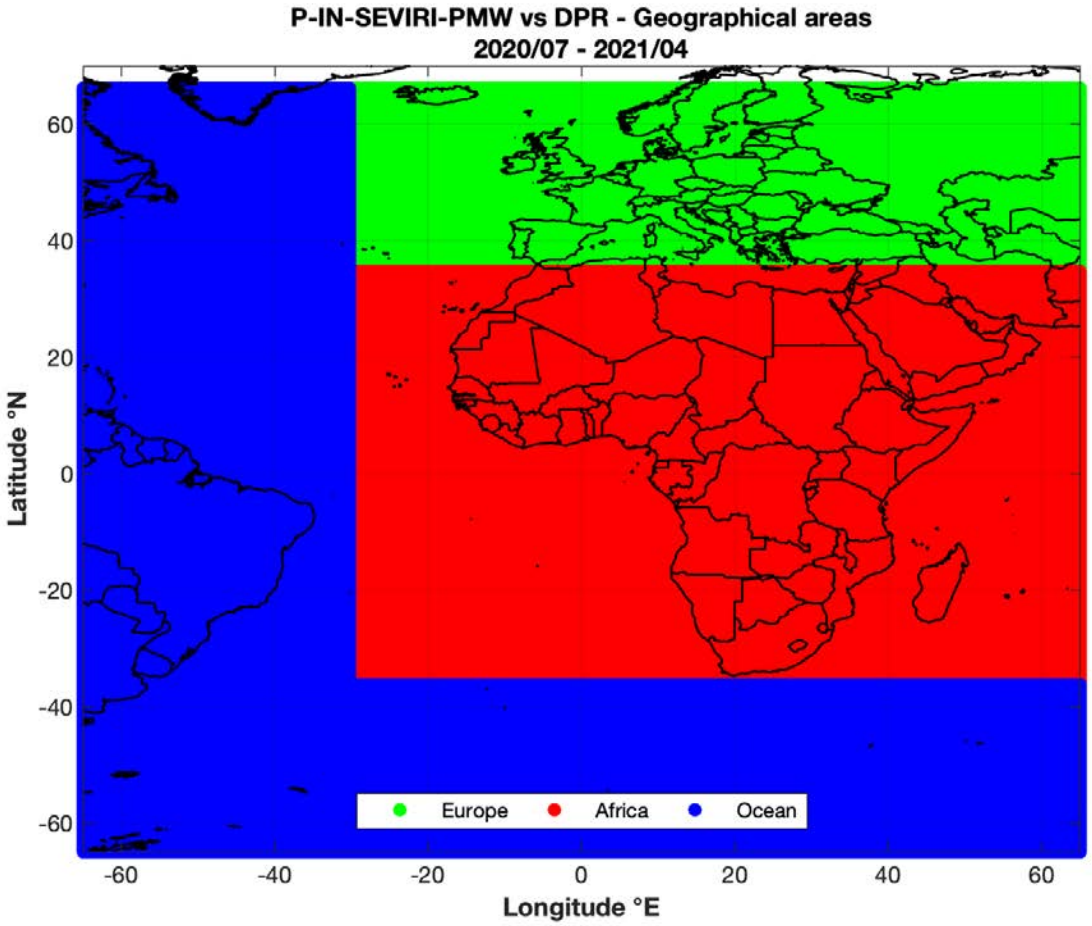

Figure 21: Spatial distribution of 0.5°x0.5° DPR-H60B intersection grid box over three geographical areas.

The tendency of the statistical scores calculated for different areas with respect to the DPR rain rates ranging between 0 and 10 mm/h are shown in Figure 22. In the panel a) the numerosity of 0.5° x 0.5° grid boxes is displayed: the full dataset contains over $2x10^7$ data (for all DPR rainfall rates) and the number of intersections decreases up to one thousand grid boxes for rain rates above 5 mm/h. The ME in panel b) highlights as it is very close to zero for all regions for low precipitation rates, while for higher precipitation rates the ME decreases. In panel c) the CC score trend is shown, for all DPR rain rates the value is between to 0.2 and 0.4 for all considered areas. Over all areas the index tends to decrease as the precipitation threshold increases. The FSE shown in the panel d) highlights as over European area the performance is better respect to all other regions.

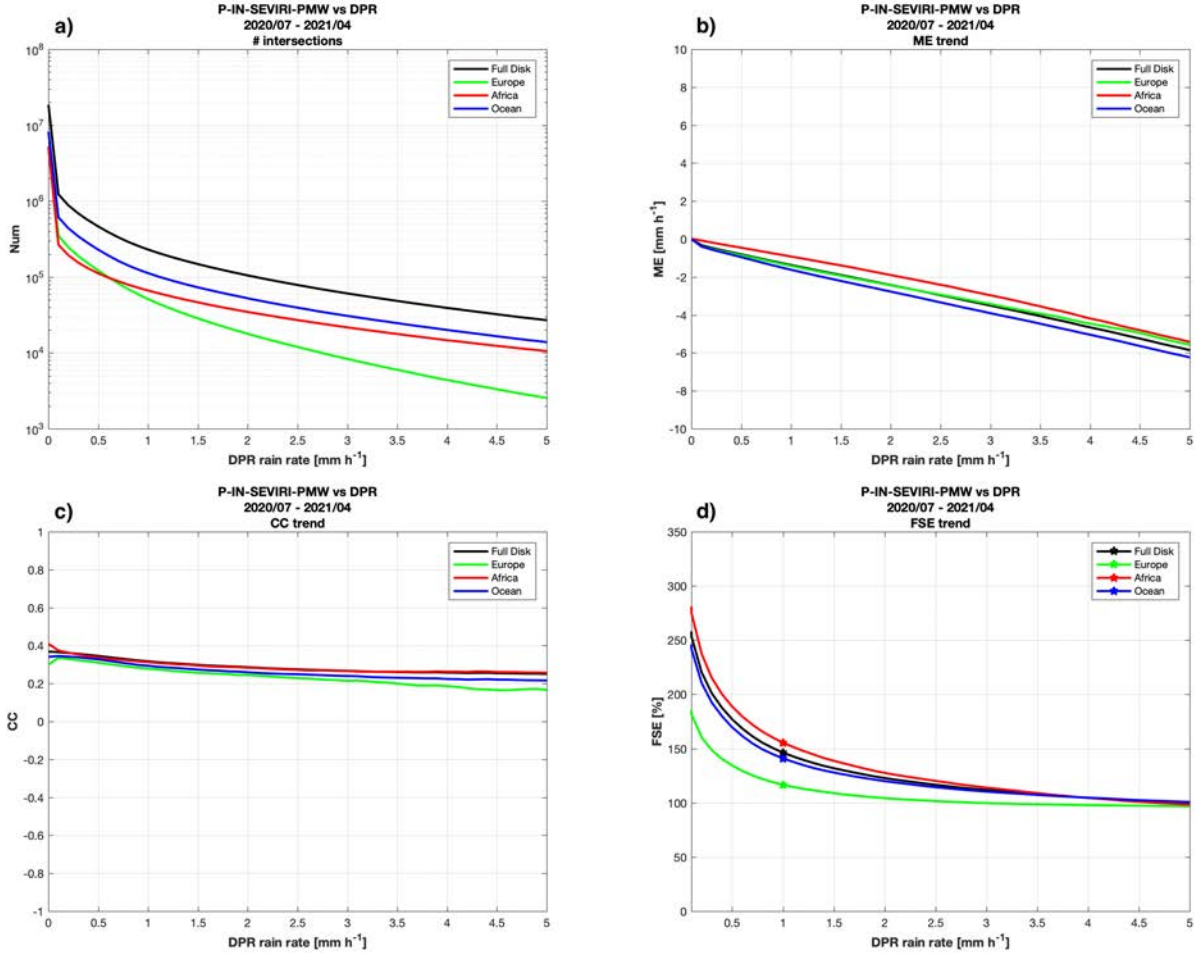

Figure 22: Tendency of some indexes (a) Numerosity of grid boxes, b) ME, c) CC and d) FSE) with respect to the DPR measurements for different geographical areas.

5 Inter-comparison results between H63 and H60B products

The results of the comparison between H60B and H63 in the overlapping area of the two products are shown here. The methodology used to compare the two products is described in Appendix 1, section A1.6 (Inter-comparison procedure between two SEVIRI FD products). The analyzed dataset available for this review is the quarter between February and April 2021. All precipitation values (rr≥0mm/h) whose grid points (between H60B and H63) are close to each other (and not far beyond 6 km) with a quality value - defined by both products themselves - not less than 50% (q> 50%) have been considered for this inter-comparison.

5.1 Large statistics analysis

The continuous statistical scores obtained by analyzing the 3 months of H63 data in comparison with H60B are shown in Table 15.

H63 vs H60B	≥0 mm/h
Num H63 [#]	313,662,875
Num H60B [#]	313,662,858
ME [mm/h]	0.01
STD [mm/h]	0.90
MAE [mm/h]	0.17
MB [-]	1.02
CC [-]	0.86
RMSE [mm/h]	0.90

Table 15: Comparison scores between H63 and H60B

The results are the intersection of over 300 million pixels. The similar number of pixels of H63 and H60B highlights how both products identify the same extension of the precipitation area. The main result is the mean error between the two products (ME) equal to 0.01 mm/h. This indicates an identical way of estimating the intensity of precipitation from one sensor and the other. Even the standard deviation of only 0.90 mm/h highlights the strong reciprocity of the two products. As expected, the correlation between the two products is also very high (0.86). Finally, the RMSE indicates an extremely low error between the two products of less than 1 mm/h (0.90 mm/h). All errors are very low and demonstrate the strong relationship between the two products, regardless of the different longitude position of the two MeteoSats.

The contingency table (Table 16) allows you to evaluate the probability of success of H63 in identifying the estimated precipitation from H60B. The POD is very good (0.81 and 0.78 for the thresholds at 0.25 and 1 mm/h). The FAR is very low and the same (0.25) for both thresholds. Even lower is the fraction of pixels with missed precipitation. The summary index (CSI) indicates good performance (0.63) for the rainfall analyzed.

H63 vs H60B		
≥0.25 mm/h	POD	0.81
	FAR	0.25
	MISS	0.19
	CSI	0.63
≥1 mm/h	POD	0.78
	FAR	0.25
	MISS	0.22
	CSI	0.62

Table 16: Probability Of Detection (POD), False Alarm Ratio (FAR), Missing (MISS) and Critical Success Index (CSI) for H63 vs H60B products for different rain rate thresholds over the overlapping area.

The results of the multi-categorical statistics for H63 in comparison with H60B are shown in Table 17. The first column indicates the precipitation classes of the H63 product, while along the columns are reported the reference (H60B product) precipitation classes. The first class detects the no-rain class (0≤PR<0.25 mm/h), the second class detects the light rain (0.25≤PR<1 mm/h), the third class identifies the stratiform rain rates (1≤PR<10 mm/h), while the last one classifies the convective rates (PR≥10 mm/h).

H63 vs H60B				
Multi-Categorical Statistics				
	[0 - 0.25[mm/h	[0.25 - 1[mm/h	[1 - 10[mm/h	≥10 mm/h
[0 - 0.25[mm/h	97%	35%	9%	1%
[0.25 - 1[mm/h	3%	44%	15%	1%
[1 - 10[mm/h	0%	21%	73%	37%
≥10 mm/h	0%	0%	3%	61%

Table 17: Multi-categorical table for product H63 in comparison with product H60B over the overlapped area. The precipitation classes along the columns (rows) are relative to H60B (H63) precipitation.

The results show that all precipitation classes are in good agreement between the two products. In particular, the non-precipitation area is in agreement in 97% of cases; the agreement between the areas of very low precipitation is 44%; stratiform precipitation is correctly identified in 73%; finally, convective precipitation is identified in 61% of total cases. In all classes, the largest percentage lies in the correct class (even in the most sensitive classes) which indicates the excellent agreement between the two products.

Finally, the density scatterplot between the estimates of H63 and H60B. As shown in the Figure 23, the rainfall population is maximum along the main bisector, up to very intense rainfall (100 mm/h). The most significant scores are also indicated at the bottom right.

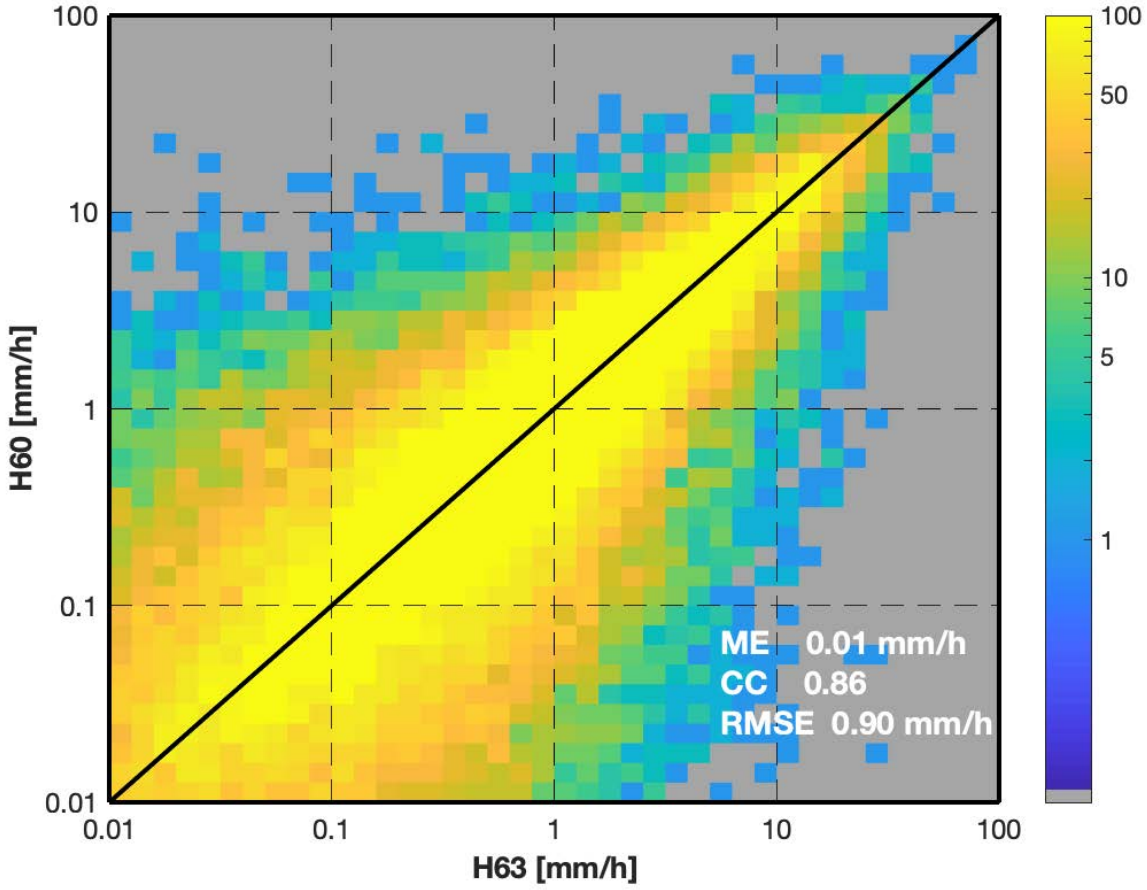

Figure 23: Density-scatterplot between H63 and H60B rainfall estimates. ME, CC and RMSE scores are also indicated.

The evaluation of H63 in comparison with H60B continues with a qualitative analysis of an event that occurred in Hungary using various products available. Hungary is well suited to this type of inter-comparison between the two products as it is positioned along the intermediate longitude of the two Meteosats.

5.2 Case study analysis

5.2.1 Case study: 22 April 2021 in Hungary (OMSZ))

PRODUCT NAME	H63 - Precipitation rate at ground by GEO/IR supported by LEO/MW (SEVIRI @ 41.5° E)
CASE STUDY PERIOD	22 April 2021
CASE STUDY AREA	Hungary
METEOROLOGICAL EVENT	Convective precipitation evolved on a cold front
VALIDATION INSTITUTE	OMSZ – Hungarian Meteorological Service
PRODUCT DEVELOPER INSTITUTE	GEO-K
OPERATIONAL CHAIN INSTITUTE	COMET

METEOROLOGICAL EVENT DESCRIPTION

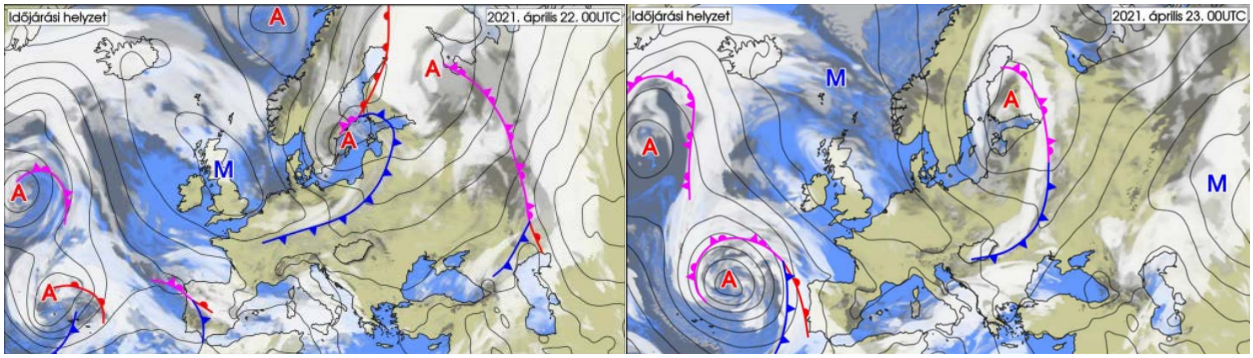

Figure 24: The location of the cold front at 00 UTC on 22nd (left) and 23rd (right) of April 2021

In the dawn of the 22nd of April 2021, a cold front spread from Finland over Poland to Luxembourg. During the day this quick-moving cold front passed over Hungary from northwest to southeast (Figure 24). The frontal cloud and the evolved convective clouds caused showers and thunderstorms in numerous places of the country, in some places even hail occurred. In the night precipitation ended in most parts of Hungary, but in the northeastern counties showers, in mountain Bükk snow shower occurred. The daily sum of precipitation was between trace and 15 mm (Figure 25).

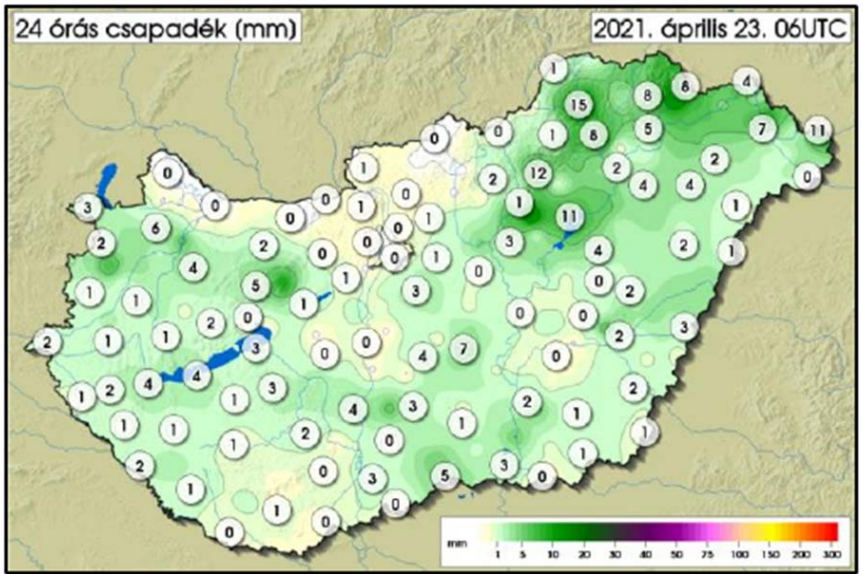

Figure 25: 24h precipitation measured until 06:00 UTC on 23rd April 2021.

DATA/PRODUCTS USED

Product to monitor:

Instantaneous precipitation values from the H63 products (EUMETSAT H SAF) derived from Meteosat-8 IODC service (41.5°E)

Reference data:

Precipitation values from the Hungarian radar network (OMSZ), precipitation from synop data, MSG IR and RGB images, lightning data of the Hungarian LINET network, operational H03B

instantaneous precipitation product (0°), H15A pre-operational instantaneous convective precipitation product (0°), H60B instantaneous precipitation product (0°) under development.

SAF products, radar images, lightning and synop maps were visualised with the **HAWK-3** (Hungarian Advanced Weather WorKStation) software, which is the operational visualisation tool developed by the Hungarian Meteorological Service.

RESULTS OF COMPARISON

During the comparison we first checked the global view of H60B and H63 (Figure 26). We also visualized the quality index maps where we can see the shades where microwave updates happened, also the 2.5x2.5 degree boxes where the histograms were calculated. The rain rate images are smoothed. Negative values can also be seen on quality maps (brown) which corresponds to -1 values on rain rate images (grey).

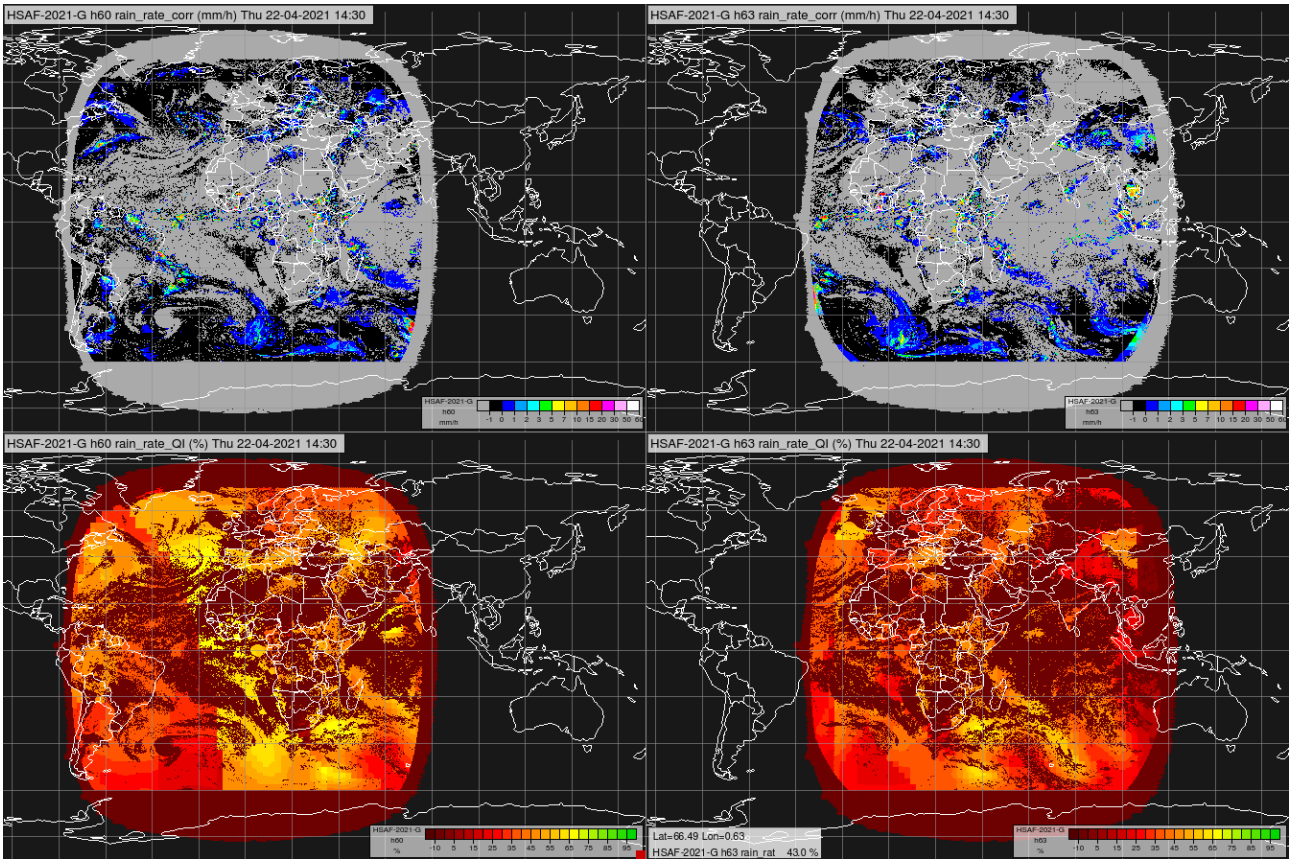

Figure 26: H60B (left)and H63 (right) products, rain rate on the top and quality index at bottom.

The closer view about the European area is shown below, in Figure 27.

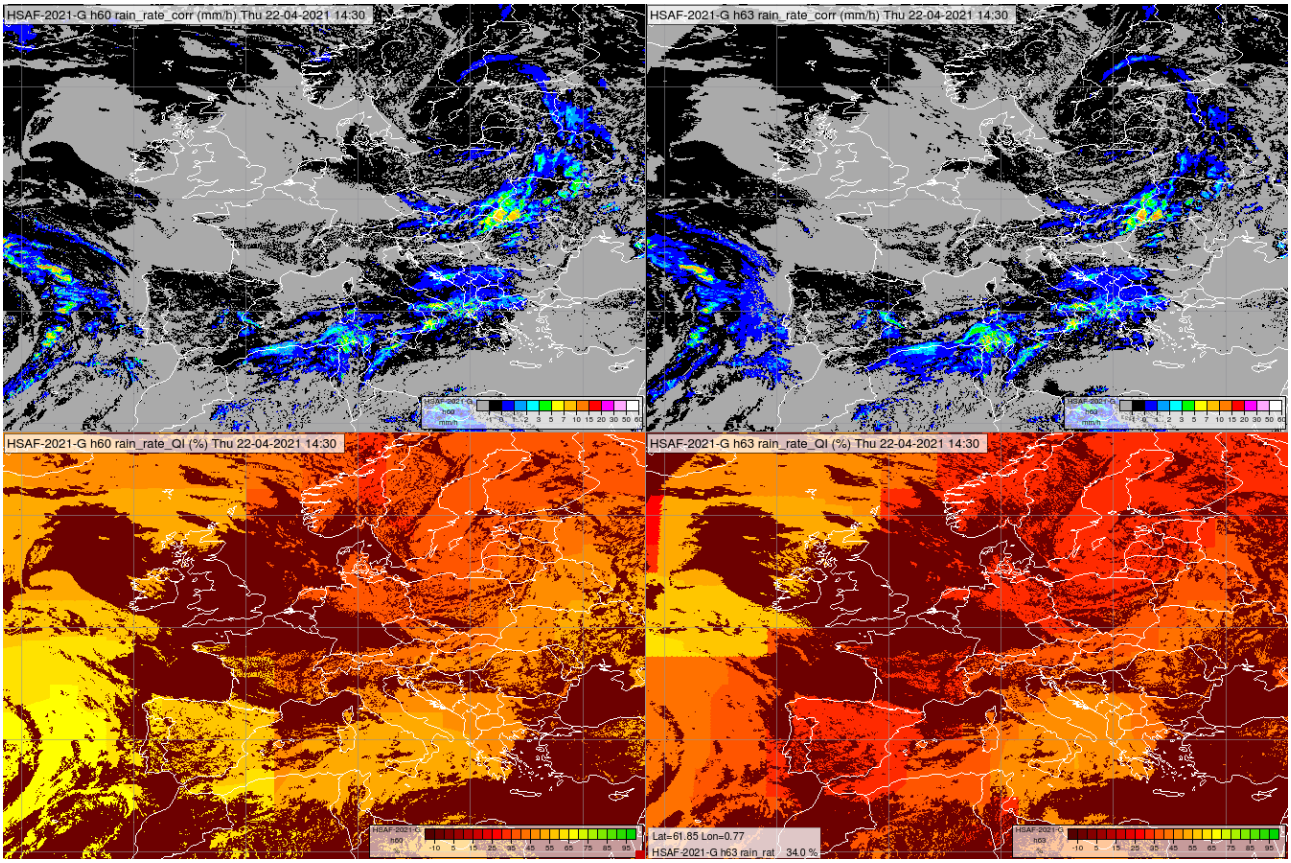

Figure 27: H60B (left)and H63 (right) products, rain rate on the top and quality index at bottom, at 14:30 UTC, 22nd April 2021.

Generally, in the overlapping area H60B (0°) and H63 (41.5° E) instantaneous precipitation products resembles to each other and also to their predecessor, the operational H03B product (0°). But locally we can find bigger differences as well (Figure 28). Because of the different inputs and updates, the differences cannot be judged without ground data. Hungary is in a good location for the comparison as it is situated between 16-23 degree latitude (East).

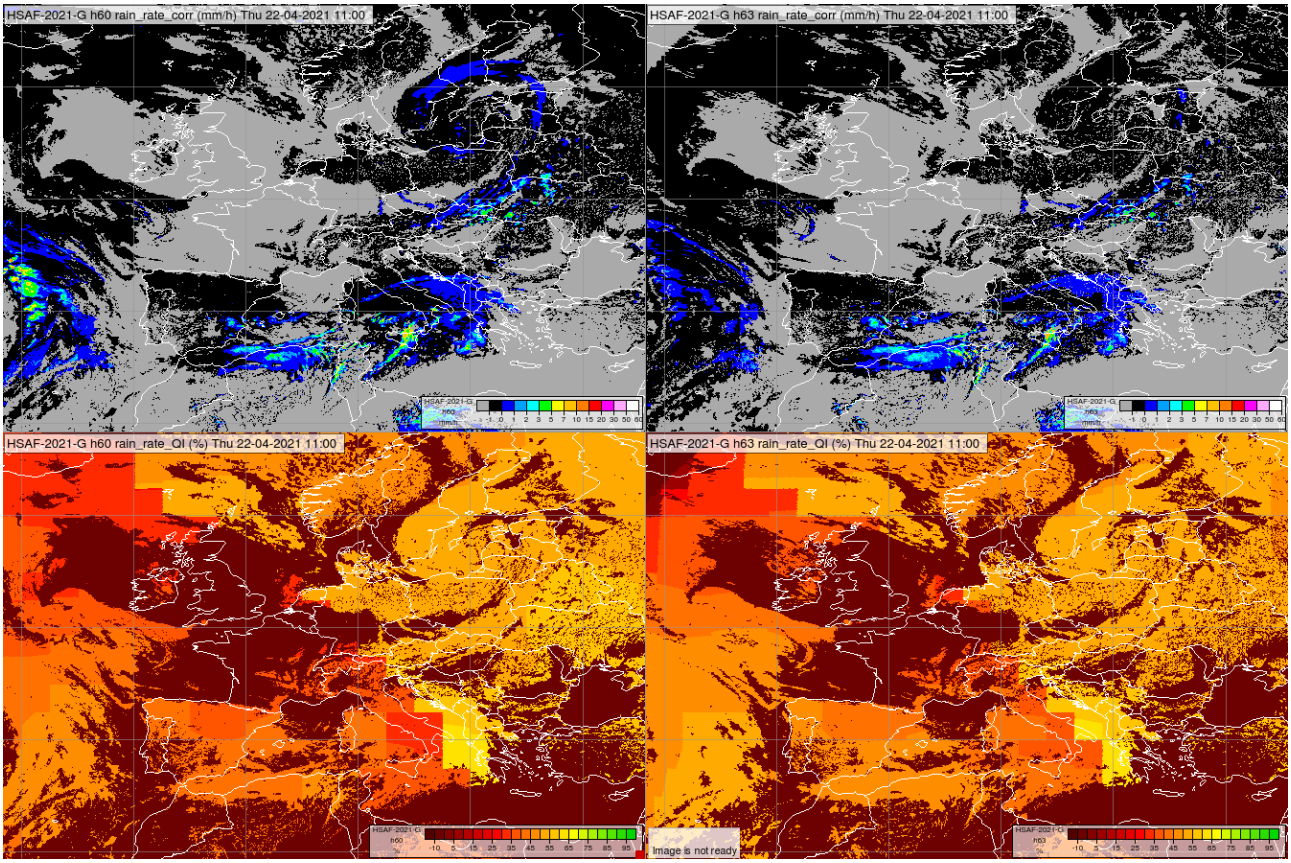

Figure 28: H60B (left)and H63 (right) products, rain rate on the top and quality index at bottom, at 11:00 UTC, 22nd April 2021.

The case was selected because on 22 April a lot of convective cloud was formed on the cold front and we wanted to compare the new product to both the general H03B and the convective H15A products. The H15A products unfortunately contained very little data as the convection was not strong enough (Figure 29).

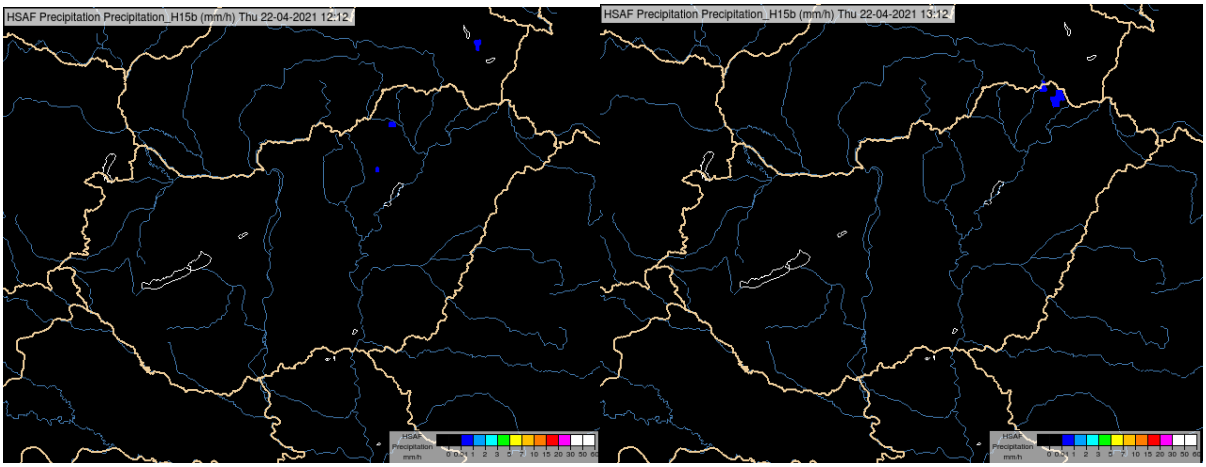

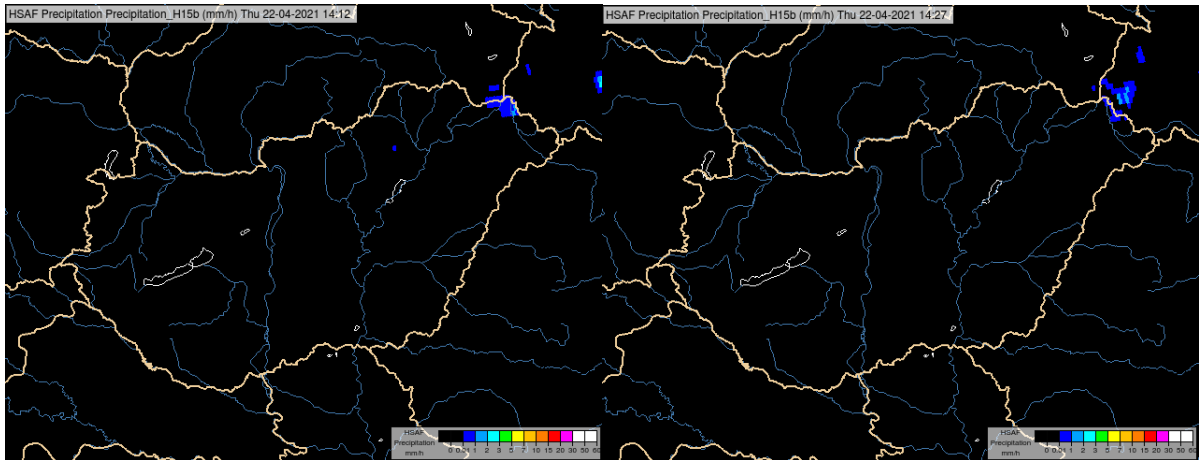

Figure 29: H15A convective precipitation product in 4 time slots from the first nonzero values until the system left Hungary (12:12 UTC top left, 13:12 UTC top right, 14:12 UTC bottom left, 14: 27 UTC bottom right)

During the detailed comparison we used the following fields, as they will appear in the images below:

1	2	3
4	5	6

1. Operational H03B instantaneous precipitation product
2. Instantaneous precipitation values from the H60B product
3. Instantaneous precipitation values from the H63 product
4. Calibrated MSG IR 10.8 µm image
5. Precipitation values from the Hungarian radar network (OMSZ) overlaid by 10 min precipitation from synop data of OMSZ.
6. SEVIRI HRV Cloud RGB image with lightning data of the Hungarian LINET network (OMSZ). Lightning of the last 1 hour is visualised, red colour represents the latest and light pink colour the oldest strokes.

In the images the IR, RGB and ground data have +10min timestamps as it is used in OMSZ, because the timestamp of the original MSG satellite images and thus most of the H SAF MSG products (excluding H15A e.g.) refer to the start of the scanning, but Hungary is scanned about 10 minutes after.

At 9 UTC the first lightning strokes appeared on the lightning map (Figure 30). At the same time the first precipitation patch appeared in H60B image. In the IR image we can see a very cold point there as top of the convective cloud. The radar composite gave precipitation earlier and in an extended area, also higher amount. But compared to H03B which still gave no precipitation, the H60B is better. H63 has the same algorithm as H60B, but this patch is missing from the image.

At 10:30 UTC H60B and H63 resembles more to each other but in H60B there are slightly higher (but max 2mm/h) intensity values, which are closer to the radar values (max above 20mm/h) (Figure 31).

At 11:00 UTC (Figure 32) the precipitating area is maybe a bit bigger in H60B and h63 than in radar image, but the intensity values are still lower in H60B and h63 than in radar. This is

acceptable here as the resolution of the satellite image is less than for the radar image. H63 and H60B are very similar now and both are much better than H03B.

The selected convective cell left Hungary at about 14:30 (Figure 33) reaching its highest precipitation intensity. The values in the radar image reach 60 mm/h. In H60B and H63 the values are between 10-15mm/h, but in a more extended area. H63 has slightly higher values. At this timeslot the H03B has similar extension for the precipitating area, but the values are much lower (less than 3mm/h). Synop stations were avoided by the highest intensity peaks, 8.4 mm/h were the maximum intensity values caught (the 10min values showed in the images should be multiplied by 6 to get mm/h values). In calibrated IR image the lowest cloud top temperature was -58°C, but only at 1 pixel.

For all the selected timeslots we can say that both H60B and H63 gives better estimate of the precipitation than H03B or H15A compared to radar data.

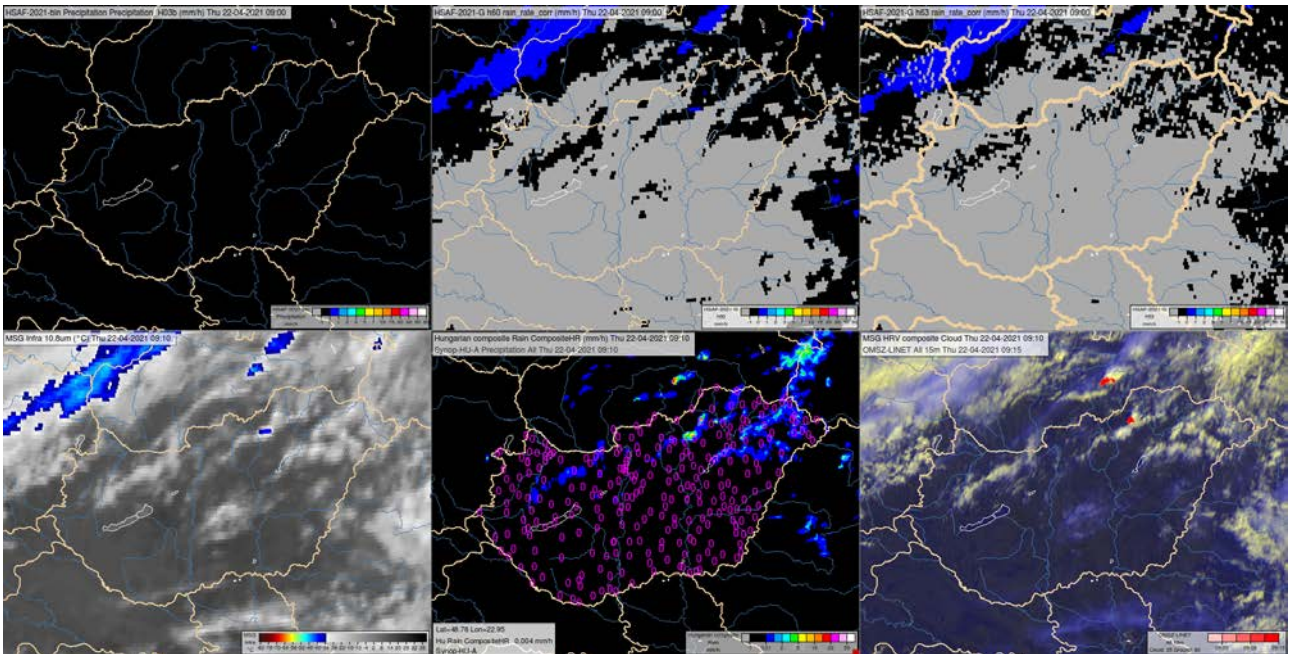

Figure 30: Precipitation fields for 22 April 2021. 09:00 UTC

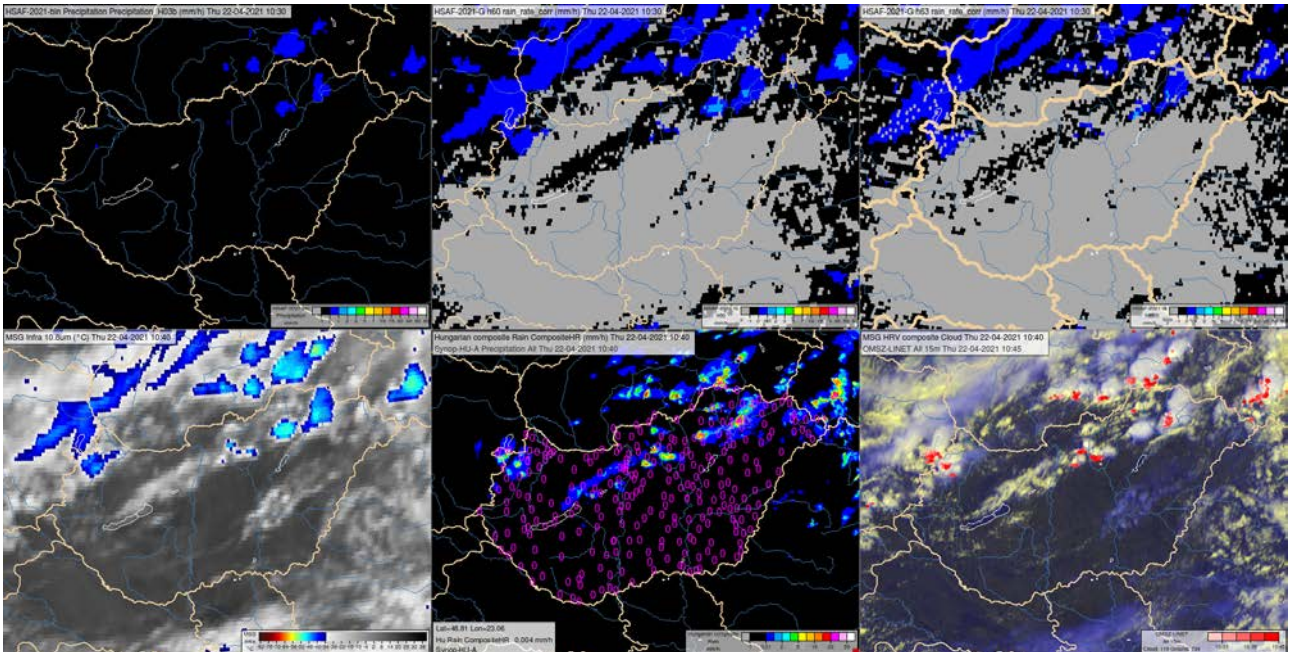

Figure 31: Precipitation fields for 22 April 2021. 10:30 UTC

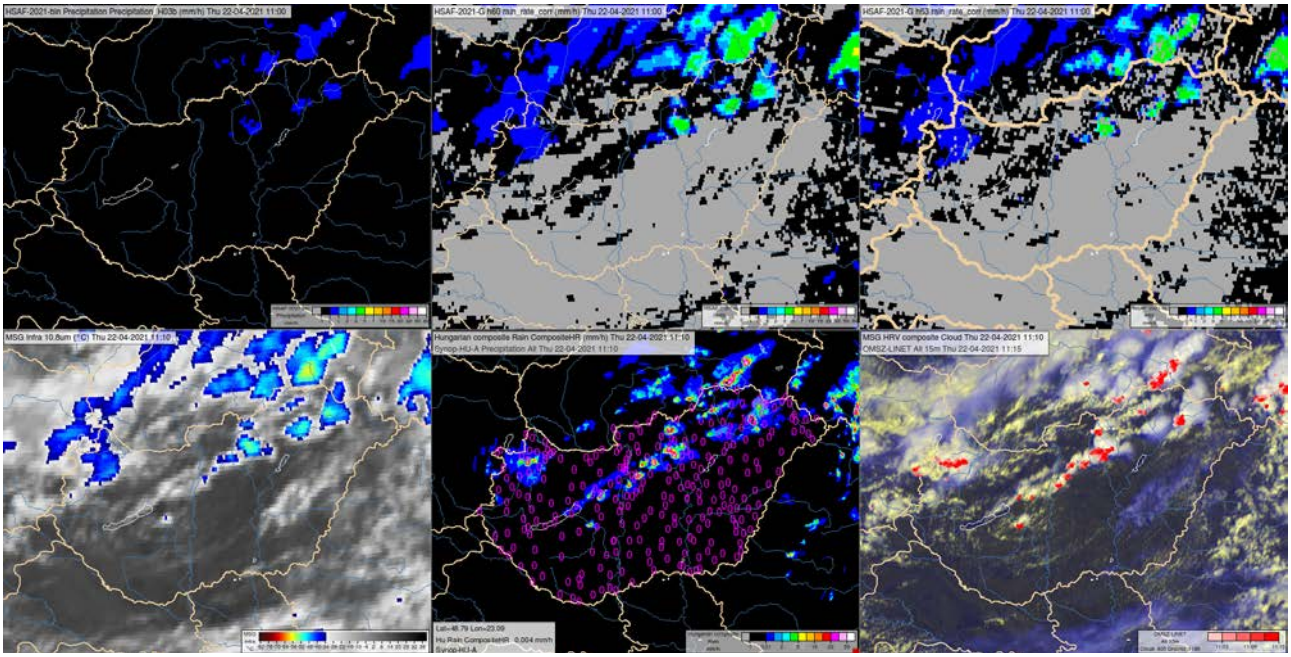

Figure 32: Precipitation fields for 22 April 2021. 11:00 UTC

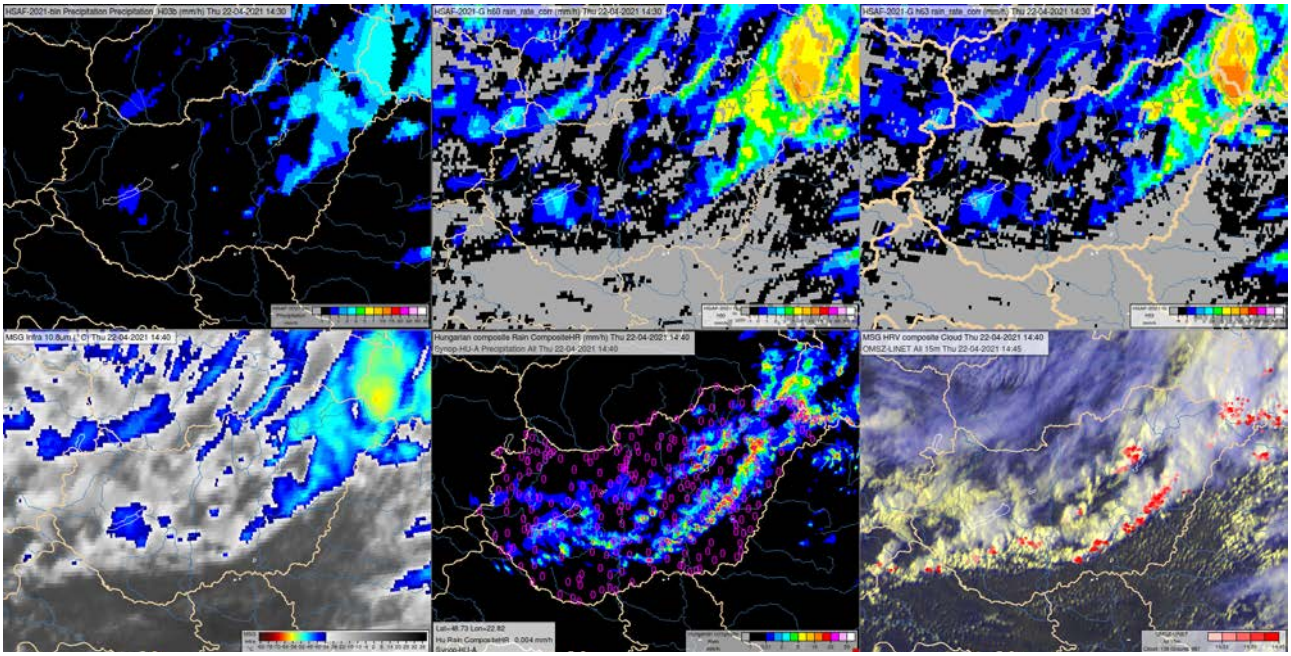

Figure 33: Precipitation fields for 22 April 2021. 14:30 UTC

FINAL COMMENTS

At this case the convective precipitation is better represented in H60B and H63 than in H03B, and much better than in H15A.

H60B and H61B resembles to each other quite well. The differences might come from the different time of the update process when IR inputs are compared to microwave inputs.

6 Conclusions

The H60B (P-IN-SEVIRI-PMW) product has been validated by the PPVG on the period of data July 2020- April 2021. Each Country/Team has provided long statistics analysis and case studies using ground data (radar and rain gauge) as reference following the common validation methodology reported in Appendix 1. A huge effort has been made in the development of the Unique Common Code (UCC) used by all members of the validation cluster to improve it. The use of a UCC guarantees that the results obtained by every partner are obtained in the same way.

In addition, a validation outside the European area was performed. The Quality Assessment of H60B product was evaluated over the full MSG disk coverage area in comparison with the DPR Normal Scan precipitation product estimated by DPR instrument onboard of GPM Core Observatory satellite. As for the UCC, the development of the validation procedure over full disk area has involved the entire Validation Cluster. Results of comparison with DPR-NS product was obtained by Italian DPC and reported in this document.

It is well known that radar and rain gauge rainfall estimation is influenced by several error sources that should be carefully handled and characterized before using these data as reference for ground validation of any satellite-based precipitation products. Each Country/Team has independently evaluated the quality of its radar data to optimize the satellite data validation.

Much effort has been made to define a standard radar quality data. Rain gauge quality data has been standardized to all members by use of the same interpolation method (GRISO).

Different case study analysis of H60B have been here reported in section 3. Case studies, analysed in different geographical regions, highlight the common behavior to underestimated precipitation intensity.

In section 4 the validation results of the H60B long statistics analysis obtained for the entire period have been presented. To assess the degree of compliance of the product with product requirements, each Country/Team has provided the monthly statistical scores. The results have been showed using both European ground (radar and rain gauge) data and DPR-NS estimates as benchmark over land, sea and coast areas.

The results of the Precipitation Validation Programme are reported in this Product Validation Report (PVR). H60B reaches the target accuracy requirement in both validation procedures. Better performances are observed in comparison with DPR estimates respect to the European ground measurements. The analysis for different geographical areas highlights as better performance is reached over European region, mainly in terms of FSE score. Contingency tables show as the precipitation areas are observed in all events. About the precipitation classes: the light intensities are well estimated, while the intermediate and heavy rainfall estimates are not always accurate and are often underestimated representing the main weakness of this product.

The inter-comparison in the overlapping area between H60B and H63 both based on SEVIRI sensors highlighted the strong relationship between the two products. The nearly zero bias (0.01 mm/h), the high correlation (0.86) and the excellent detection of areas with the same intensity of precipitation confirm the equality of the two products based on SEVIRI sensors, independent of their different position in longitude (0° vs 41.5°E).

END MAIN DOCUMENT

Appendix 1 Validation strategy, methods and tools

The quality assessment procedure, methodologies and instruments used to assess the performances of precipitation products are described in this chapter.

A1.1 Validation team and work plan

To evaluate the satellite precipitation product accuracy, a Validation Group has been established by the beginning of the Validation Phase in the H SAF project. The Precipitation Product Validation team is composed of experts from the National Meteorological and Hydrological Institutes of Belgium, Bulgaria, Germany, Hungary, Italy, Poland, Slovakia, and Turkey (Table 18). Hydrologists, meteorologists, and precipitation ground data experts, coming from these countries are involved in the product validation activities (Table 19).

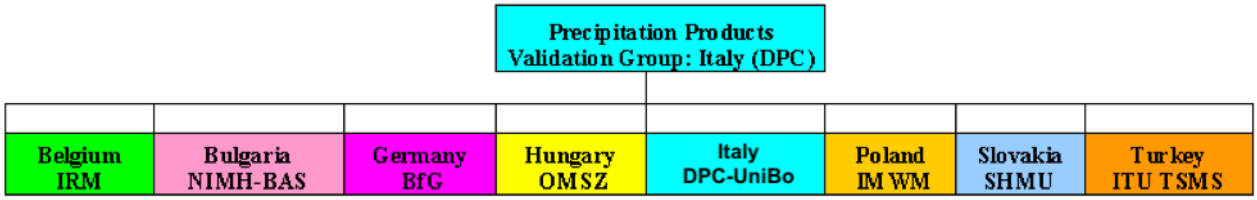

Table 18: Structure of the Precipitation products validation team.

Validation team for precipitation products			
Name	**Institute**	**Country**	**e-mail**
Silvia Puca (Leader)	Civil Protection Department (DPC)	Italy	silvia.puca@protezionecivile.it
Marco Petracca	Civil Protection Department (DPC) National Research Council (CNR - ISAC)	Italy	M.Petracca@isac.cnr.it
Alexander Toniazzo	Civil Protection Department (DPC)	Italy	alexander.toniazzo@protezionecivile.it
Alessandra Mascitelli	Civil Protection Department (DPC)	Italy	alessandra.mascitelli@protezionecivile.it
Gianfranco Vulpiani	Civil Protection Department (DPC)	Italy	gianfranco.vulpiani@protezionecivile.it
Emanuela Campione	Civil Protection Department (DPC)	Italy	emanuela.campione@protezionecivile.it
Pierre Baguis	Royal Meteorological Institute of Belgium (RMI)	Belgium	Pierre.Baguis@meteo.be
Emmanuel Roulin	Royal Meteorological Institute of Belgium (RMI)	Belgium	Emmanuel.Roulin@meteo.be
Eram Artinyan	National Institute of Meteorology and Hydrology (NIMH)	Bulgaria	eram.artinian@meteo.bg
Petko Tsarev	National Institute of Meteorology and Hydrology (NIMH)	Bulgaria	petko.tsarev@meteo.bg
Georgy Koshinchanov	National Institute of Meteorology and Hydrology (NIMH)	Bulgaria	georgy.koshinchanov@meteo.bg
Claudia Rachimow	Bundesanstalt für Gewässerkunde (BfG)	Germany	rachimow@bafg.de
Peter Krahe	Bundesanstalt für Gewässerkunde (BfG)	Germany	krahe@bafg.de
Márta Diószeghy	Hungarian Meteorological Service (OMSZ)	Hungary	dioszeghy.m@met.hu
Ildikó Szenyán	Hungarian Meteorological Service (OMSZ)	Hungary	szenyan.i@met.hu

Dóra Cséke	Hungarian Meteorological Service (OMSZ)	Hungary	cseke.d@met.hu
Federico Porcu'	Department of Physics and Astronomy, University of Bologna (UniBo)	Italy	federico.porcu@unibo.it
Bozena Lapeta	Institute of Meteorology and Water Management (IMWM)	Poland	Bozena.Lapeta@imgw.pl
Rafal Iwanski	Institute of Meteorology and Water Management (IMWM)	Poland	Rafal.Iwanski@imgw.pl
Ján Kaňák	Slovenský Hydrometeorologický Ústav (SHMÚ)	Slovakia	jan.kanak@shmu.sk
Ľuboslav Okon	Slovenský Hydrometeorologický Ústav (SHMÚ)	Slovakia	luboslav.okon@shmu.sk
Mariàn Jurasek	Slovenský Hydrometeorologický Ústav (SHMÚ)	Slovakia	marian.jurasek@shmu.sk
Ladislav Méri	Slovenský Hydrometeorologický Ústav (SHMÚ)	Slovakia	ladislav.meri@shmu.sk
Ahmet Öztopal	Istanbul Technical University (ITU)	Turkey	oztopal@itu.edu.tr

Table 19: List of the people involved in the validation of H SAF precipitation products (PPVG)

The Precipitation products validation programme started with a first workshop in Rome, 20-21 June 2006, soon after the H SAF Requirements Review (26-27 April 2006). The first activity was to lay down the Validation plan, that was finalised as first draft early as 30 September 2006. After the first Workshop, other ones followed, at least one per year to exchange experiences, problem solutions and to discuss possible improvement of the validation methodologies. Often the Precipitation Product Validation workshop are joined with the Hydrological validation group.

The results of the Product Validation Programme are reported in this Product Validation Report (PVR) and are published in the validation section of the H SAF web page. A new structure and visualization of the validation section of H SAF web page is in progress to consider the user needs. This validation web section is continuously updated with the last validation results and studies coming from the Precipitation Product Validation Group (PPVG).

A1.2 Validation objects and issues

The products validation activity has to serve multiple purposes:

- to provide input to the product developers for improving calibration for better quality of baseline products, and for guidance in the development of more advanced products;
- to characterise the product error structure in order to enable the Hydrological validation programme to appropriately use the data;
- to provide information on product error to accompany the product distribution in an open environment, after the initial phase of distribution limited to the so-called “beta users”.

Validation is a challenging task in the case of precipitation, both because the sensing principle from space is very much indirect, and because of the natural space-time variability of the precipitation field (sharing certain aspects with fractal fields), that poses severe sampling problems.

It is known that an absolute ‘ground reference’ does not exist. In the H SAF project the validation is based on comparisons of satellite products with **European ground data**: radar, rain gauge and radar integrated with rain gauge. During the Development phase some main problems have been pointed out. First of all, the importance to characterize the error associated to the ground data used

by PPVG. Secondly to develop software for all steps of the Validation Procedure, a software available to all the members of the PPVG. The radar and rain gauge Working Group (WG) have been composed to solve these problems.

In CDOP-3, with the release of more than 30 products **over the MSG full disk area,** the Validation Cluster had to develop new methodologies to compare precipitation estimates on almost global area coverage. The Associated Scientist analysis (H_AS16_03 DPC/CNR-ISAC 2016) has been identified the DPR (Dual-frequency Precipitation Radar) onboard of GPM-CO (Global Precipitation Measurement – Core Observatory) satellite as worthy instrument reference for the estimation of instantaneous precipitation on a global scale. In particular, the 2A-DPR NS V05 (**DPR**) was considered as most suitable product for potential use within the H SAF Precipitation Product Validation activity **for instantaneous precipitation estimates.** For more details, refer to Sebastianelli, 2017.

For accumulated precipitation products, instead, the Triple Collocation (**TC)** methodology (Brocca et al., 2014) was used to perform the validation activity. TC requires the simultaneous availability of three products with mutually uncorrelated errors with similar spatial coverage, resolution and accumulation time.

In the following three sections, the validation methodologies and data used as reference to perform the comparisons are described.

A1.3 Validation methodology respect to GROUND reference data

From the beginning of the project it was clear the importance to define a common validation procedure in order to make the results obtained by several institutes comparable and to better understand their meanings. The main steps of this methodology have been identified during the development phase inside the validation group, in collaboration with the product developers, and with the support of ground data experts. This common procedure has given rise to a single common code for all members of the PPVG, named Unique Common Code (UCC). This common validation methodology is based on ground data (radar and rain gauge) comparisons to produce **large statistic** (multi-categorical and continuous), and **case study analysis.** Both components (large statistic and case study analysis) are considered complementary in assessing the accuracy of the implemented algorithms. Large statistics helps in identifying existence of pathological behaviour, selected case studies are useful in identifying the roots of such behaviour, when present.
The main steps of the validation procedure are:

- ground data error analysis: radar and rain gauge;
- point measurements (rain gauge) spatial interpolation;
- up-scaling of radar data versus satellite grid (radar data gridded on satellite grid);
- temporal comparison of precipitation products (satellite and ground);
- statistical scores (continuous and multi-categorical) evaluation;
- case study analysis.

Ground data and tools used for validation

Both rain gauge and radar data have been used for H SAF product validation. Working groups have been set up to solve specific items in the validation procedure and to develop a common software. A complete knowledge of the ground-based data characteristics, used within the PPVG, was the first step necessary to define the procedure to select the most reliable data (ground reference) and to understand the validation results.

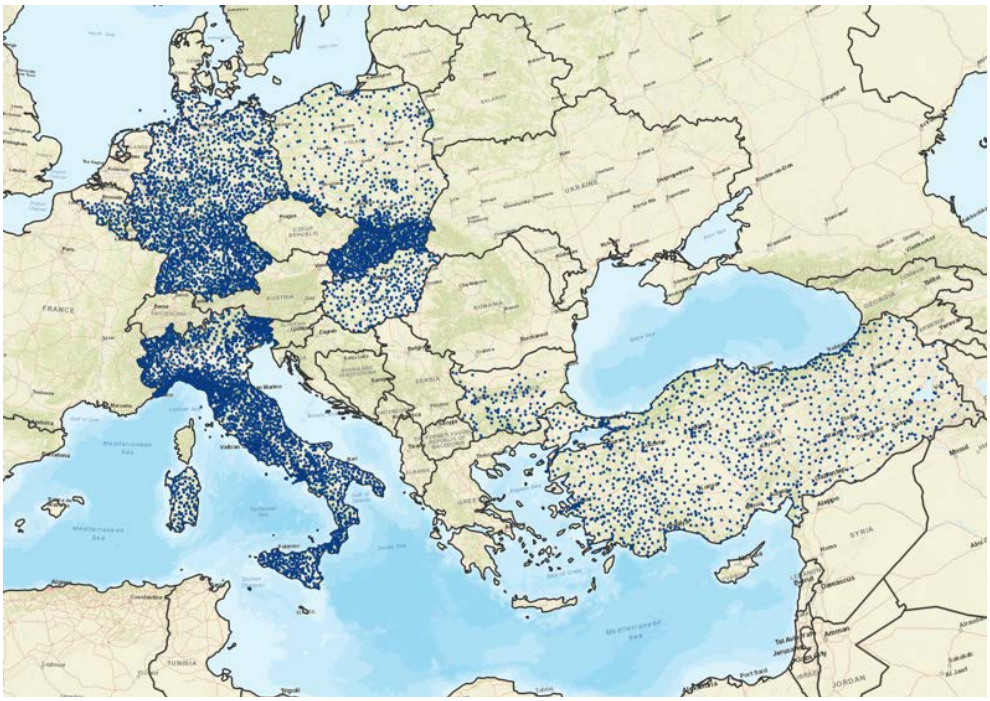

Figure 34: The network of 8,404 rain gauges used for H SAF precipitation products validation

The rain gauge networks of PPVG is composed of approximately 8400 stations across 8 Countries (Figure 34). A key characteristic of such networks is the distance between each raingauge and the closest one, averaged over all the instruments considered in the network and it is a measure of the raingauge density. Instruments number and density are summarized in the following Table 3.

Country	Total number of gauges *	Average minimum distance (km)
Belgium	92	15.2
Bulgaria	123	25.2
Germany	2,299	12.9
Hungary	270	17.0
Italy	2,934	11.3
Poland	540	24.0
Slovakia	911	13.6
Turkey	1,235	26.5

*** the number of raingauges could vary from day to day due to operational efficiency within a maximum range of 10-15%.**

Table 20: Number and density of raingauges within H SAF validation Group

Most of the gauges used in the National networks by the PPVG Partners are of the tipping bucket type, and hourly cumulated.

74 C-band radars (Figure 35**)** are used by the H SAF PPVG for assessing the satellite product accuracy. An inventory on radar data networks and products used in PPVG has pointed out that all the institutes involved in the PPVG declared the system are kept in a relatively good status and all of them apply some correction factors in their processing chain of radar data. Only the radar data, which passes the quality control of the owner Institute, are used by the PPVG for validation activities. Please note that the Validation procedure is the same for all countries of PPVG.

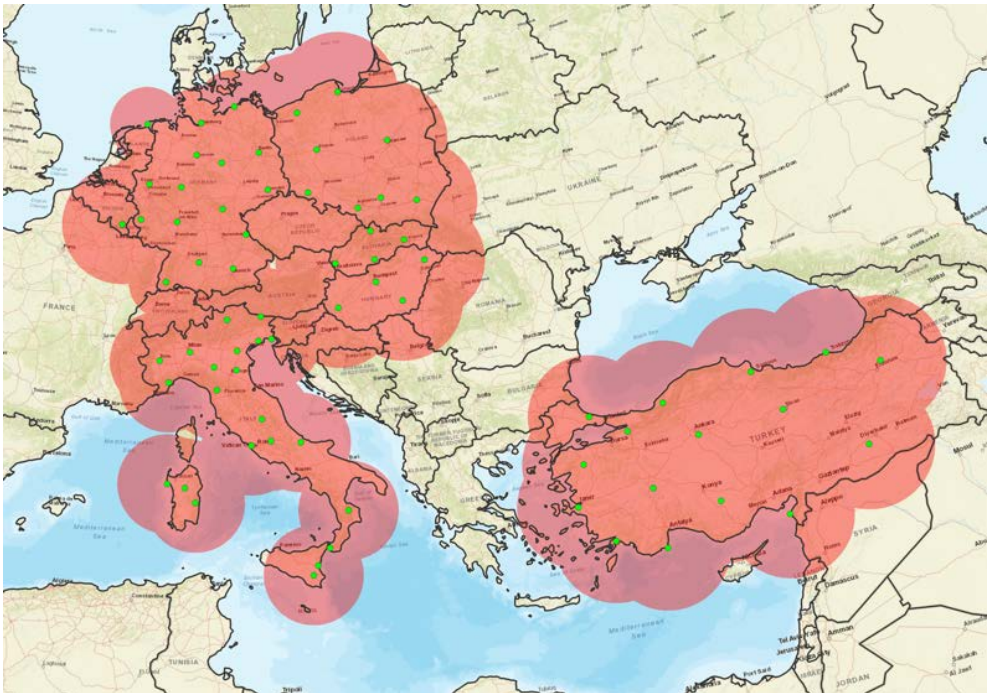

Figure 35: The networks of 74 C-band radars used by the H SAF PPVG.
Note1: Turkish radars are not used in validation activities. Note2: Only one out of four belgian radars is shown.

Instruments number and average minimum distance in each country are summarized in Table 21.

Country	Total number of radar	Average minimum distance (km)
Belgium	4	120
Bulgaria	-	-
Germany	16	163
Hungary	4	190
Italy	22	141
Poland	8	186
Slovakia	4	137
Turkey	16*	253

Table 21: Number and density of radars used by the H SAF PPVG.
*** Not used in validation activities.**

Common procedure for the validation

The UCC developed by PPVG during CDOP-2 and improved in CDOP-3 has been used to validate satellite data respect to radar and rain gauge data considered as ground reference.

Common procedure for the validation with RADAR data

Selection of satellite pixels falling into the region of interest

In order to avoid time-consuming useless calculation, every country restricts the validation to a specific Area of Interest (normally the area covered by the RADAR data of the country), which is detected implicitly by the common validation algorithm.

Taking into account quality index information

The UCC considers the quality index for each radar pixel. It depends mainly by distance from radar site and by interferences or beam-blocking. Each country independently calculates the quality of its data. This quality information is used for validation purposes since CDOP2.

Selection of the RADAR data time-synchronous with the satellite ones

The RADAR data whose temporal characteristics are congruent with the data of the satellite product to be compared (instantaneous or mean value or daily cumulated) are selected. For instantaneous acquisitions, the maximum time difference allowed for satellite comparison is 10 minutes.

Up-scaling of RADAR data at the product satellite resolution

Radar data, whose spatial resolution (0.25 ÷ 1 km) is typically greater than satellite products (5 ÷ 25 km), is rescaled to the satellite product grid (we refer it as "radar upscaled"). The information on the radar data density for each grid point is kept in order to eliminate those grid points that are not representative of the radar data (whose spatial coverage is limited or less than 50%).

Calculation of corresponding satellite and RADAR rainfall values

For each single satellite file, a separate up-scaling procedure reads the look up table and assigns to each satellite pixel the RADAR rainfall average calculated from the values of the radar pixels belonging to the satellite pixel in the look-up table.

Averaging is simply arithmetical as investigations so far have shown that the averaging method does not have an impact on the statistical scores.

The flag indicating if the satellite pixel is coast, land or sea is matched to each satellite-radar data pair calculated in this step.

Common procedure for the validation with RAIN GAUGE data

Selection of satellite pixels falling into the region of interest:

In order to avoid time-consuming useless calculation, every country restricts the validation to a specific Area of Interest (normally the area covered by the rain gauge data of the country), which is detected implicitly by the common validation algorithm.

Selection of rain gauge data synchronous with the satellite ones

Gauges with different cumulation intervals are considered, and if the interval is longer than the time resolution of the product (15 or 30 minutes), more satellite images are averaged. For H68 product two consecutive images (2 x 30' every image) are summed for comparing with one-hourly accumulated gauges.

Interpolation of the rain gauge data:
All partners of the Validation Group have been used the same interpolation technique, named GRISO (a like-Kriging interpolation technique for rain gauge data, Pignone et al. 2010; Feidas et al. 2018), to get spatially continuous rainfall maps (over 5x5 km grid) from individual gauge measurements.

The GRISO technique is the interpolation method chosen for the common validation.

Taking into account quality index information
GRISO technique produces a quality index map for each instantaneous acquisition as function of distance from each rain gauge station. This quality information was used for validation purposes in CDOP2.

Matching between satellite and rain gauge data:
The satellite data is matched with the rain gauge interpolated grid using the nearest-neighbor method.

A1.4 Validation methodology of INstantaneous precipitation products over Full Disk coverage

As the validation with respect to ground data, even this methodology was developed in communion with European experts belonging to the VC. But, differently from the first one, this is not performed by all countries but only by Italian DPC because all DPR products over global area are freely available from GPM website. All instantaneous satellite precipitation products, with extension area over FD area, are evaluated following these main steps:

- regridding of DPR and H SAF data versus a regular 0.5° equi-distance grid;
- temporal and spatial matching between precipitation products;
- statistical scores (continuous and multi-categorical) evaluation;

The methodology, as the previous one, produces **large statistic** (multi-categorical and continuous) scores.

DPR products used for validation

The spatial coverage of both rain gauge and ground radar networks is not suitable to detect precipitation on a global scale. At the contrary, satellite observations provide estimates on a synoptic scale, although there are some issues related to their accuracy. It was discussed in the Visiting Associated analysis in comparison with ground radar network (Sebastianelli, 2017). The DPR is a Dual frequency Precipitation Radar located on board of the GPM Core Observatory (Figure 36). It uses the Ka (~35 GHz) and Ku bands (~13 GHz) to construct three-dimensional precipitation and drop size distribution maps. The GPM Core Observatory (Figure 36) flies in a non-sun-synchronous orbit at 65° inclination to cover a larger latitudinal extension with respect to the TRMM orbit, which extended from 35°S to 35°N. Both Ku- and Ka-band radars perform cross-track type scans (perpendicular to the direction of the satellite motion) estimating the precipitation during the day and the night over land and ocean. The Ku-band radar performs a normal scan (NS) acquisition mode that is composed by 49 footprints (IFOV) of 5 km in diameter. In fact, away from the scanning center, footprints tend to widen and overlap (edge effects) because of a geometric

distortion. The term swath indicates the width of each scan of 245 km. The range resolution is 250 m. The Ka-band radar can perform a matched scan (MS) or a high sensitivity scan (HS) acquisition mode. The MS footprints match the central 25 footprints of the Ku-band and the range resolution is 250 m. Therefore, MS scan is composed of 25 footprints of 5 km in diameter and the swath is 125 km. When Ka-band radar operates in HS mode footprints are interlaced with the matched beams, the range resolution is 500 m and there are 24 footprints along a swath. Figure shows the different DPR scanning modes with respect the flight direction.

It must to be noted that the range resolution is different from the spatial resolution. In fact, the sampling is carried out for 19 km above the sea level and then along the vertical there are many footprints of 250 m height (range resolution). In addition, footprint size decreases as the sampling height increases due to the antenna aperture. The sampling distance between the centers of two adjacent footprints is 5.2 km, and it is constant throughout the scan to the edges. Apart the other problems which affects the DPR estimates, the main issues deal with the attenuation and the ground clutter. The K-band radar estimates are affected by attenuation when they sample through very intense precipitations (convective cells). Ground clutter is a non-meteorological echo which causes an overestimate of precipitations.

DPR products (level 2A) referred to single frequency radar are 2A-Ku, 2A-Ka-MS and 2A-Ka-HS, as showed in Figure 37. Three different DPR products combining Ka and Ku bands precipitation rate estimates (prEs) also exist depending on the IFOV to which data are referred. The IFOV can be related to the NS Ku-band, or to the MS or HS Ka-band, and the corresponding DPR products for prEs are 2A-DPR-NS, 2A-DPR-MS and 2A-DPR-HS, respectively. Results of Visiting Associated activity (Sebastianelli, 2017) highlight as 2A-DPR-NS product performs better with respect to ground-based radar estimates. For this reason, the prEs by 2A-DPR-NS product (hereafter also referred as DPR-NS) was used as precipitation reference to validate the H SAF satellite precipitation products.

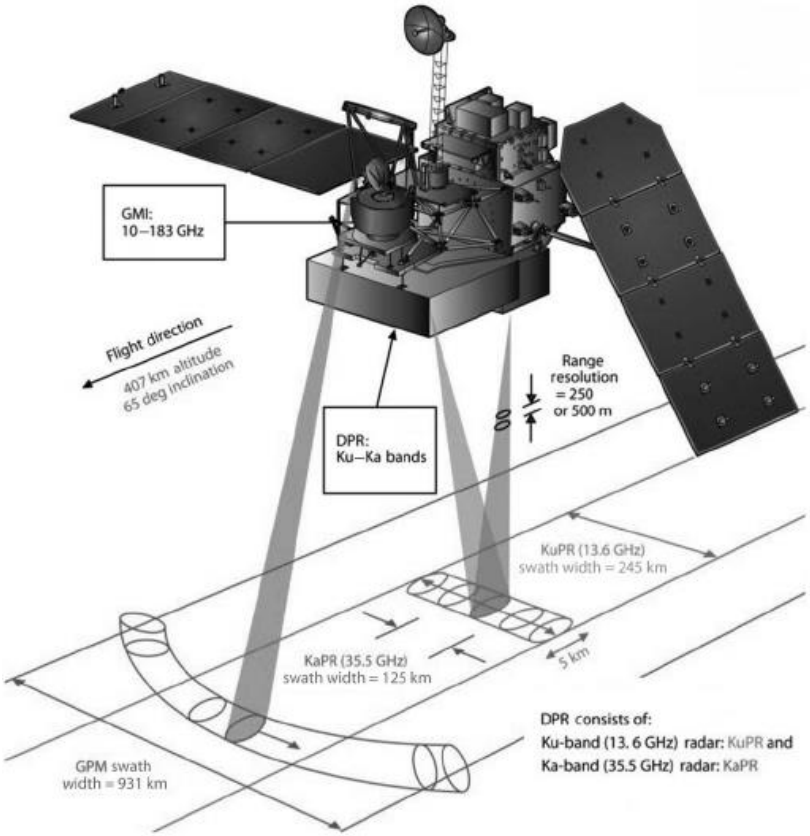

Figure 36: The GPM Core Observatory and the GMI and DPR ground tracks.

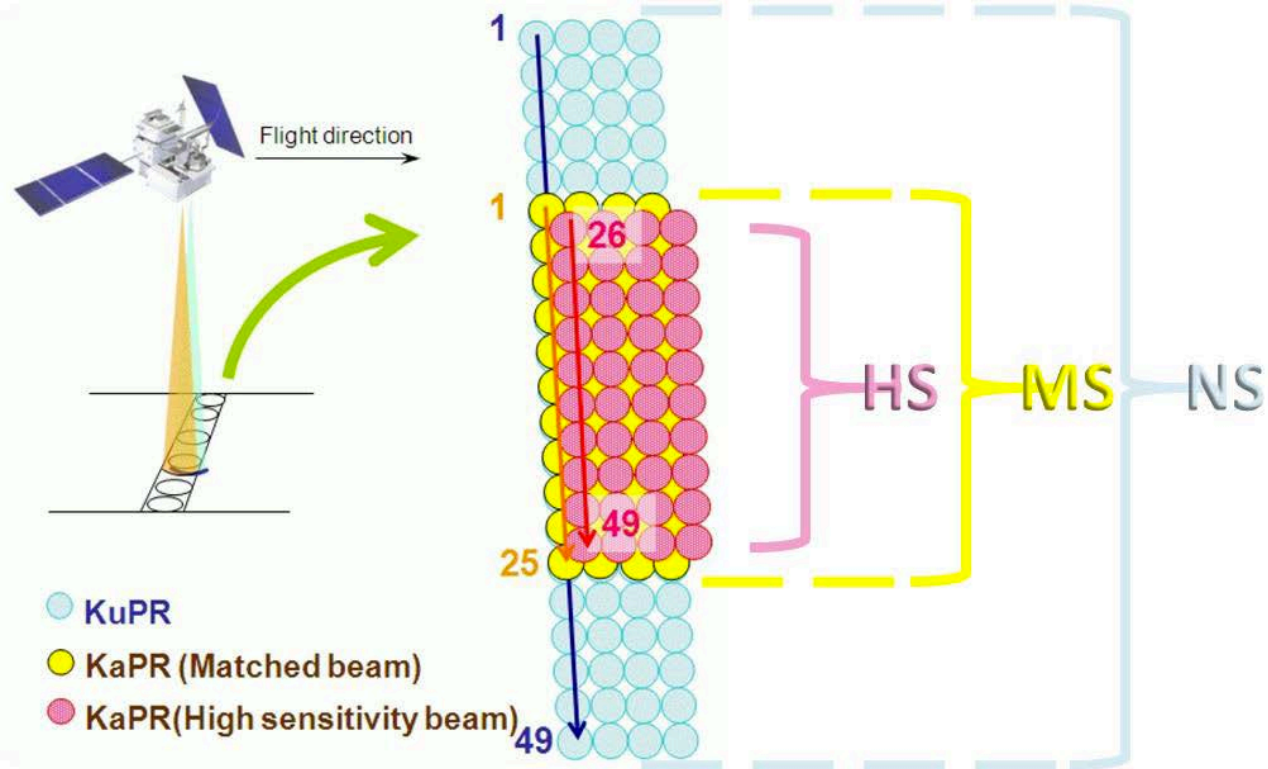

Figure 37: Different DPR scanning modes with respect to the flight direction.
The Normal Scan corresponds to Ka-band radar,
whereas matched and high sensitivity scans are performed by Ka-band radar.

Common procedure for the validation with DPR-NS

The comparison between DPR-NS and H SAF precipitation products is performed following the procedure below described.

Selection of synchronous data (first check)

Both DPR and H SAF filenames contain the start and finish time. Only files with consistent time intervals are considered and evaluated to avoid time-consuming useless computation.

Data re-gridding over regular grid

Both, DPR and H SAF data are re-gridded over the same equi-distance 0.5° grid. All satellite parameter (continuous) values are averaged over the new grid cell. For discrete parameters (such as sea/coast/land flag or precipitation phase flag) the most frequent value is considered.

Temporal and spatial matching between the two regridded data

DPR and H SAF gridded data are temporal- and spatial- matched. Only overlapping grid cells with maximum time difference within ±15 minutes (from the average time of validity of the H SAF product) are stored and evaluated for statistical score analysis.

A1.5 Validation methodology of ACcumulated precipitation products over Full Disk coverage

In order to assess the quality of accumulated precipitation products over FD area the new TC methodology analysis was successfully tested by Brocca et al. (2014). This technique requires three wholly independent rainfall datasets on global scale without the availability of ground-based rainfall accumulation data.

Given three estimates of the same variable, the main assumptions of the TC method are the (i) stationarity of the statistics, (ii) linearity between the three estimates (vs. the same target) across all timescales and (iii) existence of uncorrelated error between the three estimates.
TC provides error and correlations of three products if each of the ones is afflicted by mutually independent errors.

The main steps of the TC validation procedure are:

- temporal (daily) and spatial (0.5° x 0.5° grid) matching between three precipitation datasets;
- TC main procedure;
- statistical scores (continuous and multi-categorical) evaluation;

The methodology, as the previous one, produces **large statistic** (multi-categorical and continuous) scores.

For more details on the TC main procedure, see the H SAF Visiting Scientist Final Report titled "Leveraging coincident soil moisture and precipitation products for improved global validation of

satellite-based rainfall products" by Chen F. and Crow W. T. : https://hsaf.meteoam.it/VisitingScientist/GetDocument?fileName=Final_Report_H_AS18_04.pdf

Data and products used

In this analysis, TC is applied to the rainfall accumulation estimates derived from H SAF satellite product and by GPCC (Global Precipitation Climatology Centre, https://climatedataguide.ucar.edu/climate-data/gpcc-global-precipitation-climatology-centre) and GLDAS (Global Land Data Assimilation System, https://ldas.gsfc.nasa.gov/gldas) projects.

GPCC

The GPCC provides gridded gauge-analysis products derived from quality-controlled station data. In this analysis is used the GPCC First Guess Daily Product (hereafter named as GPCC): daily global land-surface precipitation based on the station database (SYNOP) available via the Global Telecommunication System (GTS) of the World Meteorological Organization (WMO) at the time of analysis (3 - 5 days after end of the analysis month). This product contains the daily totals for a month on a regular latitude/longitude grid with a spatial resolution of 1.0° x 1.0° latitude by longitude. Interpolation is made for the daily relative quota of the monthly total, i.e., the daily total divided by the monthly total, the latter has the DOI:**10.5676/DWD_GPCC/FG_M_100**. The temporal coverage of the dataset ranges from January 2009 to the most recent month for which GTS based SYNOP data is available, i.e. the previous month, 3-5 days after its completion. In Figure 38 is shown an example of spatial extension and resolution of the GPCC product.

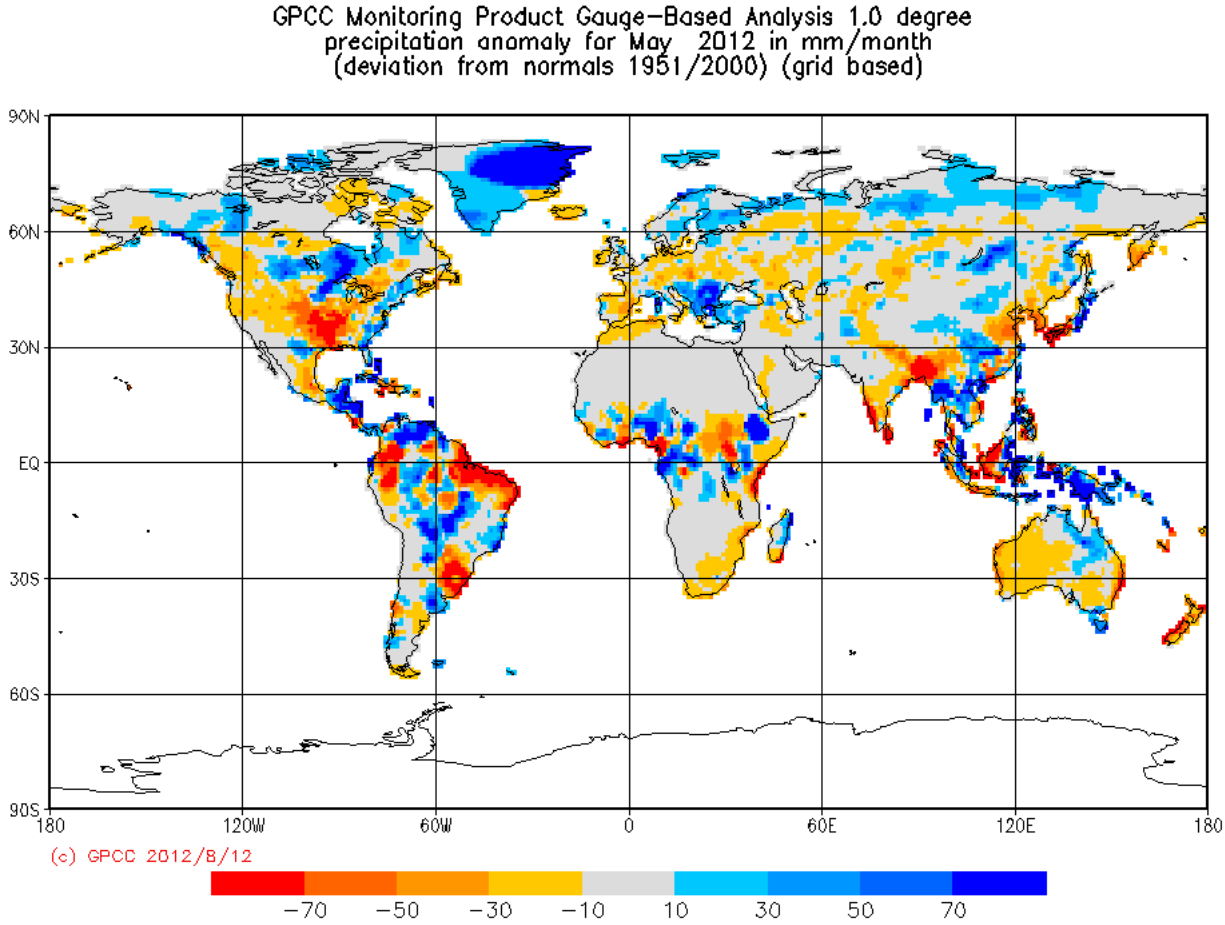

Figure 38: Example of data available in GPCC. The daily precipitation data used in TC methodology have the spatial extent as shown in the figure and the spatial resolution of 1.0 degree

GLDAS

NASA Global Land Data Assimilation System Version 2 (GLDAS-2) has three components: GLDAS-2.0, GLDAS-2.1, and GLDAS-2.2. GLDAS-2.0 is forced entirely with the Princeton meteorological forcing input data and provides a temporally consistent series from 1948 through 2014. GLDAS-2.1 is forced with a combination of model and observation data from 2000 to present. GLDAS-2.2 product suites use data assimilation (DA), whereas the GLDAS-2.0 and GLDAS-2.1 products are "open-loop" (i.e., no data assimilation). The choice of forcing data, as well as DA observation source, variable, and scheme, vary for different GLDAS-2.2 products.

The 3-hourly data product was simulated with the Noah Model 3.6 in Land Information System (LIS) Version 7 (https://lis.gsfc.nasa.gov/sites/default/files/LIS/public_7_3_releases/LIS_usersguide.06-dec-2021.pdf). The data product contains 36 land surface fields from January 2000 to present. In this analysis GLDAS-2.1 data are used. These data are archived and distributed in NetCDF format (DOI:10.5067/E7TYRXPJKWOQ). In Figure 39 is shown an example of spatial extension and resolution of the GLDAS product used.

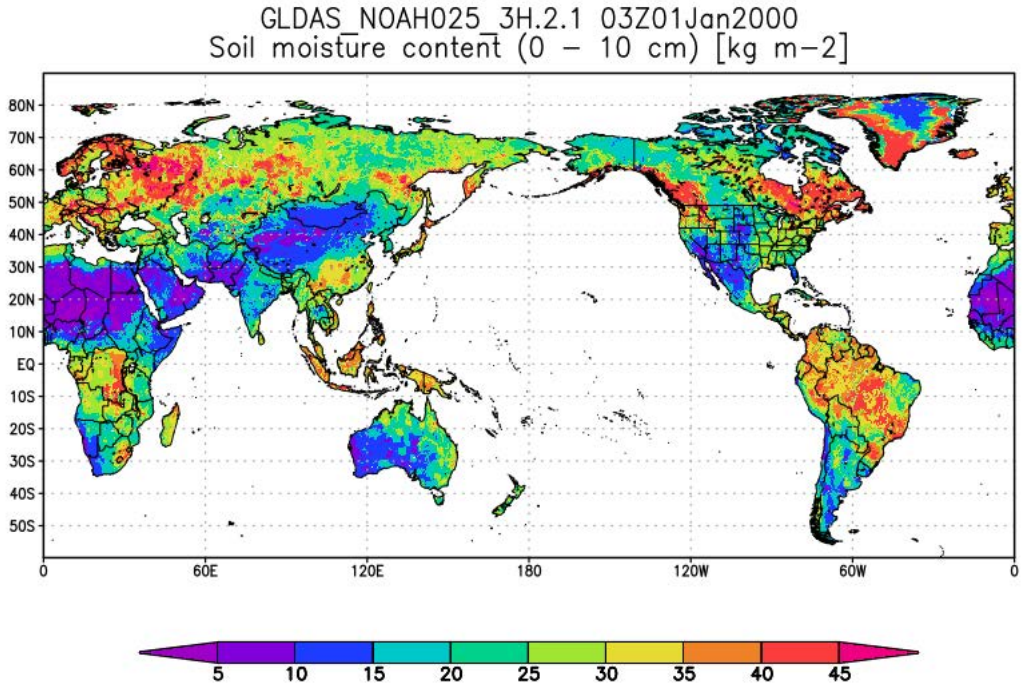

Figure 39: Example of data available in GLDAS. The 3-hourly precipitation data used in TC methodology have the spatial extent as shown in the figure and the spatial resolution of 0.25 degree

GLDAS 2.1 uses GPCC observations via the ingestion of the disaggregated Global Precipitation Climatology Project (GPCP) V1.3 Daily Analysis precipitation fields. In order to assess whether this has an impact on the TC analysis, pixel-based cross-correlated errors between GPCC and GLDAS by quadruple collocation (QC) analysis have been calculated (Perdicca et al., 2015, Gruber et al., 2016) using GPCC first guess data, GLDAS 2.1, ERA5 and SM2RAIN-ASCAT derived daily rainfall at the global scale. QC is a viable way to estimate the cross-correlated errors between two of the datasets included in the quadruplet (see Chen et al. 2020).

The analysis has been carried out at 0.25° of spatial resolution for the year 2017. Despite the use of a single year, the analysis shows that cross correlated errors between GPCC and GLDAS are very low (R=0.05 in median). If we zoom over the H SAF Extended Area (HEA) the median value decreases to 0.044 (see Figure 40 and Figure 41). In the inset it is reported the histogram of the R-values, showing how most of the pixels provided very low values of error correlation. This point should assure the independence of the datasets used for performing the analysis and thus, should allow to use TC analysis for validating H SAF products not only over the HEA, but also at the global scale.

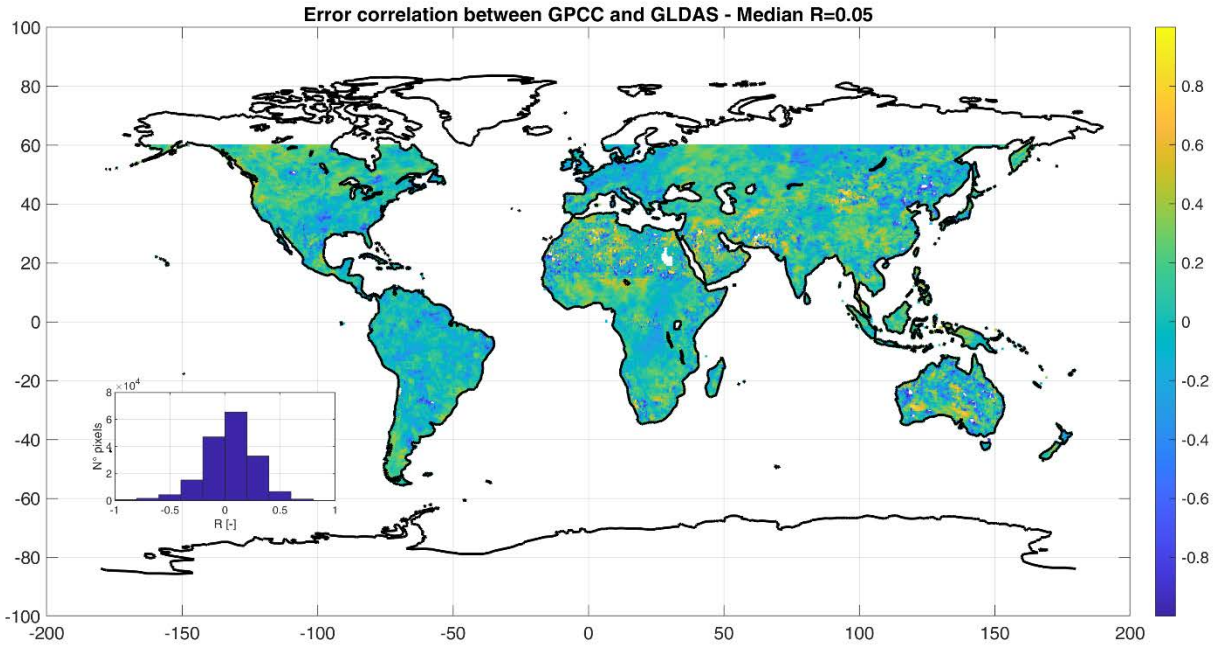

Figure 40: Cross correlated errors between GPCC and GLDAS over global scale for the year 2017.

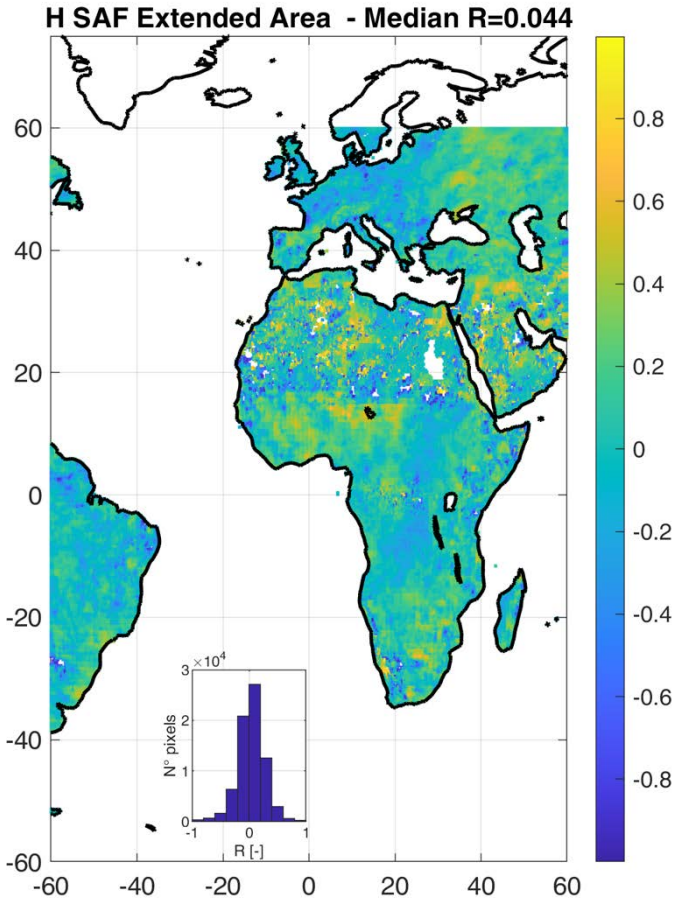

Figure 41: Cross correlated errors between GPCC and GLDAS over H SAF extened area for the year 2017.

A1.6 Inter-comparison procedure between two SEVIRI FD products

The product H63 is available from February 2021. At the time the analysis of the product started, a dataset limited to 3 months (FMA) is available. For this reason, it is not possible to assess the quality of the product H63 using the methodology as above described. It was therefore agreed to compare H63 with H60B on the common area in order to extend the Q.A. results obtained for H60B to H63. Both products share a common domain comprising Europe and Africa, as shown below in Figure 42.

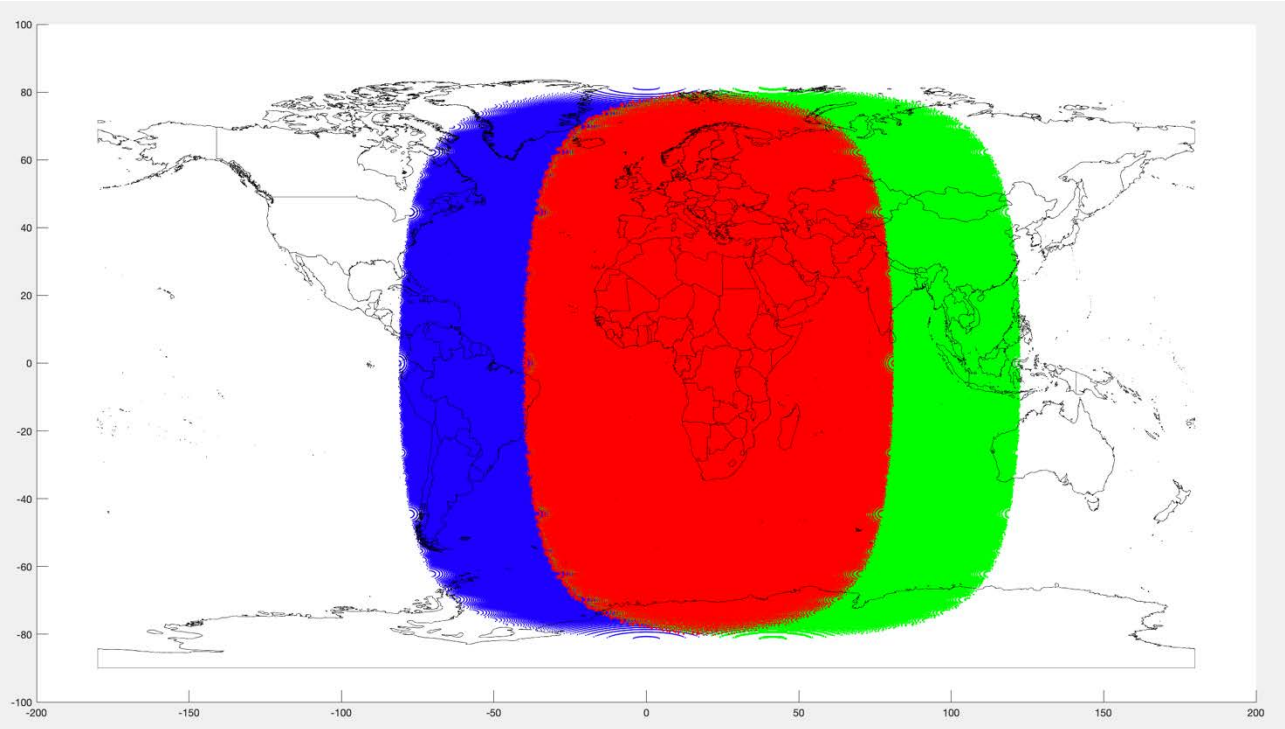

Figure 42: Coverage areas for H60B (blue) and H63 (green) products. Overlapped H63-H60B area is highlighted in red.

In order to perform the comparison, it was decided to exclude the area close to the edges as it was not observed very well by the SEVIRI sensors. An a-priori mask was then applied to both products to exclude the pixels close to the edge. In the figure below (Figure 43) the domains are shown after the application of the edge mask.

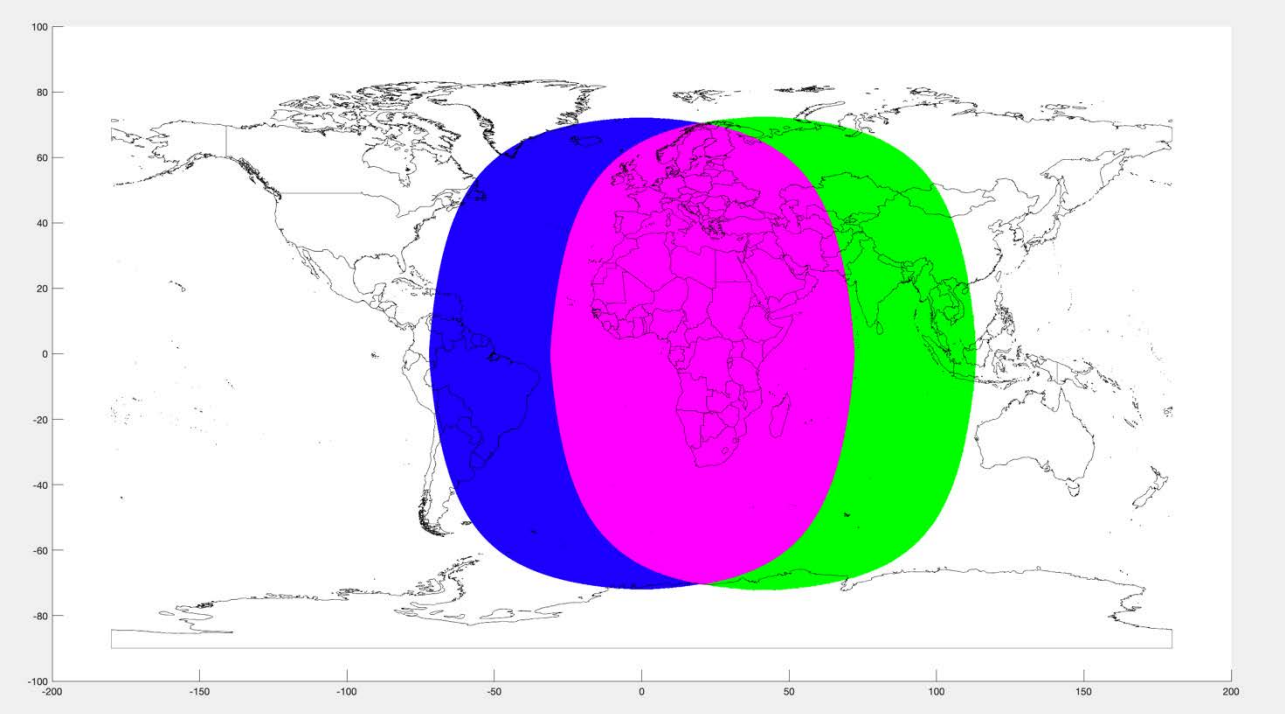

Figure 43: Border-masked areas for H60B (blue) and H63 (green) products. The overlapped H63-H60B area analyzed is highlighted in purple.

Subsequently, the corresponding nearest pixel point (NN) belonging to the domain of H60B was identified for each pixel point of H63. The search for the nearest point was limited to a distance of 6 km. The threshold was defined by assessing how the total coverage varies as a function of distance: as shown in Figure 44, at a distance of 6km the 80% of the domain is considered in the analysis, while for much greater distances the percentage of coverage does not increase appreciably.

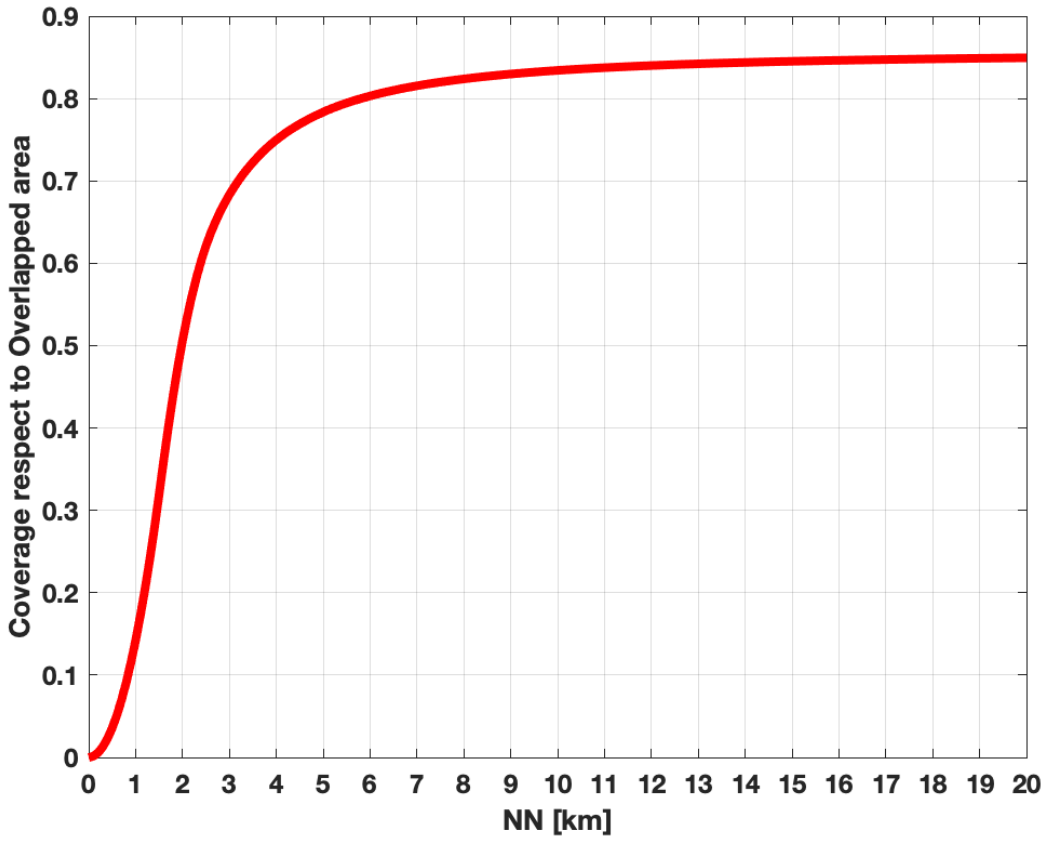

Figure 44: Extension of area (fraction) respect to the overlapped area as function of the distance among nearest neighbor (NN) pixels (H63 vs H60B). More than 80% of domain is covered for distance equals to 6 km.

The data pairs thus identified were processed and analysed in order to generate continuous and multi-categorical statistics as described below, as well as an analysis of a case study occurring in Europe within the available dataset. The results obtained are presented in the section 5.

A1.7 Large statistic

The large statistical analysis allows to point out the existence of pathological behavior in the satellite product performance. The application of the same validation technique step by step is guaranteed in all institutes take part of the PPVG and in both validation methodologies above described.

The large statistical analysis in PPVG is based on the evaluation of monthly and seasonal ***Continuous verification*** and ***Multi-Categorical*** statistical scores on one full year of data. It was decided to evaluate both continuous and multi-categorical statistics to give a complete view of the error structure associated to the H SAF product. Since the accuracy of precipitation measurements depends on the type of precipitation or, to simplify matters, on the intensity or accumulated

precipitation, the verification is carried out on three precipitation classes (for accumulated precipitation products) as descripted in Table 22: Classes for evaluating cumulated precipitation products.

Accumulated Precipitation Classes (CR)	1	2	3
	≥ 1 mm/24h	≥5 mm/24h	≥ 10 mm/24h

Table 22: Classes for evaluating cumulated precipitation products

The impact of different background is also considered in the product performances. Statistical scores are separately computed for land, sea and coast areas. The Precipitation Product Validation Leader collects all validation results as computed by European institutes, verifies the consistency of these results and evaluates the monthly and seasonal common statistical results as reported in Chapter 4.

Continuous statistics

Continuous statistics are provided for each month and season of assessment. The main statistical scores are here listed:

Score	*Acronym*	*Range*	*Perfect score*	*Calculation*
Number of Satellite samples	NS	N.A.	N.A.	N.A.
Number of Reference (radar/rain gauge) samples	N	N.A.	N.A.	N.A.
Mean Error or Bias	ME	- ∞ to ∞	0	$ME = \frac{1}{N}\sum_{k=1}^{N}(sat_k - obs_k)$
Mean Absolute Error	MAE	0 to ∞	0	$MAE = \frac{1}{N}\sum_{k=1}^{N}\lvert sat_k - obs_k \rvert$
Standard Deviation	SD	0 to ∞	0	$SD = \sqrt{\frac{1}{N}\sum_{k=1}^{N}(sat_k - obs_k - ME)^2}$
Multiplicative Bias	MB	- ∞ to ∞	1	$MB = \frac{\frac{1}{N}\sum_{1}^{N} sat_K}{\frac{1}{N}\sum_{1}^{N} obs_K}$
Correlation Coefficient	CC	- 1 to 1	1	$CC = \frac{\sum_{k=1}^{N}(sat_k - \overline{sat})(obs_k - \overline{obs})}{\sqrt{\sum_{k=1}^{N}(sat_k - \overline{sat})^2 \sum_{k=1}^{N}(obs_k - \overline{obs})^2}}$
Root Mean Square Error (or Root Mean Square Difference)	RMSE	0 to ∞	0	$RMSE = \sqrt{\frac{1}{N}\sum_{k=1}^{N}(sat_k - obs_k)^2}$
Fractional Standard Error (%)	FSE	0 to ∞	0	$FSE = [RMSE / \overline{obs}] * 100\%$

Table 23: Continuous statistical scores

In the Table 23:
- N represents the total number of observation samples and equivales to all satellite/observation pairs for computing all the statistical scores;
- NS indicates the number of product satellite estimates with given characteristics (e.g.; with estimated rain rate > 1 mm/h);
- the index "k" represents the spatial and temporal grid point at the scale of the common reference grid;
- *obs* and *sat* stand for rainfall value acquired by reference observations and satellite estimations, respectively.

The FSE score represents the accuracy for H SAF satellite precipitation products. The User requirements thresholds are below indicated:

Accuracy for CR ≥ 1 mm/daily		
Threshold	Target	Optimal
FSE% = 200%	FSE% = 150%	FSE% = 100%

Table 24: Precipitation products user requirements (UR)

The FSE score is not appropriate to define the accuracy in the TC methodology. In this case the Correlation Coefficient (CC) is used to define the product accuracy with thresholds as below indicated:

Accuracy for all precipitation rates (CR ≥ 0 mm/daily)		
Threshold	Target	Optimal
CC = 0.50	CC = 0.65	CC = 0.80

Table 25: UR for accumulated precipitation products using TC methodology

Multi Categorical statistics

Multi categorical statistics are derived by the following contingency table:

		Observation		
		yes	**no**	**total**
Satellite	**yes**	hits	false alarms	forecast yes
	no	misses	correct negatives	forecast no
	total	observed yes	observed no	total

Table 26: Multi-categorical statistics contingency table

where:

hit: $Sat_k \geq R_{th}$ and $Obs_k \geq R_{th}$

miss: $Sat_k < R_{th}$ and $Obs_k \geq R_{th}$

false alarm: $Sat_k \geq R_{th}$ and $Obs_k < R_{th}$

correct negative: $Sat_k < R_{th}$ and $Obs_k < R_{th}$

$\mathbf{R_{th}}$ is the threshold between the "rain" and "no rain" conditions. The scores evaluated from the contingency table are:

Score	Acronym	Range	Perfect score	Calculation
Probability Of Detection	POD	0 to 1	1	$POD = \frac{hits}{hits + misses} = \frac{hits}{observed\ yes}$
False Alarm Rate	FAR	0 to 1	0	$FAR = \frac{false\ alarms}{hits + false\ alarms} = \frac{false\ alarms}{forecast\ yes}$
Critical Success Index	CSI	0 to 1	1	$CSI = \frac{hits}{hits + misses + false\ alarm}$

Table 27: Multi-categorical statistics scores

A1.8 Case study analysis

Each institute, in addition to the large statistics verification, produces a case study analysis based on ***the knowledge and experience of the institute itself***, following a standard format as below reported. The institute decides whether to use ancillary data such as lightning data, SEVIRI images, the output of numerical weather prediction and nowcasting products.

The main sections of the standard format are:

- description of the meteorological event;
- comparison of ground data and satellite products;
- visualization of ancillary data;
- discussion of the satellite product performances;
- indication on the ground data (if requested) availability into the H SAF project.

Case study analysis are reported in Chapter 3.

References

Chen, F., Crow, W.T., Ciabatta, L., Filippucci, P., Panegrossi, G., Marra, A.C., Puca, S., Massari, C., 2020. Enhanced large-scale validation of satellite-based land rainfall products. Journal of Hydrometeorology 1. https://doi.org/10.1175/JHM-D-20-0056.1

Feidas, H., F. Porcù, S. Puca, A. Rinollo, C. Lagouvardos, and V. Kotroni, 2018: Validation of the H SAF precipitation prod- uct H03 over Greece using rain gauge data. Theor. Appl. Cli- matol., 131, 377–398, https://doi.org/10.1007/s00704-016-1981-9.

Gruber, A., C.-H. Su, W. T. Crow, S. Zwieback, W. A. Dorigo, and W. Wagner, 2016a: Estimating error cross-correlation in soil moisture data sets using extended collocation analysis. J. Geophys. Res. Atmos., 121, 1208–1219.

Pierdicca, N., F. Fascetti, L. Pulvirenti, R. Crapolicchio, and J. Muñoz-Sabater, 2015: Quadruple collocation analysis for soil moisture product assessment. IEEE Geosci. Remote Sens. Lett., 12, 1595–1599.

Pignone, F., N. Rebora, F. Silvestro, and F. Castelli, 2010: GRISO (Generatore Random di Interpolazioni Spaziali da Osservazioni incerte) - Piogge. Rep. 272/2010, 353 pp.

Sebastianelli, 2017: Potentials and limitations of the use of GPM-DPR for validation of H SAF precipitation products: study over the Italian territory, Associated Visiting Scientist H SAF, Final Report,116 pp. https://hsaf.meteoam.it/VisitingScientist/GetDocument?fileName=Final_Report_Stefano_Sebastianelli.pdf

Appendix 2 Ground data used for validation activities

In the following sections the precipitation ground data networks used in the PPVG are described: radar and rain gauge data the following countries: Belgium, Bulgaria, Germany, Hungary, Italy, Poland, Slovakia, and Turkey. It is well known that radar and rain gauge rainfall estimation is influenced by several error sources that should be carefully handled and characterized before using these data as reference for ground validation of any satellite-based precipitation products.

The rain gauge in PPVG is composed by more than 8000 instruments across the partner Countries. These data are, as usual, irregularly distributed over ground and are generally deduced by tipping bucket type instruments. Moreover, most of the measurements are hourly cumulated. So probably the raingauge networks used in this validation activities are surely appropriated for the validation of cumulated products (1 hour and higher), while for the validation of instantaneous estimates the use of hourly cumulated ground measurements could introduce a large error. Moreover, the revisiting time (3,4 hours) of the product makes impossible or not reasonable to validate the product for 1-24 hours cumulated interval. The first object of PPVG *(Rain Gauge- WG)* was to quantitatively estimate the errors introduced in the validation procedure comparing the instantaneous satellite precipitation estimation with the rain gauge precipitation cumulated on different intervals.

The radar data in the PPVG is composed by 74 C-band radars across the 7 countries: Belgium, Germany, Hungary, Italy, Slovakia, Poland, Turkey. The rain gauge network responsible declared that the systems are kept in a relatively good status. The rain gauge inventory pointed out that different correction factors are applied. This means that the corresponding rainfall estimates are diverse, and the estimation of their errors cannot be homogenized. The first step in PPVG *(Radar – WG)* was to define a quality index on the base of the study performed by the Slovakian team and the scheme published by J. Szturc et all. 2008. The evaluation of this quality index has allow to increase the confidence of radar estimates with the selection of more reliable radar data in the PPVG.

In this chapter a description of the ground data available in the PPVG is reported country by country. The chapter has the object to provide ground data information and to highlight their error sources.

A1.1 Ground data in Belgium (IRM)

Radar Data

The network

There are four radars in Belgium (Figure 45 and Table 28): two operated by the RMI (in Wideumont - Ardennes range - and Jabbeke - near the coast), one by Belgocontrol (Zaventem airport near Brussels) and the radar coverage is also provided by a fourth radar in France, operated by Meteo France. Of particular interest is the Wideumont radar, located in one of the highest locations of the country with clear horizon in every direction. This is very important in order to have the best possible precipitation picture in this hilly area giving rise to many tributaries of the Meuse river.

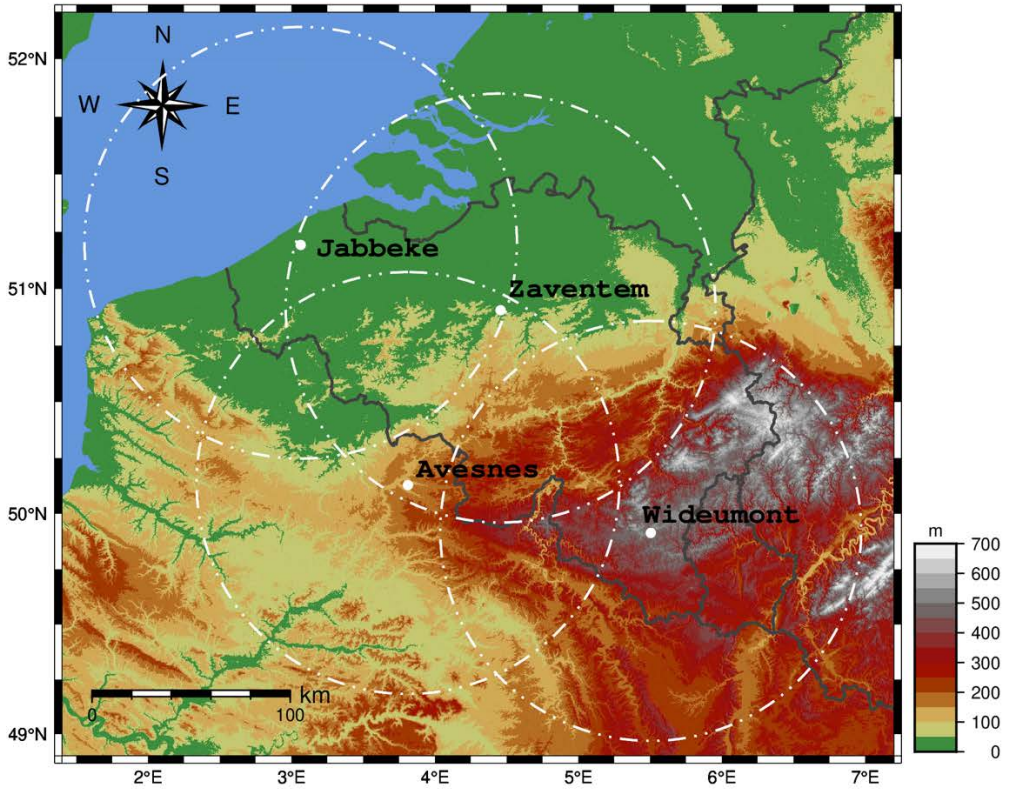

Figure 45: Meteorological radars in Belgium (elevation data from Danielson, J.J., and Gesch, D.B., 2011, Global multi-resolution terrain elevation data 2010 (GMTED2010): U.S. Geological Survey Open-File Report 2011–1073, 26 p.)

Radar location	Frequency Band	Polarization	Reflectivity Z = aR^b
Wideumont	C	Single	a = 200, b = 1.6
Jabbeke	C	Dual	a = 200, b = 1.6
Zaventem	C	Single	a = 200, b = 1.6
Avesnes	C	Dual	a = 200, b = 1.6

Table 28: Meteorological radars in Belgium, main features

Data processing

Raw reflectivity data are contaminated by off-shore wind farms and marine traffic clutter over the North Sea. The sea clutter is detected and removed using the module available in Selex Rainbow 5 software for this purpose. Rainfall rate estimation is based on a PCAPPI at a given height (depending on the radar) combined with the Marshall-Palmer relationship between reflectivity and rainrate. For grid points where several estimates are available from different radars, the maximum value is taken.
A 5-min accumulation is generated based on the rainrates at t and t-5. If the rainrate at t-5 is missing, the rainrate at t-10 is used to generate the 5-min accumulations at both t and t-5. This means than 1 missing file is tolerated. Accumulations of higher durations are made by summing accumulations of lower duration.

Acknowledgement (elevation data for the radar map)
Danielson, J.J., and Gesch, D.B., 2011, Global multi-resolution terrain elevation data 2010 (GMTED2010): U.S. Geological Survey Open-File Report 2011–1073, 26 p.

A1.2 Ground data in Bulgaria (NIMH)

Rain gauge

The network

The maximum number of available manually measured daily accumulated rain gauges is up-to 300, irregularly distributed over the country. These stations are measured every day at 6:30 UTC by emptying the collected in the past 24hours rain.
The hourly measuring automatic rain gauges are varying on daily basis and range from 70 units to 130 units. Number of stations is varying mainly because in winter months not heating gauges data is discarded from the operational database when air temperature drops below 0° C. Other specific measurement errors that are detected by the operators as funnel clogging, sensor failure etc.

The average minimum distance between closest stations is about 20 km. Most dense network of automatic gauges is built in South-Central Bulgaria where a number of European funded projects permitted to purchase and install more than 50 telemetric gauges. Spatial distribution of automatic gauges is described in (Naldzhiyan et al., 2017)[1]. One of main objectives was to consider mountain structures because of the need to measure snowfall accumulation in winter months.
This points out that the distribution of gauges could be able to describe the spatial structures of precipitation fields in case of wintertime rainfall. This objective is reached in central and South Bulgaria but much less in Western and Eastern parts of the country.

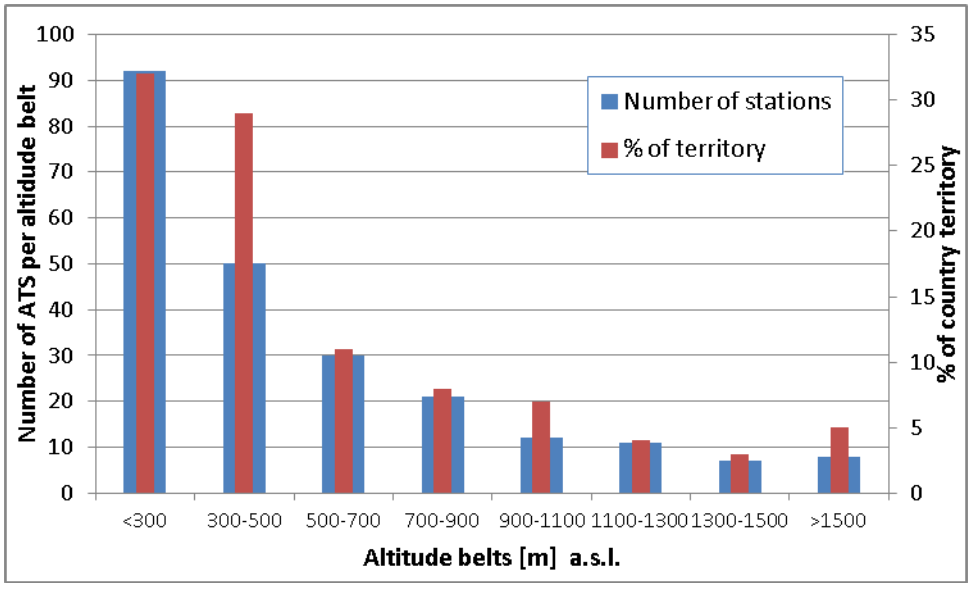

Figure 46: Spatial distribution of automatic telemetric gauges in Bulgaria (NIMH)

In following figure the distribution of working stations over Bulgaria is shown.

[1] Naldzhyian A, Georguiev O., Artinyan E., 2017: "From the sensors to the models, integrated hydro-meteorological systems in NIMH – BAS, Bulgaria". International Conference on Automatic weather stations ICAWS-2017.

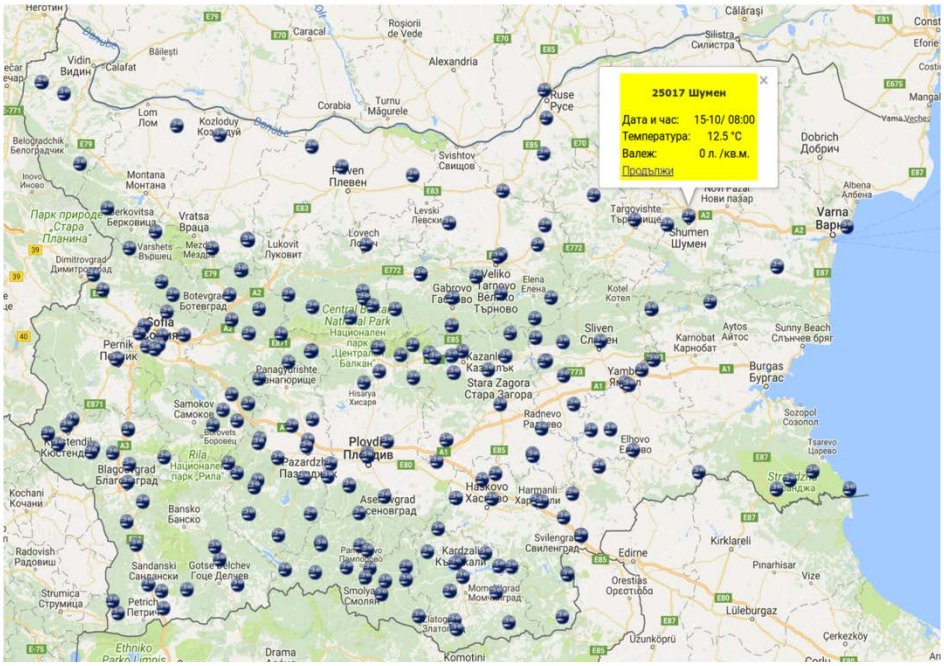

Figure 47: Distribution of the automatic stations of the Bulgaria network collected by NIMH.

The instruments – hourly measuring rain gauges:

- About 50 raingauges are of weighing type so they can measure snowfall without heating; however some of them have orifice heating (where 220V supply is available). Examples of such sensors are Vaisala VRG101, SEBA TRW 200cm^2 and SUTRON TPG
- About 80 raingauges are of tipping bucket type so they need 220 V supply to switch on the heater in winter conditions, however half of them are installed beside rivers so 220V supply is not available; The sensors types are mostly SEBA RG50, DELTA-OHM 400cm^2 and MTX 400 cm^2
- Most of the raingauges have a minimum detected quantity of 0.1 mm, others have 0.2 mm.
- The maximum rain rate (with acceptable quality) that can be measured by the gauges ranges between 33 and 120 mm^{-1} over one minute, depending on the manufacturer.

The rainrate is measured over 1 minute and 1-hour accumulation intervals depending on the hardware specifications.

At the moment, the NIMH officially provides only daily data from manually measured rain gauges. Shorter accumulation times could be available for scientific studies but not publicly distributed.

The data processing

Quality control is performed on the data, after daily visual comparison check, but only on YES/NO basis. When rain sensor fails it may be seen in few days or not be seen by the operators specially when it doesn't rain.

For NIMH internal usage hourly accumulated rain data is converted into 3 h sums and then interpolated using a kriging technique to 8 km regular grid. The method also incorporates the 24h

accumulated data from manually measured tin cans, thus enhancing the spatial and vertical quality of the field (Artinian et al., 2007)[2]

For H SAF validations a subset of country's automatic gauges is used (between 70 and 90) because of the much denser network in South-Central Bulgaria – an area of about 34000 km^2. Other parts of the country have much sparse gauge networks, data from which is not suitable to be interpolated using the GRISO technique.

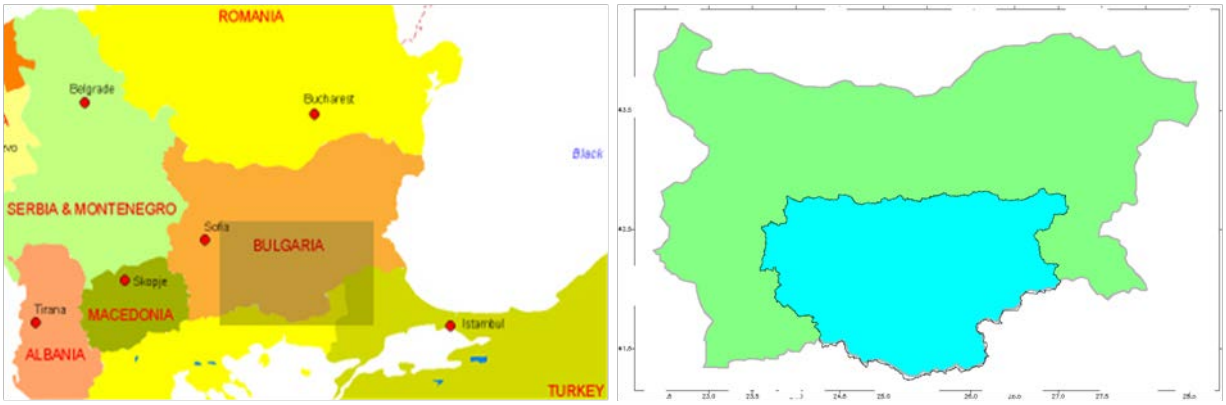

Figure 48: The area in Bulgaria used for H SAF validation with hourly accumulated rain data

[2] Artinyan, E. et al, 2007: "Modelling the water budget and the riverflows of the Maritsa basin in Bulgaria", Modelling the water budget and the riverflows of the Maritsa basin in Bulgaria. Hydrology and Earth System Sciences. 12. 10.5194/hessd-4-475-2007.

A1.3 Ground data in Germany (BfG)

The H SAF products are validated for the territory of Germany by use of two observational ground data sets: SYNOP - precipitation data based on the network of synoptical stations, provided by the German Weather Service (DWD) and RADOLAN-RW - calibrated precipitation data based on the radar network of DWD and calibrated by DWD by use of measurements at precipitation stations.

Data	Number/Resolution	Time interval	Delay	Annotation
Synoptical stations	~ 200	6h / 12h	Near-real-time	
Precipitation stations	~ 1100	hourly	Near-real-time	Automatic precipitation stations
RADOLAN RW	16 German radar sites, ~1 km x ~1 km	1 hour,	Near-real-time	Quantitative radar composite product RADOLAN RW (Radar data after adjustment with the weighted mean of two standard procedures)

Table 29: Precipitation data used at BfG for validation of H SAF products

Rain gauge

The network

The data used are compiled from ~1300 rain gauges. About 1000 are operated by DWD while about 300 are operated by other German authorities. The average minimum distance between stations is 17 km.

The instruments

The measurement instruments are precipitation sensors OTT PLUVIO of Company Ott[3] [4]. They continually and precisely measure quantity and intensity of precipitation in any weather, based on balance principle with temperature compensation (heated funnel) and by an electronic weighing cell. The absolute measuring error is less than 0.04 mm for a 10 mm precipitation amount and the long-term (12months) stability is better than 0.06 mm. The operating temperature ranges from –30°C to +45°C. The minimum detected quantity (sensitivity) is 0,05 mmh^{-1}. The maximum possible measured rain rate is 3000 mmh^{-1}. The operational accumulation interval theoretically is one minute.

The data processing

Continuous, automatic measurement of liquid and solid precipitation data are collected, accumulated (intervals: from 1hour until 1day) and provided as SYNOP tables by DWD. These data are error corrected and quality controlled in four steps with checks of completeness, climatologic temporal/spatial consistency and marginal checks.

[3] http://www.ott.com/web/ott_de.nsf/id/pa_ottpluvio2_vorteile.html?OpenDocument&Click=

[4] **Precipitation amount and intensity measurements with the Ott Pluvio, Wiel Wauben, Instrumental Department, INSA-IO, KNMI, August 26, 2004**

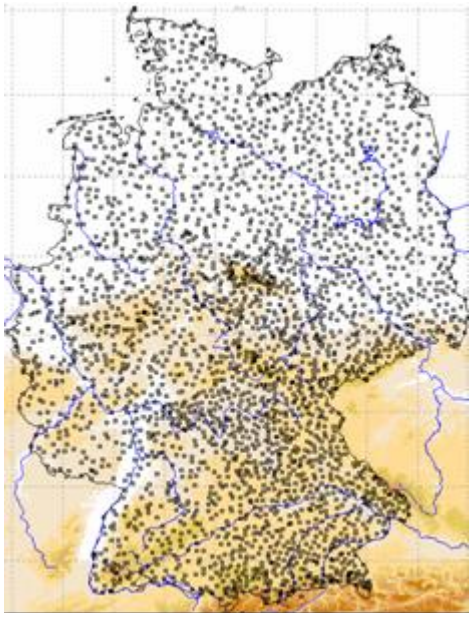

Figure 49: (left): Network of rain gauges in Germany - Figure 50: (right): Pluvio with Remote Monitoring Module

Radar data

Radar-based real-time analyses of hourly precipitation amounts for Germany (RADOLAN) is a quantitative radar composite product provided in near-real time by DWD. Spatial and temporal high-resolution, quantitative precipitation data are derived from online adjusted radar measurements in real-time production for Germany. Radar data are calibrated with hourly precipitation data from automatic surface precipitation stations. [5]

The combination of hourly point measurements at the precipitation stations with the five-minute-interval radar signals of the 16 weather radars (C-Band Doppler) provides gauge-adjusted hourly precipitation sums for a ~1km x ~1km raster for Germany in a polar stereographic projection.

Radar site	Latitude (N)	Longitude (E)	WMO No.	Radar site	Latitude (N)	Longitude (E)	WMO No.
München	48° 20’ 14’’	11° 36’ 46’’	10871	Rostock	54° 10’ 35’’	12° 03’ 33’’	10169
Frankfurt	50° 01’ 25’’	08° 33’ 34’’	10630	Ummendorf	52° 09’ 39’’	11° 10’ 38’’	10356
Hamburg	53° 37’ 19’’	09° 59’ 52’’	10147	Feldberg	47° 52’ 28’’	08° 00’ 18’’	10908
Berlin-Tempelhof	52° 28’ 43’’	13° 23 17’’	10384	Eisberg	49° 32’ 29’’	12° 24’ 15’’	10780
Essen	51° 24’ 22’’	06° 58’ 05’’	10410	Flechtdorf	51° 18’ 43’’	08° 48’ 12’’	10440
Hannover	52° 27’ 47’’	09° 41’ 54’’	10338	Neuheilenbach	50° 06’ 38’’	06° 32’ 59’’	10605
Emden	53° 20’	07° 01’	10204	Türkheim	48° 35’	09° 47’	10832

5 http://www.dwd.de/bvbw/appmanager/bvbw/dwdwwwDesktop?_nfpb=true&_windowLabel=dwdwww_main_book&T14609949251144921180881gsbDocumentPath=Navigation%2FWasserwirtschaft%2FUnsere__Leistungen%2FRadarniederschlagsprodukte%2FRADOLAN%2Fradolan__node.html%3F__nnn%3Dtrue&switchLang=en&_pageLabel=_dwdwww_spezielle_nutzer_forschung_fkradar

	22''	30''			10''	02''	
Neuhaus	50° 30' 03''	11° 08' 10''	10557	Dresden	51° 07' 31''	13° 46' 11''	10488

Table 30: Location of the 16 meteorological radar sites of the DWD

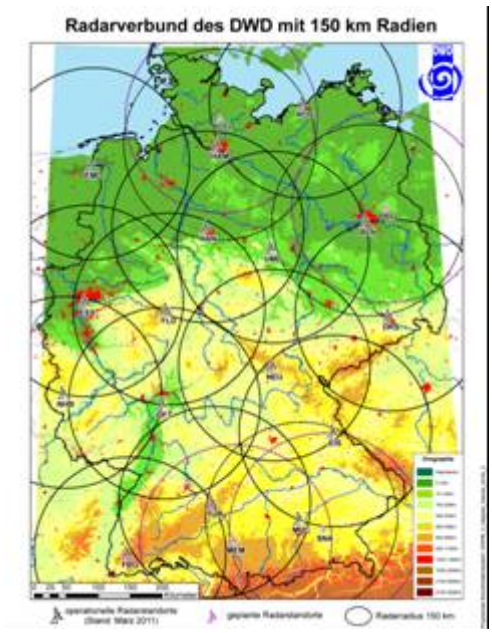

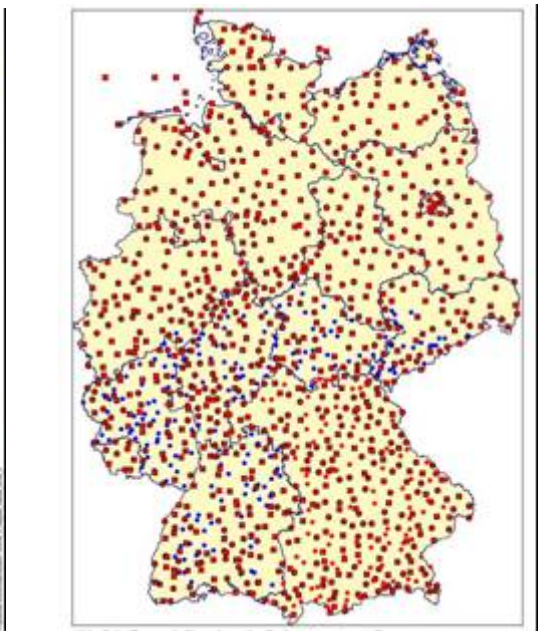

Figure 51: (left) radar compound in Germany (March 2011) ; Figure 52: (right) location of ombrometers for online calibration in RADOLAN; squares: hourly data provision (about 500), circles: event-based hourly data provision (about 800 stations)6.

The flowchart of online calibration method applied in RADOLAN is depicted in Figure 53.

[6] Bartels, H.: Projekt RADOLAN. Routineverfahren zur Online-Aneichung der Radarniederschlagsdaten mit Hilfe von automatischen Bodenniederschlagsstationen (Ombrometer), Abschlussbericht 2004

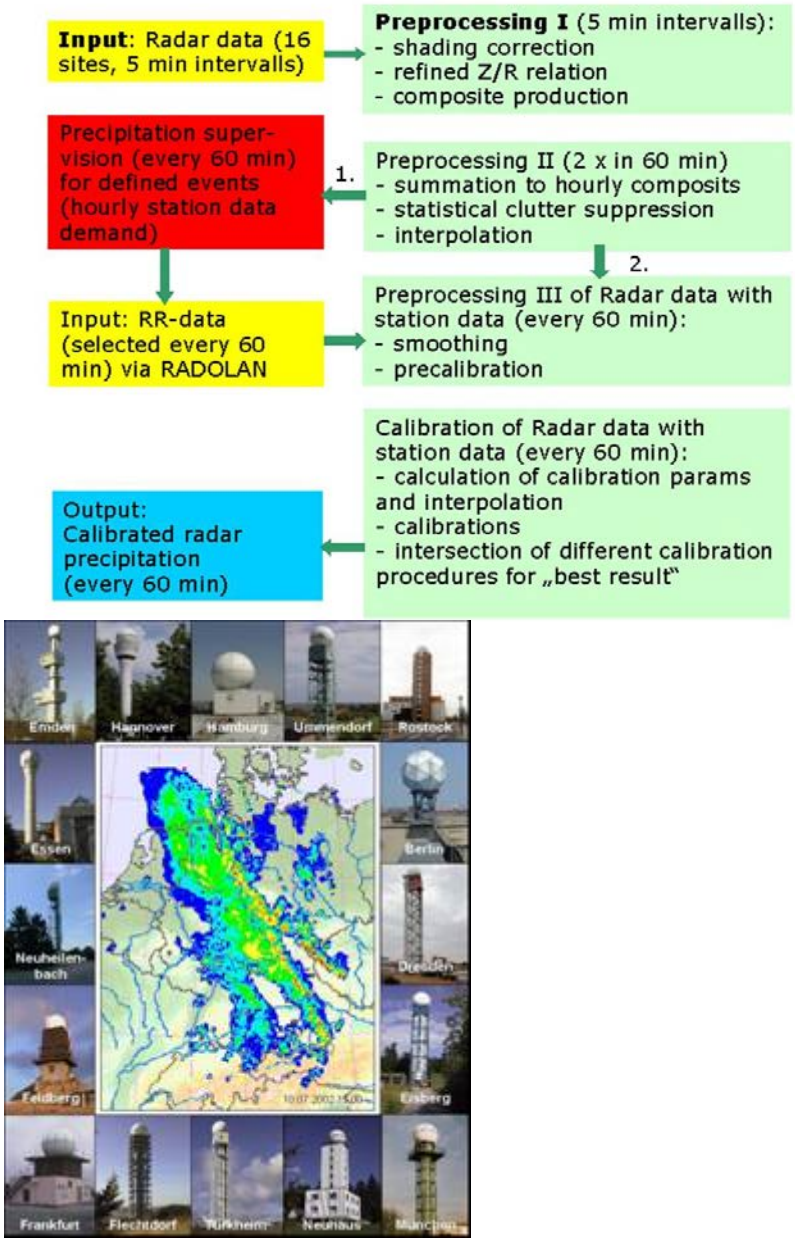

Figure 53: Flowchart of online calibration RADOLAN (DWD, 2004)

A1.4 Ground data in Hungary (OMSZ)

The radar network

The main data used for validation in Hungary would be the data of meteorological radars. There are four C-band dual polarized Doppler weather radars operated routinely by the OMSZ-Hungarian Meteorological Service. The location of the four Hungarian radars and the measurement characteristics are listed in Table 31. All four radars are calibrated periodically, with an external (calibrated) TSG, the periodicity is kept every 1 year.

Year of installation	***Location***	***Radar type***	***Parameters measured***
1999	*Budapest*	*Dual-polarimetric Doppler radar*	Z,Z_{DR},K_{DP},Φ_{DP}
2003	*Napkor*	*Dual-polarimetric Doppler radar*	Z,Z_{DR},K_{DP},Φ_{DP}
2004	*Poganyvar*	*Dual-polarimetric Doppler radar*	Z,Z_{DR},K_{DP},Φ_{DP}
2014	Szentes	*Dual-polarimetric Doppler radar*	Z,Z_{DR},K_{DP},Φ_{DP}

Table 31: Main characteristics of the Hungarian radar network

Instrument characteristics

The Hungarian radar network is composed by four Doppler radars, which are measuring in the C-band, mainly at same frequencies. The scan strategy is the same for all the radars. The parameters of the instruments and the measurement campaigns are listed in Table 32.

	Budapest	***Napkor***	***Poganyvar***	***Szentes***
Frequency band	C-Band, 5625MHz	C-Band, 5610MHz	C-Band, 5610MHz	C-Band, 5640MHz
Polarization (Single/Double)	double	double	double	double
Doppler capability (Yes/No)	Yes	Yes	Yes	Yes
Scan strategy: elevations, maximum nominal range distance, range	*scan freq: 5 min Elevaions(deg): 0 0.5 1.1 1.9 3.0 4.7 7.0 10.0 14.2*	*scan freq: 5 min Elevaions(deg): 0 0.5 1.1 1.9 3.0 4.7 7.0 10.0 14.2*	scan freq: 5 min Elevaions(deg): *0 0.5 1.1 1.9 3.0 4.7 7.0 10.0 14.2*	scan freq: 5 min Elevaions(deg): *0 0.5 1.1 1.9 3.0 4.7 7.0 10.0 14.2*

resolution	*Range 240 Km Resolution:125 m*	*Range 240 Km Resolution:125 m*	Range 240 Km Resolution:125 m	Range 240 Km Resolution:125 m

Table 32: Characteristics of the four radar instruments in Hungary

Data processing and radar products

Radar field corrections

Radar measurements are influenced by many error sources that should be minimized as much as possible. As such, in case of the Hungarian radar data many correction methods are applied to filter out false radar reflectivity measurements. Clutter removal, WLAN filter and clear-air echo filter is implemented in the processing chain of all four-radar data. The beam blockage correction is also implemented in the processing chain in order to correct serious underestimation of precipitation amounts behind mountains. Attenuation correction (the attenuation of electromagnetic waves in water environment, water drops) was implemented in 2019. Hungary does not apply VPR (Vertical Profile Reflectivity) correction.

Precipitation intensity is derived from radar reflectivity with the help of an empirical formula, the Marshall-Palmer equation (R=a*Z^b, where a=200, b=1.6). From the four radar images a composite image over the territory of Hungary is derived every 5 minutes applying the maximum reflectivity in one column method, in order to make adjustments in overlapping regions.

Rain gauge correction of the radar precipitation fields

The non-corrected precipitation field can be corrected by rain gauge measurements. In Hungary, we do not make corrections to instantaneous 5 minutes radar data. In our institute, we only use a correction for the total precipitation for 1, 3-, 6-, 12- and 24-hour periods.

For the accumulated products, we use a special method to accumulate rainfalls: we interpolate the 5-minutes measurements for 1-minute grid by the help of displacement vectors also measured by the radar, and then sum up the images which we got after the interpolation. It is more precise especially when we have storm cells on the radar picture, because a storm cell moves for 5 minutes and thus we do not get continuous precipitation fields when we sum up only with 5 minute periods. This provides satisfying results. However, there is still a need for rain-gauge adjustment because there are obviously places (behind mountains) that the radar does not see.

The radars are corrected with rain gauge data every hour. The correction method using rain gauge data for 1-hour total precipitation consists of two kinds of corrections: the spatial correction which becomes dominant in the case of precipitation extended over a large area, whereas the other factor, the distance correction factor prevails in the case of sparse precipitation. These two factors are weighted according to the actual situation. The weighting factor depends on the actual effective local station density, and also on the variance of the differences of the bias between radar and rain gauge measurements. On the whole, we can say that our correction method is efficient within a radius of 100 km from the radar. In this region, it gives a final underestimation of about 10%, while at bigger distance; the underestimation of precipitation fields slightly increases.

Resolution, projection, threshold of detection

The resolution of the radar data used for validation is 1km by 1km. This is true for the accumulated and the instantaneous products as well. Hungarian radar data is available operationally in stereographic (S60) projection.

References

Péter Németh: Complex method for quantitative precipitation estimation using polarimetric relationships for C-band radars. Proceed. of 5th European Radar Conference (ERAD), Helsinki (Finland) (http://erad2008.fmi.fi/proceedings/extended/erad2008-0270-extended.pdf)

Raingauge network

Distribution of the raingauge stations in Hungary

The automated precipitation measurement network of OMSZ Hungarian Meteorological Service (OMSZ) consist of the following types of instruments:

96 instruments are tipping bucket type (34 Lambrecht Lambrecht 15183H, 62 Lambrecht 15180H), and 37 instruments are weighing type (4 Lambrecht 15184H, 23 OTT Pluvio2, 8 Geonica Datarain4000, 2 EWS HWI).

In addition, 142 weighing type instruments (OTT Pluvio2) belonging to the General Directorate of Water Management of Hungary (OVF) are also maintained by OMSZ and integrated into its network.

Altogether more than 270 automated raingauges are available, but the number is constantly increasing with new installations.

All data of the precipitation network are collected in every 10 minutes and they undergo on a quality check procedure.

Traditional precipitation measurements by human observers (either spacialists or amateurs) are not used for HSAF validation work in Hungary.

The map below shows the Hungarian automated precipitation measurement network, the stations of OMSZ are red and the stations of OVF are green.

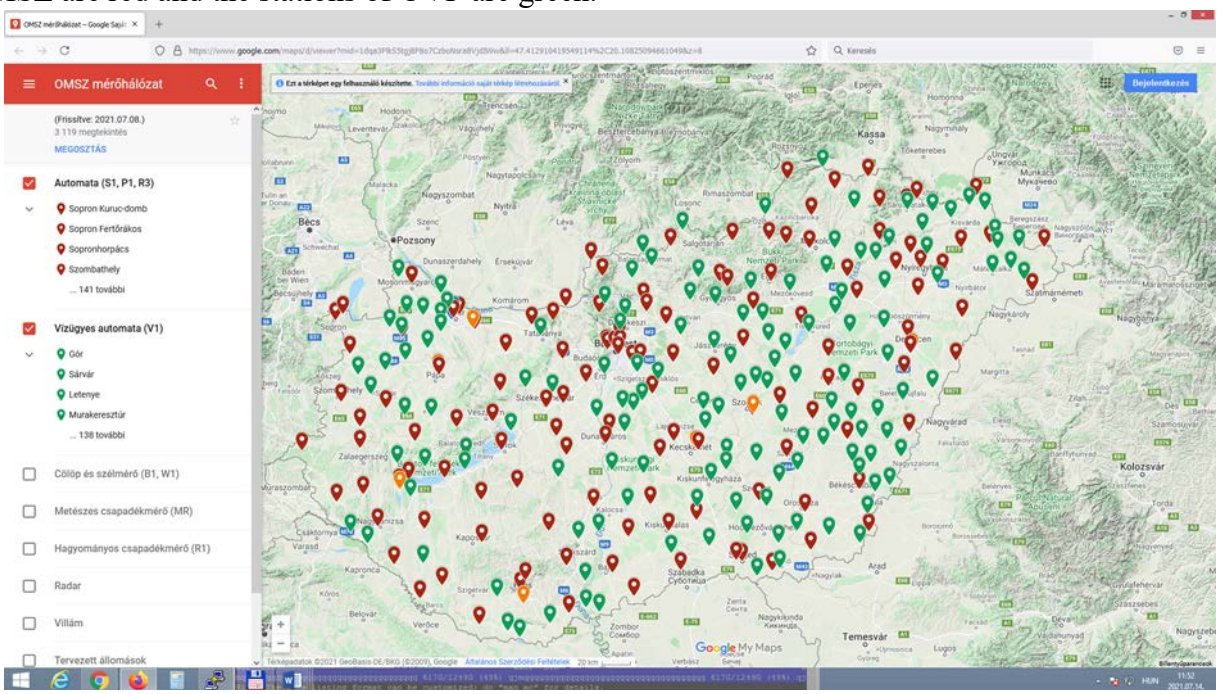

Figure 54: Hungarian automated precipitation measurement network.

A1.5 Ground data in Italy (DPC, UniBo)

Rain gauge

The network

The maximum number of available raingauges is about 3000, irregularly distributed over the surface. On the average, however, a number of stations have low quality data, failure or data transmission problems and their data are missing (-9999 recorded). This number of no data stations is highly varying on hourly/daily basis and ranges from few units to a hundred. In case of data acquired but not transmitted/recorded, the first transmitted measure is the cumulated value over the time when the data were not transmitted.

The average minimum distance between closest stations is about 11 km, with a very high variance: in some regions (such as Tuscany in central Italy) it is below 5 km, while in Emilia Romagna (Po Valley) it is more than 20 km. A study of the decorrelation distance between stations as function of the mutual distance has been carried out for the 2009 dataset. The decorrelation distance is defined as the minimum distance between two observations that makes the Pearson correlation coefficient between the two measures decrease below e^{-1}. Results are shown in Figure 55, where the decorrelation distance is plotted as function of the distance between stations. It appears that there is a large variability of this parameter from higher values (around 60 km for cold months when large precipitating systems dominate and reduces to roughly 10 km when small scale convection is more likely to occur (warm months).
This points out that the distribution of gauges could be able to describe the spatial structures of precipitation fields in case of wintertime rainfall, while may be inadequate for spring/summer convective events.

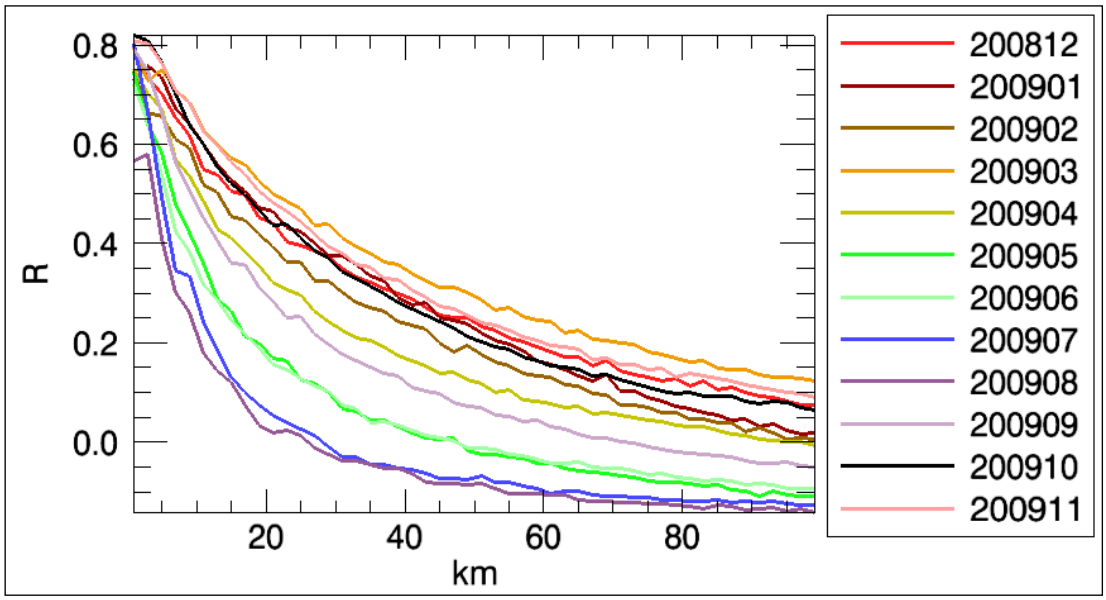

Figure 55: Correlation between rainrates detected by two close stations as function of the distance between the two stations. Colors refer to the month along 2009

In Figure 56 the distribution of working stations over Italy is shown.

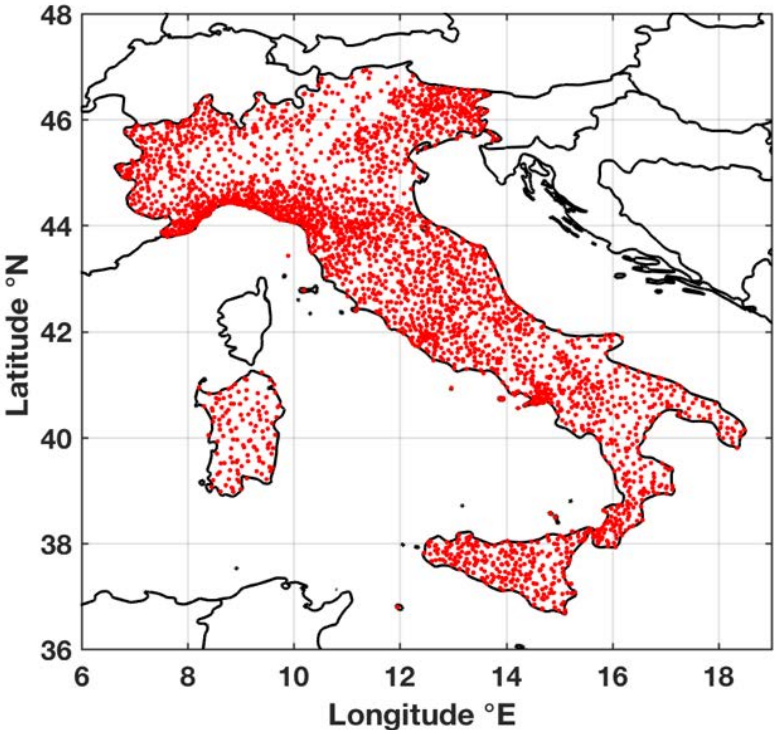

Figure 56: Distribution of the raingauge stations of the Italian network collected by DPC.

The instruments

This section provides the following information:

- All the available raingauge are of tipping bucket type;
- Most of the raingauge have a minimum detected quantity of 0.2 mm, others have 0.1 mm.
- The maximum rainrate that can be measured by the gauges ranges between 300 and 500 mm^{-1} over one minute, depending on the manufacturer.

The rainrate is measured over different cumulation intervals by the different local administrations managing the network, but the data disseminated are all integrated over 60 minutes.

At the moment, the National network made available by DPC provides only hourly data, shorter cumulation times could be available for case studies after specific agreements with local management authorities.

Only a small subset (about 300 stations) of gauges have heated funnel, especially in alpine regions (such as Valle d'Aosta and Piedmont), and this is a clear source of errors in both summer (due to hailfall) and in autumn/winter (due to snowfall).

The data processing

To homogenize the two ground datasets, rain gauge data, preprocessed according to range, persistence, step, and spatial consistency (Shafer et al. 2000) to screen out suspect values, have been interpolated over a regular grid (5 km x 5 km) through the Random Generator of Spatial Interpolation from uncertain Observations (GRISO). The GRISO (Pignone et al. 2010; Feidas et al. 2018) is an improved kriging-based technique implemented by the International Centre on Environmental Monitoring (CIMA Research Foundation). This technique preserves the values observed at

the rain gauge location, allowing for a dynamical definition of the covariance structure associated with each rain gauge by the interpolation procedure. Each correlation structure depends both on the rain gauge location and on the accumulation time considered. GRISO is adopted by all European participating countries in the H SAF validation procedure (Puca et al. 2014). The resulting grid is a 5x5 km regular grid with 240 columns and 288 lines. Moreover, a Digital elevation model is used to provide a mask of Italy in order to: 1) screen out sea-pixels too far from the coastlines and 2) process the pixels with the elevation above sea level.

Radar data

The network

The Italian Department of Civil Protection (DPC) is the authority leading the national radar coverage project in order to integrate the pre-existent regional systems. Currently, the radar network is composed by 22 systems (20 C-band and 2 X-band systems), most of them with dual-polarization. The network is composed by 8 C-band fixed regional installations (five of them are polarimetric), five systems owned by the Italian company for air navigation services (ENAV), 9 dual-polarization systems managed by DPC (7 using C-band and 2 X-band).

The Figure 57 shows the spatial radar coverage of the Italian territory.

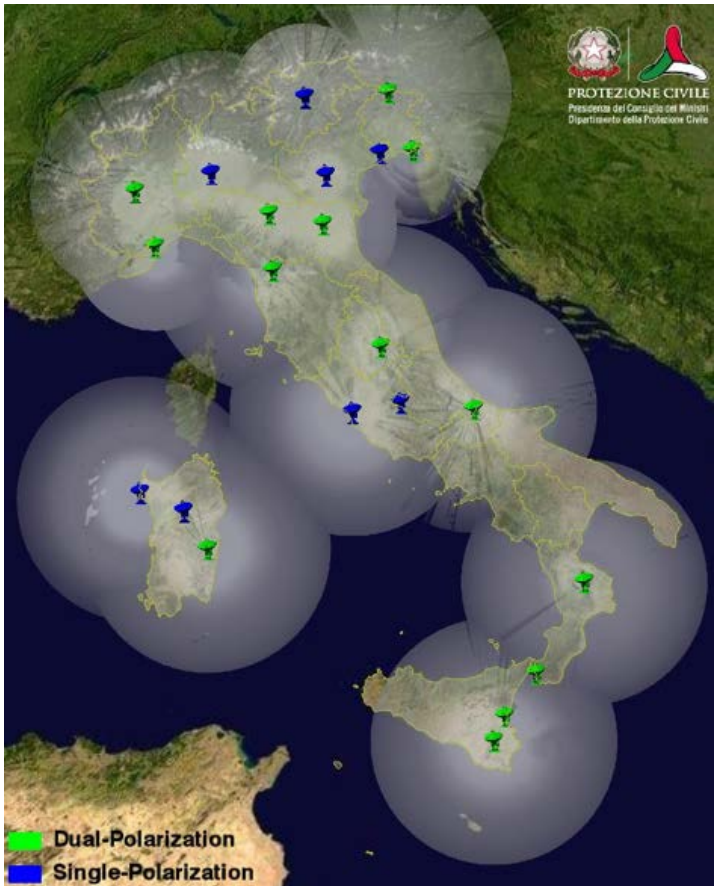

Figure 57: Italian radar network coverage. The green and blue radar symbol stands for dual- and single-polarization system, respectively.

Radar Data processing

The operational radar processing chain is briefly described in this section.
It aims at compensating or at least identifying most of the uncertainty sources conditioning the radar rainfall estimation process (Friedrich et al., 2006). Among them, the following error sources are primarily considered: contamination by non-weather returns (clutter), Partial Beam Blocking (PBB), beam broadening at increasing distances, vertical variability of precipitation (Germann and Joss, 2002; Joss and Lee, 1995; Marzano et al., 2004) and rain path attenuation (Bringi and Chandrasekar, 2001; Carey et al., 2000; Testud et al., 2000; Vulpiani et al., 2008). Every error source is quantified through specific tests ending with the estimation of specific (partial) quality matrices and, when possibile, is compensated for. The overall data quality (Q) is then obtained as a combination of the partial quality matrices. The quality model described in Rinollo et al. (2013) is embedded within the overall processing chain schematically depicted in Figure 24.
In this schematic representation, the sequential flow among consecutive computational steps is specified by black arrows, while the blue ones identify the data input (or output) to (or from) a specific processing module.
The processing chain can be summarized through the following few steps as follows:

i. As typical, the raw volumetric data must be first filtered from non-weather returns. This step is here achieved using the fuzzy-logic approach proposed in Vulpiani et al. (2012) for polarimetric radar systems.
ii. The next step is the correction for Partial Beam Blocking (PBB) based on the retrieved 3-D occlusion map (Bech et al., 2003) that, assuming the e.m. waves propagate in a standard atmosphere, is evaluated only once for a given radar scanning strategy.
iii. The rain path attenuation is just qualitatively evaluated in case the considered radar system has single-polarization capability (Rinollo et al., 2013), otherwise it is compensated for by means of the differential phase shift that needs to be preliminarly processed. In this framework, the iterative moving-window range derivative approach proposed in Vulpiani et al. (2012) is applied here.
iv. The range-related deterioration of radar data quality is modeled through a non-linear function as in Rinollo et al. (2013).
v. Once the attenuation is evaluated and, eventually, compensated for through the so-called ZPHI method (Testud et al., 2000), the overall data quality is computed as geometric mean of the partial quality matrices.

$$Q = q_{clutter} \cdot q_{vertical} \cdot q_{PBB} \cdot q_{distance} \cdot q_{attenuation}$$

vi. The retrieved mean Vertical Profile of Reflectivity (VPR) is applied to the entire volumetric scan with the aim to use all the observations along the vertical to retrieve the surface rainfall rate. All the clutter-filtered and attenuation-corrected (if applicable) PPIs are projected at ground by means of the average Vertical Profile of Reflectivity (VPR).
vii. The Surface Rainfall Intensity (SRI) map is computed as a quality-weighted average of each rain rate map, obtained by each ground-projected reflectivity sweep (Vulpiani et al., 2014).
viii. The SRI composite is built by combining the single-radar rainfall maps through a squared-quality-weighted approach. In case of dual-polarization systems, the composite rainfall retrieval algorithm proposed in Vulpiani and Baldini (2013).

As descripted in Petracca et al. (2018), only radar data with Q values greater than 0.60 are used for comparison with satellite data.

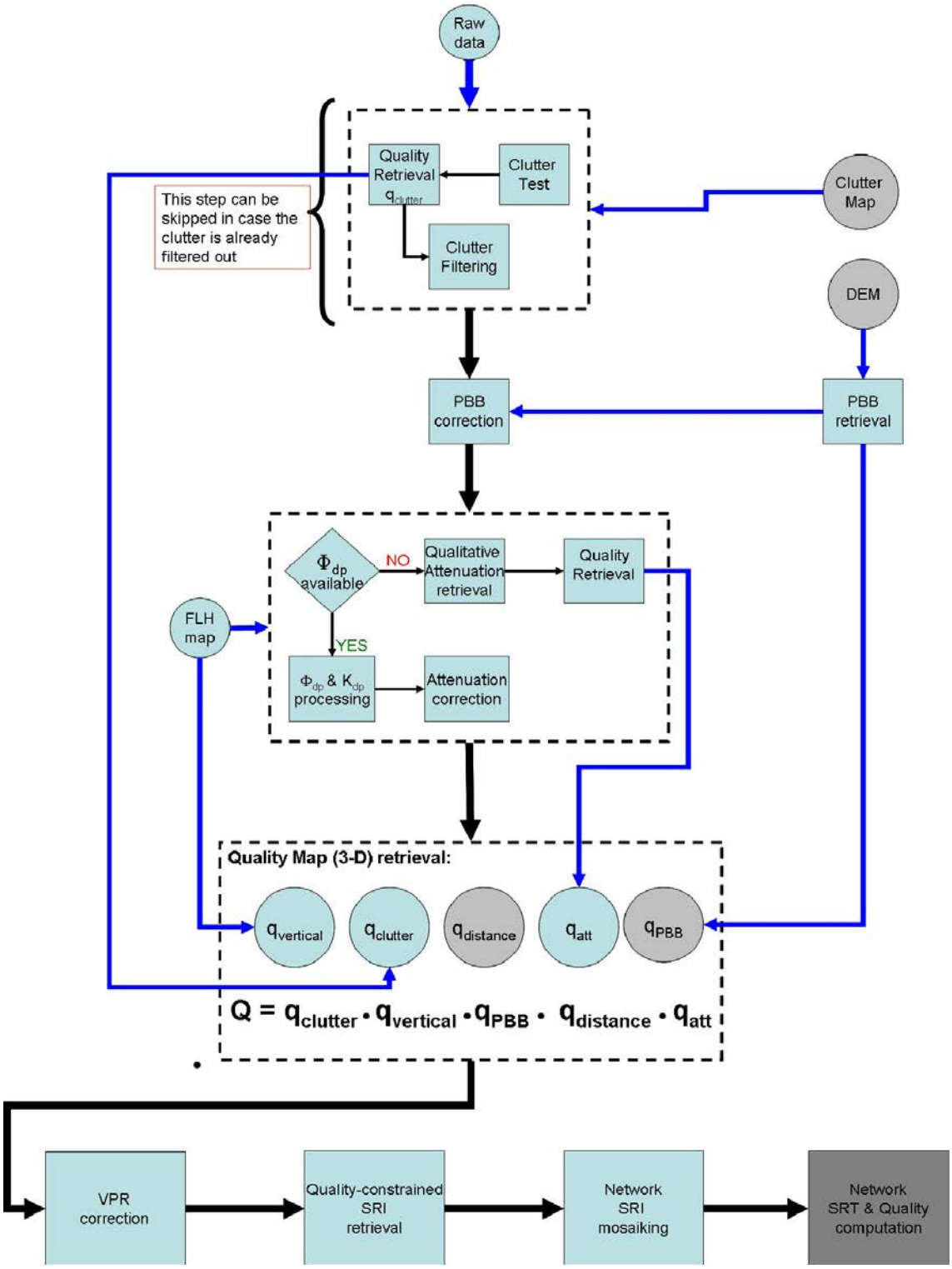

Figure 58: Schematic representation of the Italian radar data processing chain.

References

Bech, J., B. Codina, J. Lorente, and D. Bebbington, 2003: The sensitivity of single polarization weather radar beam blockage correction to variability in the vertical refractivity gradient. J. Atmos. Oceanic Technol., 20, 845–855.

Bringi, V. N. and V. Chandrasekar, 2001: Polarimetric doppler weather radar. Cambridge University Press, 636 pp.

Carey, L. D., S. A. Rutledge, and D. A. Ahijevych, 2000: Correcting propagation effects in c-band polarimetric radar observations of tropical convection using differential propagation phase. J. Appl. Meteor., 39, 1405–1433.

Feidas, H., F. Porcù, S. Puca, A. Rinollo, C. Lagouvardos, and V. Kotroni, 2018: Validation of the H SAF precipitation prod- uct H03 over Greece using rain gauge data. Theor. Appl. Cli- matol., 131, 377–398, https://doi.org/10.1007/s00704-016-1981-9.

Friedrich, K., M. Hagen, and T. Einfalt, 2006: A quality control concept for radar reflectivity, polarimetric parameters, and doppler velocity. J. Atmos. Ocean. Tech., 23, 865–887.

Germann, U. and J. Joss, 2002: Mesobeta profiles to extrapolate radar precipitation measurements above the alps to the ground level. J. Appl. Meteorol., 41, 542–557.

Joss, J. and R. Lee, 1995: The application of radar-gauge comparisons to operational precipitation profile corrections. J. Appl. Meteorol., 34, 2612–2630.

Petracca, M., D'Adderio, L.P., Porcù, F., Vulpiani, G., Sebastianelli, S., Puca, S., Validation of GPM Dual-frequency Precipitation Radar (DPR) rainfall products over Italy, Journal of Hydrometeorology, 19, 907-925, 2018, doi: 10.1175/JHM-D-17-0144.1

Pignone, F., N. Rebora, F. Silvestro, and F. Castelli, 2010: GRISO (Generatore Random di Interpolazioni Spaziali da Osservazioni incerte)-Piogge. Rep. 272/2010, 353 pp.

Puca, S., Baguis, P., Campione, E., Ertürk, A., Gabellani, S., Iwański, R., Jurašek, M., Kaňák, J., Kerényi, J., Koshinchanov, G., Kozinarova, G., Krahe, P., Łapeta, B., Lábó, E., Milani, L., Okon, L., Öztopal, A., Pagliara, P., Pignone, F., Porcù, F., Rachimow, C., Rebora, N., Rinollo, A., Roulin, E., Sönmez, İ., Toniazzo, A., Vulpiani, G., Biron, D., Casella, D., Cattani, E., Dietrich, S., Laviola, S., Levizzani, V., Melfi, D., Mugnai, A., Panegrossi, G., Petracca, M., Sanò, P., Zauli, F., Rosci, P., De Leonibus, L. "The validation service of the hydrological SAF geostationary and polar satellite precipitation products", Nat. Hazards Earth Syst. Sci., 14, 871–889, 2014 www.nat-hazards-earth-systsci.net/14/871/2014/ doi:10.5194/nhess-14-871-2014

Rinollo, A., Vulpiani, G., Puca, S., Pagliara, P., Kanák, J., Lábó, E., Okon, L'., Roulin, E., Baguis, P., Cattani, E., Laviola, S., and Levizzani, V.: Definition and impact of a quality index for radar-based reference measurements in the H SAF precipitation product validation, Nat. Hazards Earth Syst. Sci., 13, 2695–2705, doi:10.5194/nhess-13-2695-2013, 2013.

Shafer, M. A.,C.A. Fiebrich, D. S. Arndt, S. E. Fredrickson, andT.W. Hughes, 2000: Quality assurance procedures in the Oklahoma Mesonetwork. J. Atmos. Oceanic Technol., 17, 474–494, https:// doi.org/10.1175/1520-0426(2000)017,0474:QAPITO.2.0.CO;2.

Testud, J., E. L. Bouar, E. Obligis, and M. Ali-Mehenni, 2000: The rain profiling algorithm applied to polarimetric weather radar. J. Atmos. Oceanic Technol., 17, 332–356.

Vulpiani, G. and L. Baldini, 2013: Observations of a severe hail-bearing storm by an operational X-band polarimetric radar in the mediterranean area. Proceed. of the 36th AMS Conference on Radar Meteorology, Breckenridge, CO, USA.

Vulpiani, G., M. Montopoli, L. D. Passeri, A. Gioia, P. Giordano, and F. S. Marzano, 2012: On the use of dual-polarized C-band radar for operational rainfall retrieval in mountainous areas. J. Appl. Meteor and Clim., 51, 405–425.

Vulpiani, G., P. Tabary, J. P. D. Chatelet, and F. S. Marzano, 2008: Comparison of advanced radar polarimetric techniques for operational attenuation correction at c band. J. Atmos. Oceanic Technol., 25, 1118–1135.

Vulpiani, G., A. Rinollo, S. Puca, m. Montopoli, 2014: A quality-based approach for radar rain field reconstruction and the H SAF precipitation products validation. The eighth European Radar conference on radar in meteorology and hydrology. Garmish-Partenkirken (Germany) 1-5 Sept., 2014.

A1.6 Ground data in Poland (IMWM)

Rain gauge

The network

The maximum number of rain gauges in the Polish ATS (Automatic Telemetric Station) national network is 950. Each ATS post is equipped with two independent rain gauges of the same sort. One of them is heated during the winter period and the other one is not. Therefore precipitation information is derived from 475 points at the time. Fact that rainfall is measured by two equally sensitive instruments two meters away from each other at the same post, enables to apply simple in situ data quality control during summertime. During winter non-heated rain gauge is covered with a cup to prevent it from being clogged by the ice and damaged. Because of that the precipitation information derived from ATS network in winter cannot be verified using this method. It can be stated that during the wintertime precipitation information might be a slightly bigger measuring error.

The number of rain gauges available for H SAF validation activities varies from day to day due to operational efficiency of ATS network in Poland and depends on large number of independent factors. It can be stated that the number varies between 330 and 475 rain gauges for each day of operational work.

Mean minimum distance between precipitation measuring ATS posts (between each pair of rain gauges) in Polish national network is 13,3 km.

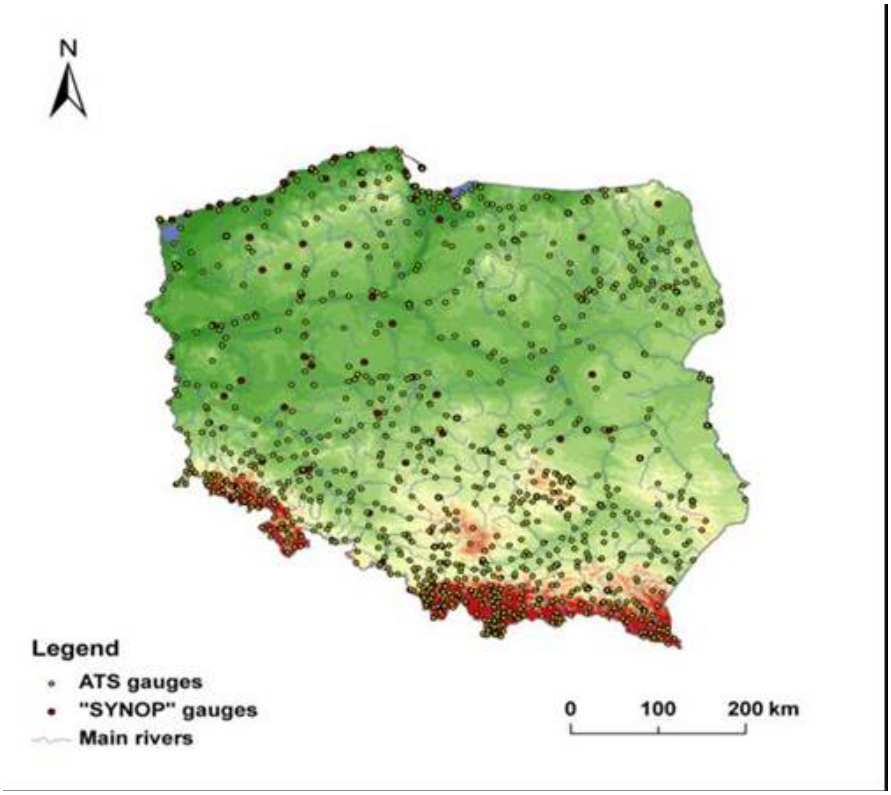

Figure 59: ATS national network in Poland

The instruments

All rain gauges working within Polish ATS national network are MetOne tipping bucket type instruments. Minimum detected quantity that can be measured by those rain gauges is 0,1 mm/h which means that each tilt of rain gauge bucket adds 0,1mm to the total sum of the measured precipitation. During very heavy precipitation events MetOne rain gauges tend to underestimate real

precipitation by factor of 10%. Maximum measured rainrate *(mmh^{-1})* by MetOne instruments in Poland was recorded in 5.06.2007 at ATSO Koscielisko Kiry at the foot of Tatra Mountains. The recorded values reached 65 mm/h. Operational cumulation interval *(min)* of ATS network rain gauges is set for 10 minutes and can be adjusted according to given needs. There is possibility to have very short cumulation intervals for case studies - theoretically 1 minute - but not on every given precipitation post. It depends on local DCS settings.

The data processing

As stated above the data quality control can be achieved by comparison on two rainfall datasets collected by two independent rain gauges at the same ATS post. It is done operationally during summertime. There is no such possibility during the winter because of lack of non-heated rain gauge dataset. In case that one pair of rain gauges at the same ATS post provide two different rainfall readings the higher one is taken into account.

No specialization technique is used for standard validation process. However, for some case studies, the Natural Neighbor technique is applied for satellite and ground precipitation data. To match the precipitation information with satellite data spatial and temporal matching are applied.

- Spatial matching: for each given satellite pixel, the posts situated within that pixel were found. The pixel size was taken into account, however, its shape was assumed to be rectangular. If more than one rain gauge were found within one satellite pixel, the ground rain rate value was calculated as a mean of all rain gauges measurements recorded within that pixel;
- Temporal matching: satellite derived product is combined with the next corresponding ground measurement. As the ground measurements are made with 10 minute time resolution, the maximum interval between satellite and ground precipitation is 5 minutes.

Radar data

The Polish meteorological radar network called POLRAD (initially Doppler Radar System METEOR) consists of eight devices and was produced by Gematronic Weather Radar Systems GmbH SELEX Sistemi Integrati GmbH. The system had been installed in Poland starting from year 2001 and has its 20th anniversary this year. The software running within this system is Rainbow 5 (and it's later updates). The radars are using band C (frequency 5,6 GHz and subsequently 5,4 cm wavelength). All of the radars are Doppler instruments operationally run in 10 min. scan frequency and two of them (Ramża and Pastewnik) in dual polarisation mode.

Eight basic radars working within the POLRAD network.

Station location	Latitude	Longitude	Elevation a.m.s.l.	Antenna height a.t.l.	Radar type
Legionowo	52°24'18,79''	20°57'39,28''	89,0 m	29,0 m	Doppler radar METEOR 1500 C
Rzeszów	50°06'49,79''	22°02'12,09''	206,5 m	30,0 m	Doppler radar METEOR 1500 C
Brzuchania	50°23'39,13''	20°05'00,35''	388,5 m	35,0 m	Doppler radar METEOR 500 C
Ramża	50°09'04,59''	18°43'29,86''	320,7 m	36,0 m	Dual polarisation Doppler radar METEOR 1600C

Pastewnik	50°53’32,81’’	16°02’22,17’’	666,5 m	23,5 m	Dual polarisation Doppler radar METEOR 1600C
Poznań	52°24’47,73’’	16°47’49,40’’	95,1 m	35,0 m	Doppler radar METEOR 500 C
Świdwin	53°47'40,25"	15°50'16,97"	121,1 m	30,0 m	Doppler radar METEOR 500 C
Gdańsk	54°23’03,17’’	18°27’23,00’’	135,2 m	20,0 m	Doppler radar METEOR 1500 C

Table 33: Radars in Poland

The original radar arrangement in Poland (when installed).

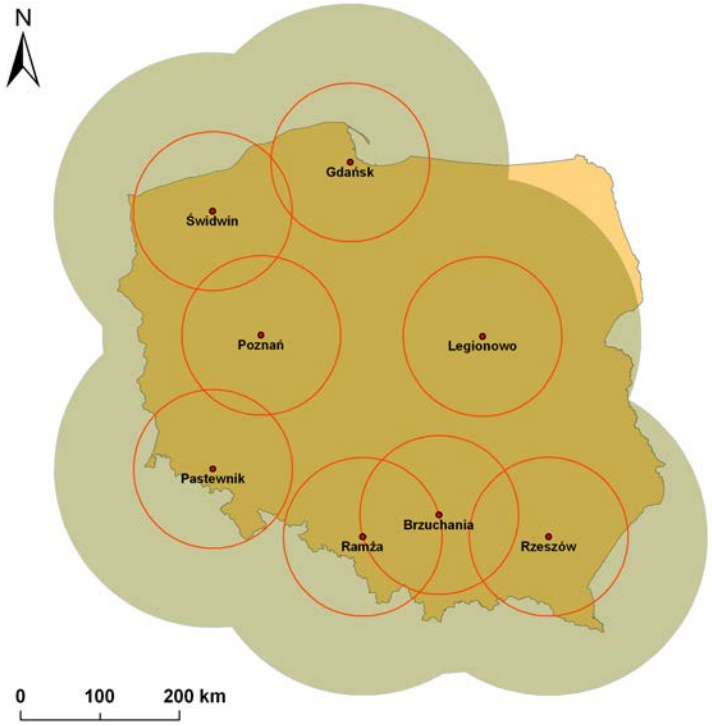

Figure 60: Radar dislocation in Poland

The radar ranges drawn above represent both 125 km and 250 km ranges respectively.

The spatial resolution of the radar scan is 1 km, the data resolution in azimuth is 1° on average, hence within a circumference of a given radius 200 km one elevation angle returns 72 000 virtual measurement points. The basic max reflectance radar information is gathered from 10 elevation angles so one measurement cycle (max reflectance only, no Doppler wind information received) returns 720 000 points. To make this information valid, one point requires 256 levels – 8 bits of information. Concluding, one reflectance only measurement cycle requires 720 kB.

Since the beginning of the millennium Poland has operational meteorological radar data exchange with neighbouring countries. The current composite radar map of Poland looks as follows (incorporating radar data received on the basis of transnational radar data exchange).

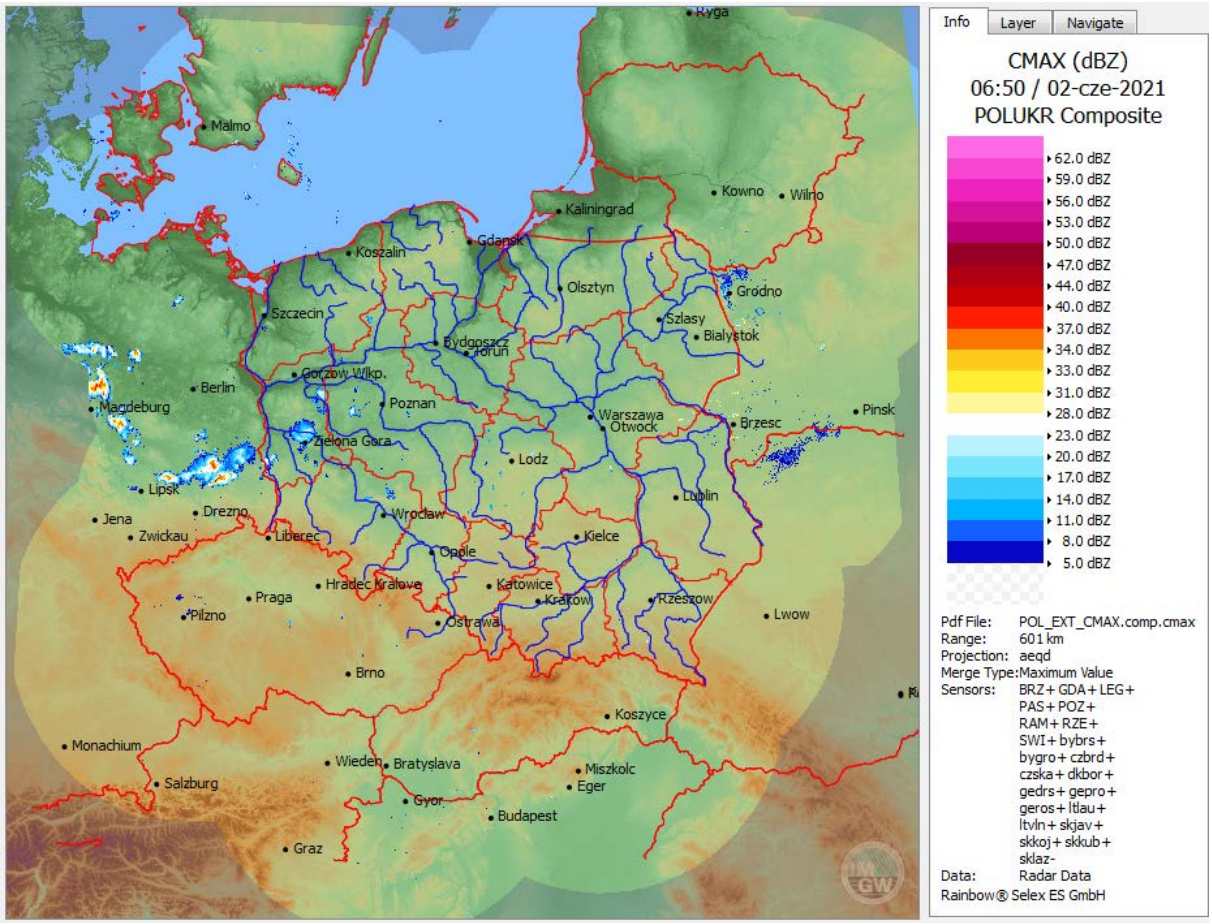

Figure 61: Radar composite map in Poland

The operational radar data exchange is maintained with Germany, Czechia, Denmark and Slovak Republic. The cooperation was initiated in 1998 within Baltrad and Opera projects and is still kept valid.

Foreign radars that provide data on operational basis.

Station location	Longitude	Latitude
Brdy-Praha	13.817800	49.658300
Skalky	16.788500	49.501100
Kojsovska	20.987277	48.782895
Maly Javornik	17.153100	48.256100
Kubinska Hola	19.249350	49.271670
Spani Laz	19.257430	48.240430
Protzel	13.858210	52.648660
Rostock	12.058070	54.175660
Dresden	13.768630	51.124630
Bornholm	14.887517	55.112750

Table 34: Operational foreign radars.

The non-operational radar data exchange is carried out with Belarus, Ukraine and Latvia. The data aren't operationally provided and sometimes are very burdened with artificial errors, hence they are not included in the operational composite radar map of Poland.

Foreign radars that provide test or non-operational data.

Station location	Longitude	Latitude
Laukuva	22.239500	55.609040
Traky	25.106780	54.626220
Grodno	24.048889	53.651943
Minsk	28.040277	53.865833
Brzesc	23.898611	52.115276
Lviv	23.900514	49.848378

Table 35: Non-operational foreign radars.

It is worth mentioning that in the current year 2022 the POLRAD system is being upgraded to new instruments and software. The work will continue in the next year (2023). All new radars will be Doppler class magnetron instruments with dual polarisation. In addition, there will be two completely new radars located in Użranki and Góra Św. Anny.

The new radars that will be installed in 2023.

Station location	Longitude	Latitude
Użranki	21,4121	53,8557
Góra Św. Anny	18,1530	50,4640

Table 36: New radars with forthcoming installation

A1.7 Ground data in Slovakia (SHMÚ)

Rain gauge

The network

In Slovakia there are overall 98 automatic rain gauge stations potentially available for the H SAF project. The real number of usable gauges varies with time because on average about 20 of them are out of operation.

Mean minimum distance between rain-gauges in the complete network is 7,74 km. Map of the rain gauge network in Slovakia containing also climatological and selected hydrological stations is shown in next figure.

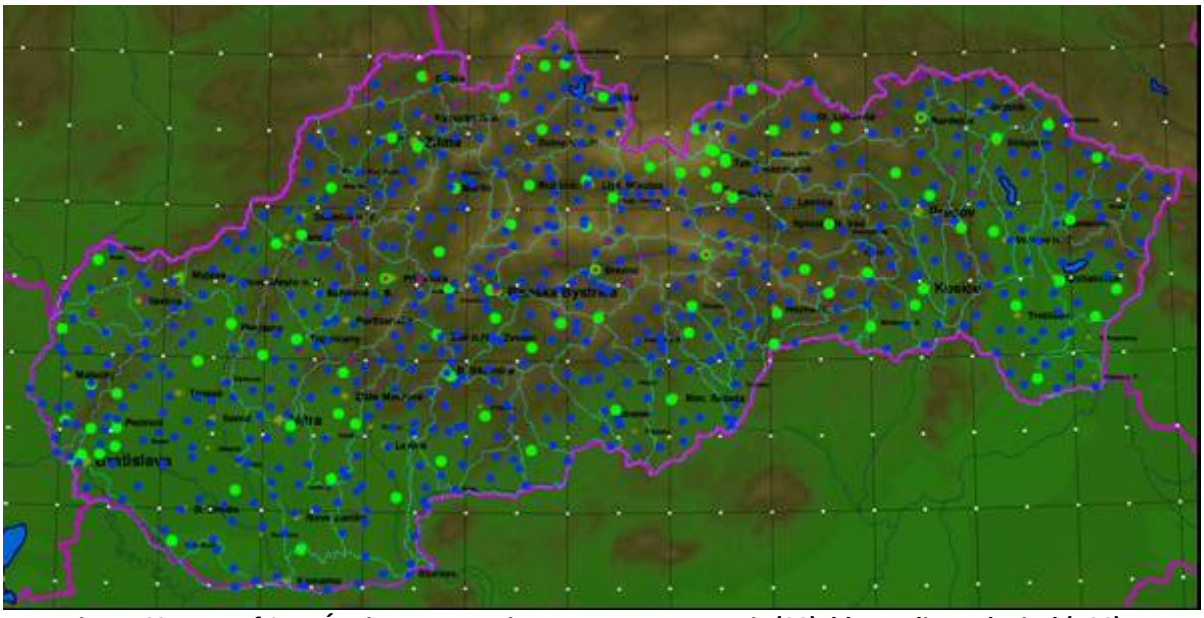

Figure 62: Map of SHMÚ rain gauge stations: green – automatic (98), blue – climatological (586), red - hydrological stations in H SAF selected test basins (37)

The instruments

Type of all the automatic rain gauges is tipping bucket (without heating of the funnel). The gauges are able to measure precipitation rates ranging from 0,1 to 200 mm/h at 10 min operational accumulation interval. Shorter accumulation interval of 1 min is also possible which makes the instruments suitable for case studies in the H SAF project.

The data processing

The rain gauge data are not used at SHMÚ directly for the H SAF precipitation validation but they are utilized as the input to the INCA precipitation analysis system which is supposed to become a new validation tool. Prior the INCA analysis the rain gauge data are interpolated onto the regular 1x1 km grid using the inverse-distance-squared (IDS) interpolation method. Only the 8 nearest rain gauge stations are taken into account in the interpolation in order to reduce occurrence of precipitation bull-eyes artifact.

SHMÚ performs the offline automatic and manual quality check of the rain gauge data. In frame of the INCA system a quality control technique called blacklisting has been developed which avoids the data from systematically erroneous rain gauges to enter the analysis. Currently the blacklisting is used in manual mode only.

Radar data

The network

The Slovak meteorological radar network consists of 4 radars (see next figure). One is situated at the top of Maly Javornik hill near city Bratislava, second one is on the top of Kojsovska hola hill close to the city Kosice. The third and fourth radars are installed on Kubinska hola in Orava region and on Spani laz in the south of Central Slovakia. All of them are Doppler, dual-polarization C-band radars of the same type.

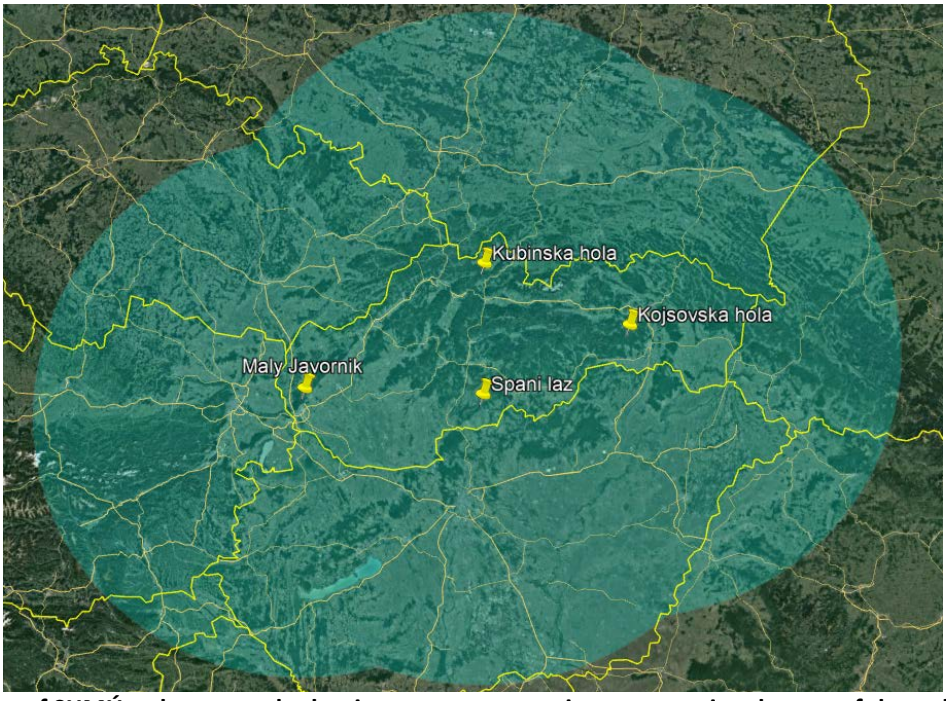

Figure 63: Map of SHMÚ radar network; the rings represent maximum operational range of the radars – 240 km

The instruments

The radars are operated and technically maintained by SHMÚ. Receivers of radars are calibrated regularly by means of internal test signal generator (TSG) every 6 months. The peak power of the transmitted pulses is calibrated with the same periodicity using calibrated power meters.

The basic parameters of SHMÚ radars are summarized in following table.

	Maly Javornik	*Kojsovska hola*	*Kubinska hola*	*Spani laz*
Frequency band	C-Band, Yes 5605 MHz	C-Band, Yes 5645 MHz	C-Band, Yes 5630 MHz	C-Band, Yes 5615 MHz
Polarization (Single/Double)	Double	Double	Double	Double
Doppler capability (Yes/No)	Yes	Yes	Yes	Yes
Scan strategy: scan frequency, elevations,	*Scan frequency: 5 min*	*Scan frequency: 5 min*	*Scan frequency: 5 min*	*Scan frequency: 5 min*

maximum nominal range distance, range resolution	*Elevations (deg): 0.0 0.5 1.0 1.5 2.0 2.7 3.4 4.4 7.0 11.4 18.3 26.7* *Range: 240 km* *Resolution: 250m*	*Elevations (deg): 0.0 0.5 1.0 1.5 2.0 2.7 3.4 4.4 7.0 11.4 18.3 26.7* *Range: 240 km* *Resolution: 250m*	*Elevations (deg): 0.0 0.5 1.0 1.5 2.0 2.7 3.4 4.4 7.0 11.4 18.3 26.7* *Range: 240 km* *Resolution: 250m*	*Elevations (deg): 0.0 0.5 1.0 1.5 2.0 2.7 3.4 4.4 7.0 11.4 18.3 26.7* *Range: 240 km* *Resolution: 250m*

Table 37: Characteristics of the SHMÚ radars

<u>The data processing</u>

For ground clutter removal the GIP frequency domain filter is used. Isolated bins in the range and azimuth direction are removed by the speckle removal filters. The data with intensities around the noise level and below are eliminated using the LOG threshold.

The measured radar reflectivity is corrected for atmospheric (clear-air) attenuation of the radar beam. RLAN interference is removed using the Interference filter and SQI thresholding in the signal processor. The radar reflectivity is then corrected for attenuation of the radar beam in the precipitation. In the final step, dual-pol filtering of the non-meteorological echoes is applied on the reflectivity data which removes also most of the remaining interference.

Correction for vertical profile of reflectivity (VPR) is not applied at SHMÚ. However beam blocking correction is being used in the quality-checking step for the H SAF validation due to complicated orographical conditions in Slovakia. Software filter for the RLAN interference detected by radars is currently in development at SHMÚ.

Quality-based radar composite CAPPI 2 km products from all radars is used for the H SAF validation. The composition algorithm uses several quality-checking algorithms, where distance from radar, beam-blockage, spike-detection (similarity with neighbor values) and comparison with NWCSAF cloud-type and clout-top-height are considered and evaluated as quality indexes. The resulting value in the overlapping area of several radars is computed as weighted average of values from different radars, where weights are evaluated quality indexes.

Precipitation intensity is derived from radar reflectivity according to the Marshall-Palmer equation (Z=a*R^b) with constant coefficients valid for stratiform rain (a=200, b=1.6).

No raingauge correction of the derived instantaneous precipitation is applied. Effect of elevating radar beam with increasing range and beam attenuation is reduced by limiting the validation area to rain effective range of 120 km for both radars in the composite.

The instantaneous precipitation products are provided in Mercator projection with approximately 1 km resolution. Threshold for precipitation detection is 0,02 mm/h. Time resolution of the current instantaneous products is 5 minutes, for the products prior to April 2010 it was 10 minutes and prior to August 2009 15 minutes.

Precipitation accumulation in case of 3-hourly interval is based on integration of 5 (10 or 15) minutes instantaneous measurements in time period of 3 hours. Accumulated precipitation for intervals of 6, 12 and 24 hours is calculated as a sum of the 3-hourly accumulated precipitation. At least 92% of instantaneous measurements must exist in relevant time period for the 3-hourly accumulated product to be produced.

No rain gauge correction of the accumulated precipitation is applied but the same limitation of validation area is used as for the instantaneous product. Threshold for precipitation detection of the 3-hourly accumulated product is 0,5 mm. Geographical projection and space resolution of the accumulated products are the same as those of instantaneous product (see above).

For validation of H SAF precipitation products it is necessary to know errors distribution of used ground truth data – in case of SHMÚ it is precipitation intensity and accumulated precipitation measured by Slovak radar network. For this purpose a study called "SHMU study on evaluation of radar measurements quality indicator with regards to terrain visibility" has been elaborated (/hsaf/WP6000/WP6100/precipitation/WG_groups/WG2-radar/WG-2-3_radar quality indication_v1.doc). To find distribution of errors in radar range next steps had to be done:

- simulations of terrain visibility by radar network using 90m digital terrain model
- statistical comparison of radar data against independent rain gauge data measurements
- derivation of dependence (regression equation) describing the errors distribution in radar range with regard to terrain visibility, based on rain gauge and radar data statistical evaluation computation of error distribution maps using regression equation and terrain visibility

Main results of this study are shown in next figure. It is evident that the best visibility of SHMU radars corresponds to the lowest PR-RMSE-RMSE of 60% displayed by light violet colors. PR-RMSE-RMSE is of quite homogeneous distribution with average of 69% in prevalent lowlands of Slovakia displayed by bluish colors. But in central and north-west mountainous areas this error exceeds 100%.

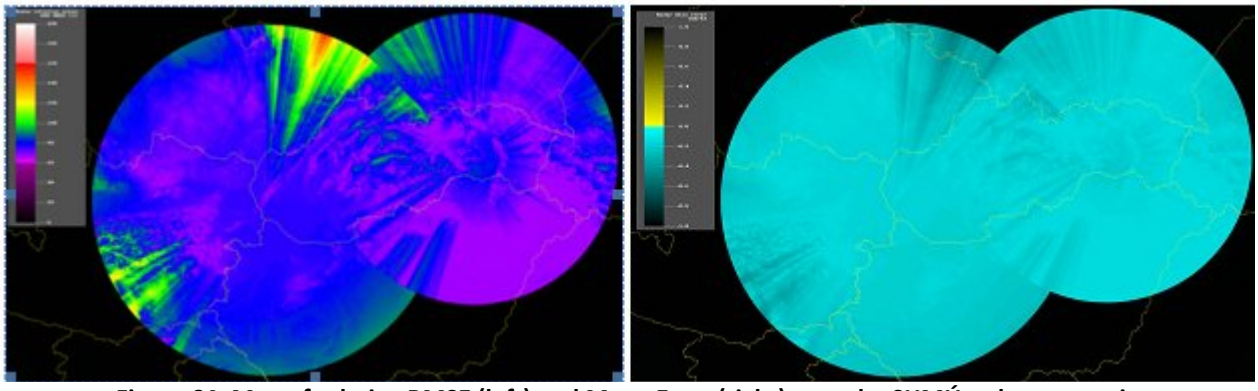

Figure 64: Map of relative RMSE (left) and Mean Error (right) over the SHMÚ radar composite

Similar studies that have been carried out in the PPVG on comparison of radar data with rain gauge data have shown in general that RMSE error associated with radar fields depends considerably on radar minimum visible height above the rain gauge especially in mountainous countries. In lowlands this dependence is not so significant, but no negligible. The reason can be the location of radar sites at the top of hills and impossibility of the lowest elevation to reach the lowland's surface. In case of Slovakia the PR-RMSE error of radar accumulated fields is between 60-90%, with an average PR-RMSE value of 69,3%. Mean Error specified for 24-hours cumulated precipitation is -4,42mm or converted into instantaneous precipitation -0,184 mm/h. RMSE specified for 24-hours cumulated precipitation is 9,48mm or converted into instantaneous precipitation 0,395 mm/h.
Complete SHMU study is available on the H SAF ftp server:
/hsaf/WP6000/WP6100/precipitation/WG_groups/WG2-radar/WG-2-3_radar quality indication_v1.doc

A1.8 Ground Data in Turkey

Rain gauge

The network

356 Automated Weather Observation Station (AWOS) distributed over the country are used for the validation of the satellite precipitation products in the H SAF project. The average distance between the AWOS sites is 40.5 km.

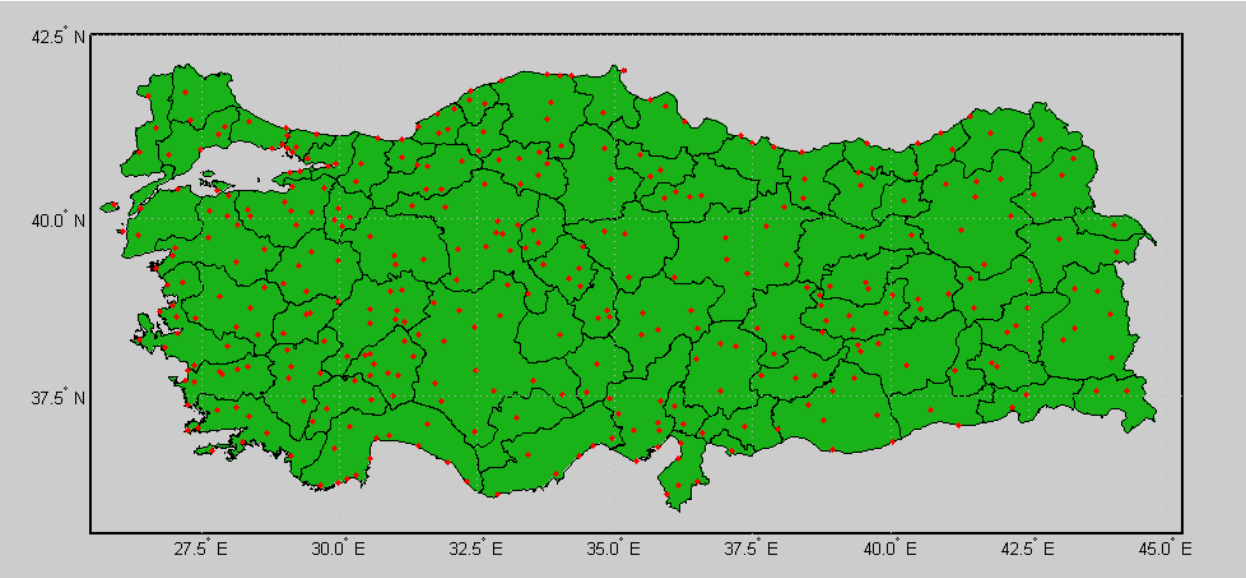

Figure 65: Map Turkish rain gauge stations

The instruments

The gauge type of the network is tipping bucket where each has a heated funnel. The minimum detection capability of the gauge is 0.2 mm per tip. In the maximum capacity of the instrument is 720 mm/h at most. The operational accumulation interval is 1 minute, so that alternative cumulation intervals such as 5, 10, 20, 30 minutes are possible.

Data processing

Quality control

High quality of the ground data is critical for performing the validation of the precipitation products. The validation results or statistics can provide meaningful feedbacks for the product developers and additionally the products can be used reliably only if there is a confidence present about the ground data at a certain level. For this reason, some predefined quality assurance (QA) tests are considered for the precipitation data in order to define the confidence level. First of all, a flagging procedure is defined as described in next table

QA Flag Value	QA Status	Brief Description
0	Good	Datum has passed all QA Test
1	Suspect	There is concern about accuracy of datum
2	Failure	Datum is unstable

Table 38: The precipitation data QA tests are summarized as follows.

Range Test

This test is used to see if any individual precipitation observation falls within the climatological lower and upper limits. The test procedures applied in the study are as follows.

IF $Lim_{Lower} \leq Obser_{j,t} \leq Lim_{Upper}$ **THEN** $Obser_{j,t}$ flag is **'Good'**
IF $Obser_i > Lim_{Upper}$ **OR** $Obser_{j,t} < Lim_{Lower}$ **THEN** $Obser_{j,t}$ flag is **'Failure'**

Lim_{Lower} and Lim_{Upper} thresholds are separately determined for each station on a monthly basis. At any specific site, all the observed monthly data is considered for determination of the upper and lower limits. By applying this test, each observation is flagged either by 'Good' or 'Failure' label depending on the comparison tests mentioned above.

Step Test

It is used to see if increment/decrement between sequential observations in time domain is in acceptable range or not. The applied test procedure is,

IF $|Obser_{j,t}-Obser_{j,t-1}| < Step_j$ **THEN** $Obser_{i,t}$ flag is **'Good'**
IF $|Obser_{j,t}-Obser_{j,t-1}| > Step_j$ **THEN** $Obser_{i,t}$ flag is **'Suspect'**

$Step_j$ threshold is determined again for each site on a monthly basis. For each site, the dataset containing the absolute difference of the sequential observations is determined by considering the observations for the matching month. The 99.9 % cumulative histogram value of the dataset is set as the $Step_j$ threshold for the related site and month.

Persistence Test

Persistence test is used to determine if any group of observations are due to instrument failures. The test procedure applied is defined as,

IF T < Δ THEN Flag for all Obser in T **: 'Good'**
IF T > Δ THEN Flag for **all** Obser in T **: 'Suspect'**

where T is the total number of the sequentially repeating observations forward in time and Δ is the possible maximum number of sequentially repeating observations. As in the other two tests, Δ threshold is determined for each site on a monthly basis. For any site, the data belonging to the same month is taken into account to determine the repeating number of the sequential observations. Then, 99.9 % cumulative histogram value of the repeating number dataset is assigned as the Δ amount for the corresponding site and month. Since there is a high possibility of no-precipitation data (zero), the sequential zero observations are excluded in this test during the determination of the Δ threshold amount and application of the test.

QA Test procedure

By applying the control procedures of the QA test mentioned above, each individual precipitation observation receives three flags referring to the corresponding test. For the corresponding observation if all the test flag is not 'Good' then the observation is excluded from the validation process.

Use of spatialization technique

Due to the time and space structure of precipitation and to the sampling characteristics of both the precipitation products and observations used for validation, care has to be taken to bring data into comparable and acceptable range. At a given place, precipitation occurs intermittently and at highly fluctuating rates. Various maps, time series analysis, statistical and probabilistic methodologies are employed in the validation procedure classically, but some additional new aspects such as the

spatial coverage verification model of point cumulative semivariogram (PCSV) approach (Şen and Habib, 1998) are proposed for usage in this work.

Each precipitation product within the H SAF project represents a foot print geometry. Among these, H01 and H02 products represent an elliptical geometry while H03B and H05 have a rectangular geometry. On the other hand, the ground observation (rain gauge) network consists of point observations. The main problem in the precipitation product cal/val activities occurs in the dimension disagreement between the product space (area) and the ground observation space (point). To be able to compare both cases, either area to point (product to site) or point to area (site to product) procedure has to be defined. However, the first alternative seems easier. The basic assumption in such an approach is that the product value is homogenous within the product footprint. Next figure presents satellite footprint (FOV) centers of the H01 and H02 products, an elliptical footprint for the corresponding center (area within the yellow dots) and Awos ground observation sites. The comparison statistic can be performed by considering just the sites in the footprint area. Although this approach is reasonable on the average but it is less useful in spatial precipitation variability representation. The comparison is not possible when no site is available within the footprint area.

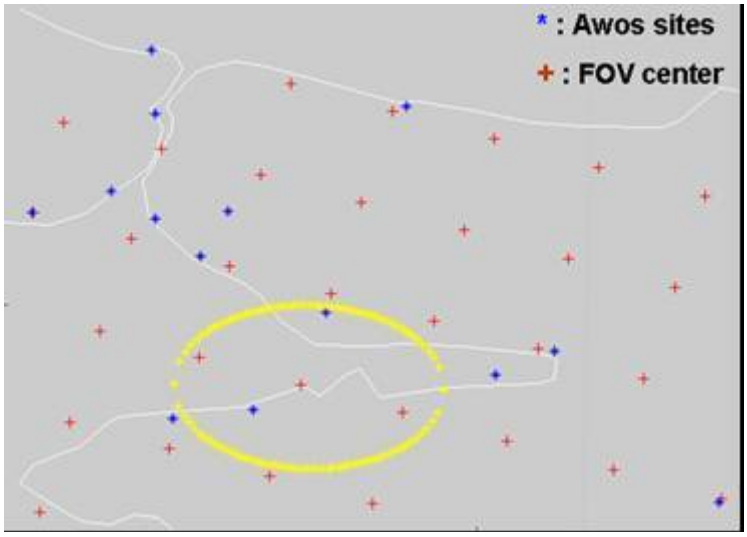

Figure 66: H01 and H02 products footprint centers with a sample footprint area as well as the Awos ground observation sites.

Alternatively, the point to area approach is more appealing for the realistic comparison of the precipitation product and the ground observation. This approach is simply based on the determination of the true precipitation field underneath the product footprint area. To do so, the footprint area is meshed and precipitation amounts are estimated at each grid point by using the precipitation observations at the neighboring Awos sites as shown in Figure 67. A 3x3 km grid spacing is considered for the products with elliptical geometry while 2x2 km spacing is considered for the products with rectangular geometry. For any grid point, Awos sites within the 45 km for the time period of April-September (convective type) and 125km for the rest (stratiform type) are taken into consideration. At each grid point, the precipitation amount is estimated by,

$$Z_m = \frac{\sum_{i=1}^{n} W(r_{i,m}) Z_i}{\sum_{i=1}^{n} W(r_{i,m})} \qquad (4.13.1)$$

where Z_m is the estimated value and $W(r_{i,m})$ is the spatially varying weighting function between the i-th site and the grid point m.

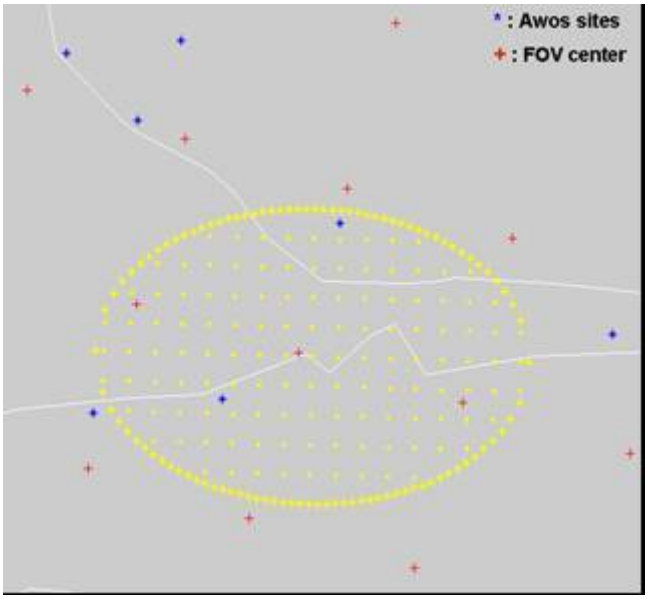

Figure 67: Meshed structure of the sample H01 and H02 products footprint.

Determination of the $W(r_{i,m})$ weighting function in Equation 1 is crucial. In open literature, various approaches are proposed for determining this function. For instance, Thiebaux and Pedder (1987) suggested weightings in general as,

$$W(r_{i,m}) = \begin{cases} \left(\frac{R^2 - r_{i,m}^2}{R^2 + r_{i,m}^2} \right)^{\alpha} & \text{for} \quad r_{i,m} \le R \\ 0 & \text{for} \quad r_{i,m} \ge R \end{cases} \qquad (4.13.2)$$

where R is the radius of influence, $r_{i,m}$ is the distance from point i to point m to the point and α is a power parameter that reflects the curvature of the weighting function. Another form of geometrical weighting function was proposed by Barnes (1964) as,

$$W(r_{i,m}) = \exp\left[-4 \left(\frac{r_{i,m}}{R} \right)^{\alpha} \right] \qquad (4.13.3)$$

Unfortunately, none of these functions are observation dependent but suggested on the basis of the logical and geometrical conceptualizations only. They are based only on the configuration, i.e. geometry of the measurement stations and do not take into consideration the natural variability of the meteorological phenomenon concerned. In addition, the weighting functions are always the same from site to site and time to time. However, in reality, it is expected that the weights should reflect to a certain extent the regional and temporal dependence behavior of the phenomenon concerned.

For the validation activities, the point cumulative semi-variogram technique proposed by Şen and Habib (1998) is used to determine the spatially varying weighting functions. In this approach, the weightings not only vary from site to site, but also from time to time since the observed data is used. In this way, the spatial and temporal variability of the parameter is introduced more realistically to the validation activity.

Matching approach

The temporal and spatial matching approaches are applied separately in the validation of the satellite products. As for the temporal matching, the product time is taken into account and 5 minute window (t-2 to t+3) is considered for estimation of the average rainrate for each site.

For the spatial matching, the mesh grid size of 3kmX3km is constructed for each IFOV area. For each grid point, the rainrate is estimated by taking the 5 minute averaged rainrate amounts observed at the nearby AWOS sites within the radius distance of 45 km(for convective type) or 125 km(for stratiform type) considering the weighting of each site with respect to the grid point(Equation 1). The weighting amounts are derived from the spatially varying weighting functions obtained by using the semi-variogram approach (Şen and Habib,1998). Finally, the Gaussian filter is applied to the estimations at the mesh grid of the IFOV area to get the average rainrate. Then, this amount is compared with the satellite precipitation product amount for the validation purposes.

Appendix 3 Continuous statistical scores

H60B vs Grd	RADAR LAND		RADAR SEA		RADAR COAST		GAUGE LAND		OVERALL	
	≥1 mm/h	≥10 mm/h	≥1 mm/h	≥10 mm/h	≥1 mm/h	≥10 mm/h	≥1 mm/h	≥10 mm/h	≥1 mm/h	≥10 mm/h
Nsat	1'329'158	28'465	345'458	12'341	321'171	10'197	2'281'090	36'827	4'276'877	87'830
Nref	848'255	43'083	471'758	25'355	346'884	18'119	1'731'400	45'612	3'398'297	132'169
ME	-2.45	-17.82	-2.48	-15.71	-2.53	-16.62	-1.63	-11.37	-2.05	-15.02
SD	5.71	16.12	5.33	14.39	5.40	14.69	3.04	7.31	4.47	13.42
MAE	3.18	18.00	3.26	15.95	3.25	16.82	2.33	11.59	2.77	15.23
MB	0.33	0.14	0.33	0.18	0.31	0.16	0.43	0.26	0.37	0.19
CC	0.21	0.17	0.23	0.16	0.22	0.17	0.30	0.17	0.23	0.14
RMSE	6.21	24.03	5.88	21.31	5.96	22.18	3.45	13.52	4.91	20.14

Table 39: Continuous statistical scores for H60B vs Ground over European area.

H60B vs DPR	LAND			SEA			COAST			OVERALL		
	≥0 mm/h	≥1 mm/h	≥10 mm/h	≥0 mm/h	≥1 mm/h	≥10 mm/h	≥0 mm/h	≥1 mm/h	≥10 mm/h	≥0 mm/h	≥1 mm/h	≥10 mm/h
Nsat	5'389'732	89'129	4'386	11'299'398	158'776	6'116	1'914'021	17'155	482	18'603'151	265'060	10'984
Nref	5'389'732	59'555	1'751	11'299'398	149'927	5'403	1'914'021	20'576	495	18'603'151	230'058	7'649
ME	0.03	-0.75	-8.95	-0.01	-1.57	-12.60	-0.01	-1.75	-14.23	0.00	-1.37	-11.87
SD	0.64	4.41	10.87	0.61	4.00	10.33	0.50	3.55	9.78	0.61	4.09	10.55
MAE	0.08	2.65	11.55	0.09	2.59	13.32	0.07	2.35	14.69	0.08	2.59	13.01
MB	1.56	0.74	0.46	0.90	0.48	0.30	0.73	0.32	0.18	1.03	0.53	0.33
CC	0.39	0.31	0.17	0.38	0.34	0.27	0.25	0.21	0.10	0.37	0.32	0.22
RMSE	0.64	4.47	14.08	0.61	4.30	16.29	0.50	3.96	17.27	0.61	4.31	15.88

Table 40: Continuous statistical scores for H60B vs DPR-NS product over MSG full disk area.

Appendix 4 Multi-categorical statistics

H60B VS Ground		RADAR LAND	RADAR SEA	RADAR COAST	GAUGE LAND	OVERALL
≥0.25 mm/h	POD	0.35	0.34	0.34	0.41	0.38
	FAR	0.78	0.54	0.63	0.70	0.71
	MISS	0.65	0.66	0.66	0.59	0.62
	CSI	0.15	0.24	0.22	0.21	0.20
≥1 mm/h	POD	0.28	0.27	0.26	0.32	0.30
	FAR	0.82	0.63	0.72	0.76	0.76
	MISS	0.72	0.73	0.74	0.68	0.70
	CSI	0.12	0.19	0.16	0.16	0.15

Table 41: Probability Of Detection (POD), False Alarm Ratio (FAR), Missing (MISS) and Critical Success Index (CSI) for H60B vs Radar over Land, Sea, Coast, Gauge over Land and Overall surfaces for different rain rate thresholds over the European area.

H60B VS DPR		LAND	SEA	COAST	OVERALL
≥0.25 mm/h	POD	0.39	0.25	0.17	0.27
	FAR	0.68	0.63	0.70	0.65
	MISS	0.61	0.75	0.83	0.73
	CSI	0.21	0.18	0.12	0.18
≥1 mm/h	POD	0.41	0.30	0.18	0.32
	FAR	0.73	0.71	0.78	0.72
	MISS	0.59	0.70	0.82	0.68
	CSI	0.19	0.17	0.11	0.17
≥10 mm/h	POD	0.27	0.19	0.11	0.20
	FAR	0.89	0.83	0.89	0.86
	MISS	0.73	0.81	0.89	0.80
	CSI	0.08	0.10	0.06	0.09

Table 42: Probability Of Detection (POD), False Alarm Ratio (FAR), Missing (MISS) and Critical Success Index (CSI) over Land, Sea, Coast and Overall surfaces for different rain rate thresholds for H60B vs DPR-NS product over the MSG full disk area.

Appendix 5 H60B versus DPR maps over MSG full disk area

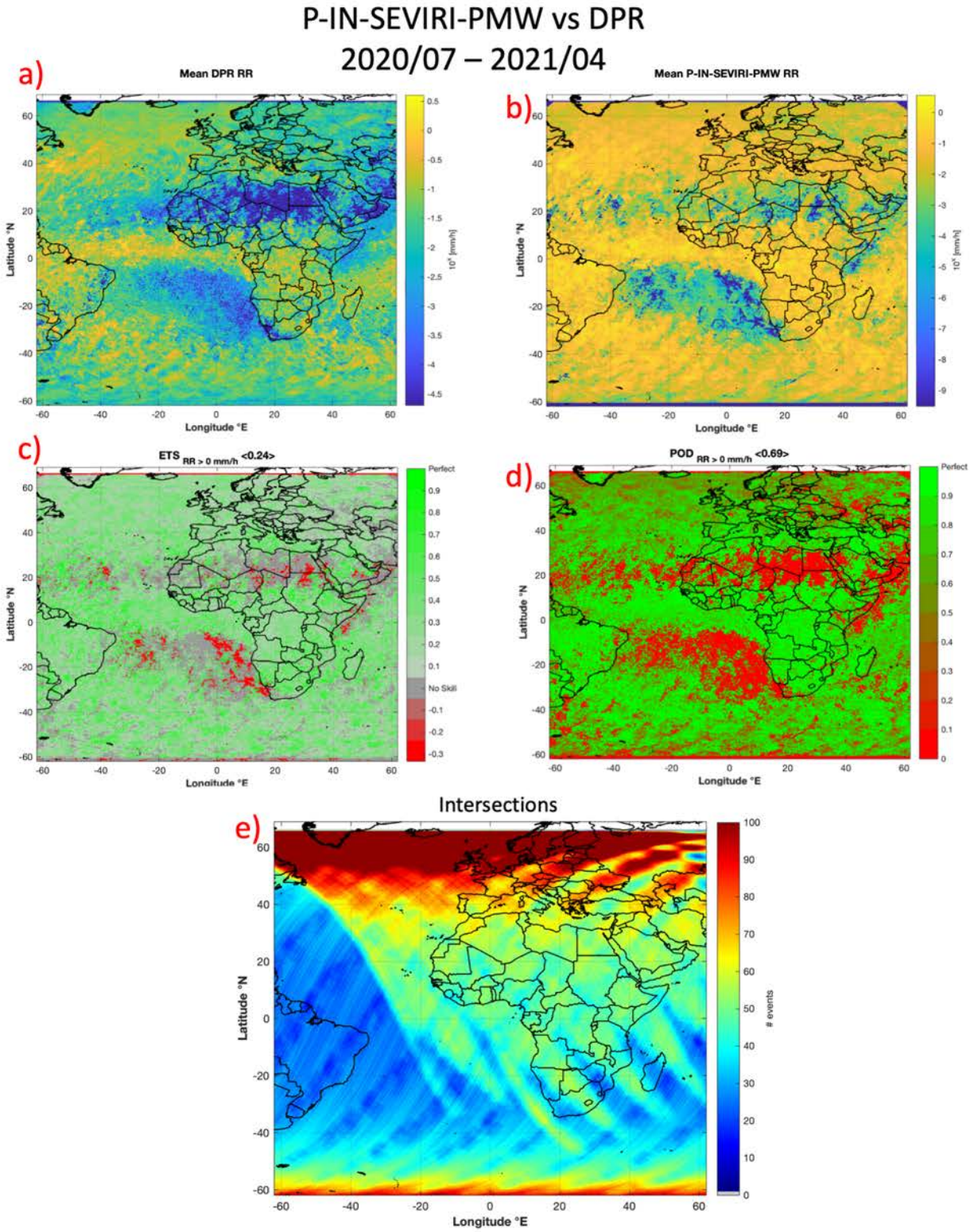

Figure 68: Regular gridded maps (0.5° x 0.5°) of comparison between H60B and DPR-NS products. a) Mean DPR RR. b) Mean P-IN-SEVIRI-PMW RR. c) ETS for RR > 0 mm/h. d) POD for RR > 0 mm/h. e) Number of intersections.

Appendix 6 Acronyms

AMSU	Advanced Microwave Sounding Unit
ATMS	Advanced Technology Microwave Sounder
ATS	Automatic Telemetric Station
AWOS	Automated Weather Observation Station
BE	Belgium
BfG	German Federal Institute of Hydrology
CAPPI	Constant altitude plan position indicator
CSI	Critical Success Index
DE	Germany
DPC	Italian Department of Civil Protection
ECMWF	European Centre for Medium-Range Weather Forecasts
EFOV	pixel Extension Field Of View
ENAV	Italian air navigation service provider
EU	European
FAR	False Alarm Ratio
FD	Full Disk
FMI	Finnish Meteorological Institute
GRISO	Rainfall Generator of Spatial Interpolation from Observation
HU	Hungary
IFOV	Instantaneous Field Of View
IMWM	Institute of Meteorology and Water Management - Poland
INCA	Integrated Nitrogen model for CAtchments
IRM	Institut Royal Météorologique - Belgium
IT	Italy
ITAF-COMET	ITalian Air Force – Operational Meteorological Center
MAE	Multiplicative Absolute Error
MB	Multiplicative Bias
ME	Mean Error
METOP	Meteorological Operational Satellites
MHS	Microwave Humidity Sounder
MW	MicroWave
NE	North-East
NW	North-West
OMSZ	Hungarian Meteorological Service
PL	Poland
POD	Probability Of Detection
PPVG	Precipitation Product Validation Group
PR	Precipitation Rate
PR-RMSE	Product Requirement Root Mean Square Error
PUM	Product User Manual
PVR	Product Validation Report
RD	Radar
RG	Raingauge
RMSE	Root Mean Square Error

SAF	Satellite Application Facility
SE	South-East
SHMU	Slovak hydrometeorological institute
SK	Slovakia
SRI	Surface Rainfall Intensity
STD	Standard Deviation
SW	South-West
TSMS	Turkish State Meteorological Service
TU	Turkey
UCC	Unique Common Code
WG	Working Group
ZAMG	Zentralanstalt für Meteorologie und Geodynamik